January 1986 ANL-PRISM-8

MODELING OF THE AIR-SIDE PERFORMANCE OF THE RVACS SHUTDOWN HEAT REMOVAL SYSTEM--STATUS OF EXPERIMENTAL PROGRAM

by

T. C. Chawla, F. B. Cheung, R. R. Stewart, D. R. Pedersen,
J. H. Tessier, R. L. Webb,* H. J. Haupt, T. T. Anderson,
E. W. Johanson, C. August, and J. R. Pavlik

Reactor Analysis and Safety Division
Argonne National Laboratory
9700 South Cass Avenue
Argonne, Illinois 60439

~~LIMITED DISTRIBUTION~~

~~The ANL-~~ ...r the ANL tasks perfo... ...M series is prepared p... ...eported are preliminary... ...quoted or ~~referenced~~

~~Any furthe~~ ...n therein to third partie... ...companies and foreign... ...ld be coordinated with the Deputy Assistant Secretary for Breeder Reactor Programs, U. S. Department of Energy.~~

*Consultant; Pennsylvania State University

Table of Contents

Table of Contents (cont'd)

List of Figures

List of Tables

1.0 INTRODUCTION

The use of a natural circulating air stream as a means of shutdown heat removal from the reactor vessel has been a key feature of the advanced liquid metal reactor concepts initiated in FY 1985 by vendors selected by DOE as a part of a competitive procurement process. The Department of Energy has selected GE and AI to develop their innovative design concepts aimed at improving safety, lowering plant costs, simplifying plant operation, reducing construction times, and most of all, enhancing the plant licensability. GE is developing a small modular, pool-type reactor, capable of being factory fabricated and transported by rail. The reactor program at Argonne has been providing support to evaluate the vitalities of both designs.

The method of shutdown heat removal proposed in the GE design employs a totally passive cooling system referred to as the Radiant Vessel Air Cooling System RVACS that rejects heat from the reactor by radiation and natural convection to air. The system is inherently reliable since it is not subject to the types of failure modes normally associated with active auxiliary cooling systems. Specifically, the RVACS is designed to assure adequate cooling of the reactor vessel under abnormal operational conditions associated with loss of heat removal through the normal heat transport path via the steam generator system. The RVACS air cooling system consists of several concentrical segments. The reactor vessel is located at the center of the system surrounded by the guard vessel which is the containment of the advanced liquid metal reactor. The space between the reactor vessel and the guard vessel is closed and is filled with an inert gas such as argon or helium. Outside of the guard vessel is a cylindrical structure referred to as the finned shell or the duct wall. Radial fins or repeated ribs can be attached to the duct wall and/or the guard vessel. The annular region outside of the duct wall provides

a natural circulation path for downward flow of air from the environment. The air draft turns at the bottom and flows upward in the gap or flow channel formed by the guard vessel and the duct wall.

Previous scoping calculations have indicated the validity of the air-cooled shutdown heat removal method. However, uncertainties remain with respect to the particular design concerning the width of the flow channel, the repeated-rib/fin arrangements and their locations, the rib/fin height, and the rib/fin spacing. In addition, the effects of the inlet air temperature, the pressure loss at the inlet and outlet, the stack height, the thermal loading, and material properties including surface emissivity on the performance of the air cooling system are not clearly understood. Previous studies of turbulent flow and heat transfer in channels with or without fins/ribs have been restricted to the case of forced convection flow [1-8] and the case of combined free and forced convection flow [9-12]. No study has been made of purely buoyancy-induced turbulent flow in channels. The purpose of this report is to summarize the status of the analytical and experimental work as a part of the ANL effort on the development of an optimum design configuration for the air cooling system. Results of the analysis provide basic information needed to evaluate the performance of various design options. They also provide useful guidance to the ongoing experimental effort at ANL which is described in Section 8.0 of this report.

2.0 DESIGN OPTIONS

Six different design options have been identified for the air cooling systems. These are shown schematically in Figure 2.1. In design option A (smooth wall option), the flow channel is simply the annulus space between the guard vessel and the cylindrical duct wall. The primary parameters are the width, H, of the gap between the two bounding walls and the ratio H/R, where R is the radius of the guard vessel. Generally, the curvature effect is negligible since $R \gg H$. Hence the flow channel may be approximated by the one formed between two parallel flat plates. This is the simplest design option among the others and may be treated as the base case for comparison. Design option B involves placement of repeated-rib roughness circumferentially on the bounding walls. The repeated ribs are employed to enhance heat transfer in the air cooling system. Note that the roughness elements may be placed on either one or both surfaces. The primary parameters are the height, e, the pitch, p, and the shape of the roughness elements, see Fig. 2.2. In design options C, D, and E, vertically-spaced straight fins are employed to enhance the total heat transfer surface area. Design option C involves placement of all of the fins on the guard-vessel side. The primary parameters are the fin height, H, the fin spacing, S, and the clearance, C, between the tips of the fins and the duct wall. Other parameters that would affect the performance of the system include the thickness and shape of the fins and the fin geometry (e.g., continuous fins vs. staggered fins). Design option D involves placement of all the fins on the duct wall. The important parameters are the same as those for option C. Design option E is a combination of design options C and D. It involves placement of half of the fins on the duct wall and the other half on the guard vessel, being arranged in an alternative manner. Design option F is a variation of design option E. It involves

simultaneous placement of short fins on both the guard vessel and the duct wall with $H_{GV} + H_D = H$. Note that for a given sodium pool temperature, a higher heat transfer per unit area can be achieved for fins placed on the guard vessel rather than on the duct wall. This is because the guard-vessel temperature is always higher than the duct-wall temperature so that a higher rate of radiative and convective cooling can be achieved by using extended surfaces from the guard vessel. This, however, must be weighted against the disadvantages in fabrication cost, in-service inspection, and containment boundary complications associated with putting fins on the guard vessel.

General Electric is interested in Design Options A, B and D and therefore the heat transfer characteristics of these options will be presented. In the analysis of the various system the primary criteria for evaluation are :

1. What is the reactor vessel temperature?
2. What is the air exit temperature?
3. What impact does the system have on the structural concrete temperatures?

The major impact of the guard vessel temperature is on the reactor vessel temperature. The heat transfer from the reactor vessel to guard vessel is dominated by radiation heat transfer. Assuming planar surfaces, the reactor vessel temperature, T_{RV}, as a function of surface emissivity, ε, heat flux, Q, and the guard vessel temperature, T_{GV}, is given by

$$T_{RV} = \left(\frac{Q}{\sigma\, \varepsilon_A} + T_{GV}^4\right)^{1/4} \qquad (2\text{-}1)$$

$$\text{where} \quad \varepsilon_A = \frac{1}{\frac{2}{\varepsilon} - 1} \qquad (2\text{-}2)$$

neglecting conduction and convection heat transfer. Figure 2.3 shows the reactor vessel temperature as a function of the guard vessel temperature for heat fluxes of 10 and 20 kW/m^2 and emissivities of 0.7, 0.85, and 1.0. In the GE RVACS design the typical peak heat fluxes will be in the range from 10-15 kW/m^2. The results shown in Fig. 2.3 demonstrate the relatively weak dependence of reactor vessel temperature upon guard vessel temperature for guard vessel temperatures less than ~ 300°C; as well as the strong effect of emissivity. For higher guard vessel temperature the effect is increased. Thus one must be aware of the relationship between guard vessel temperature and reactor vessel temperature in the assessment of air-side performance.

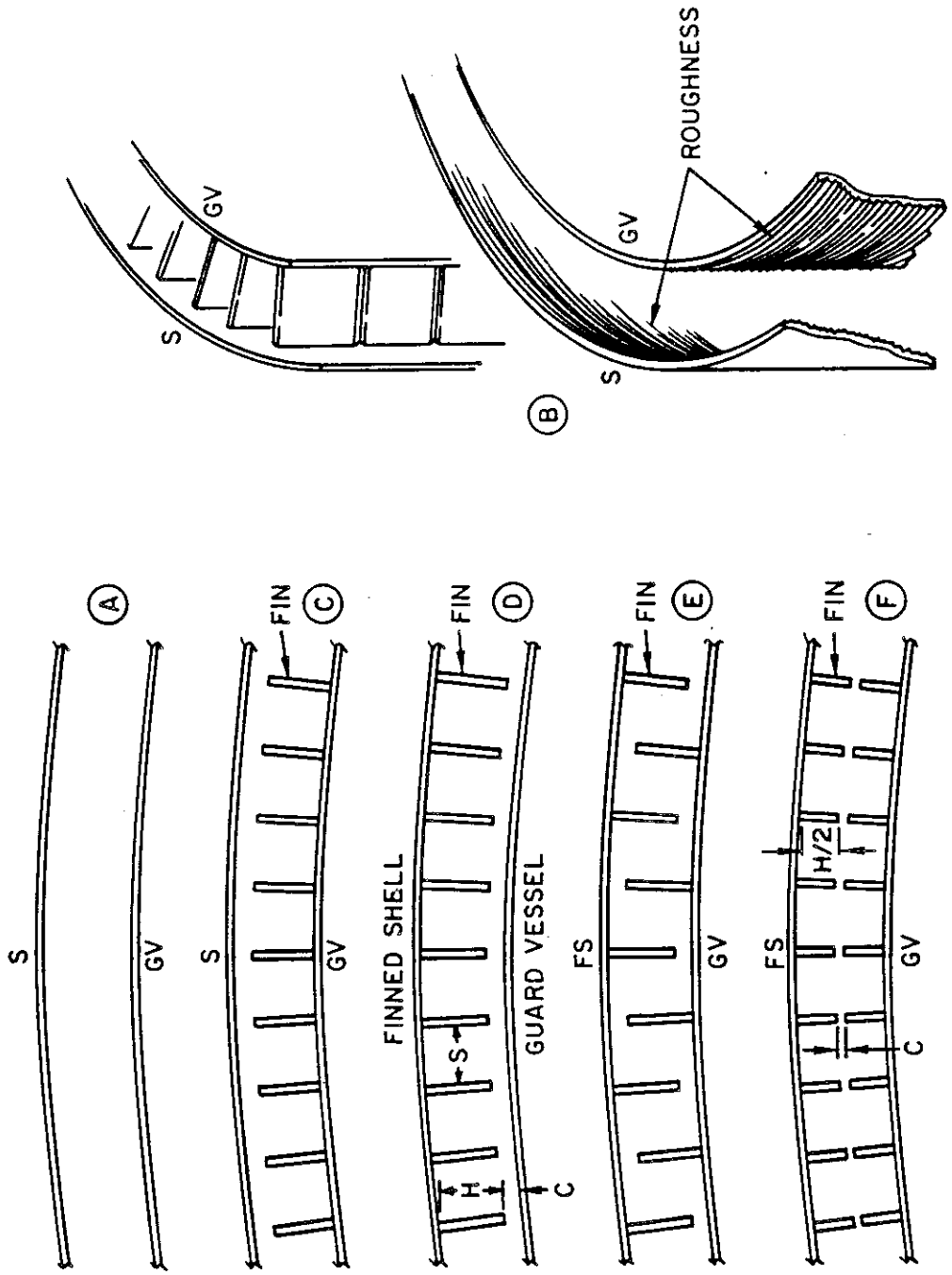

Fig. 2.1 Schematic Representations of Six Designs

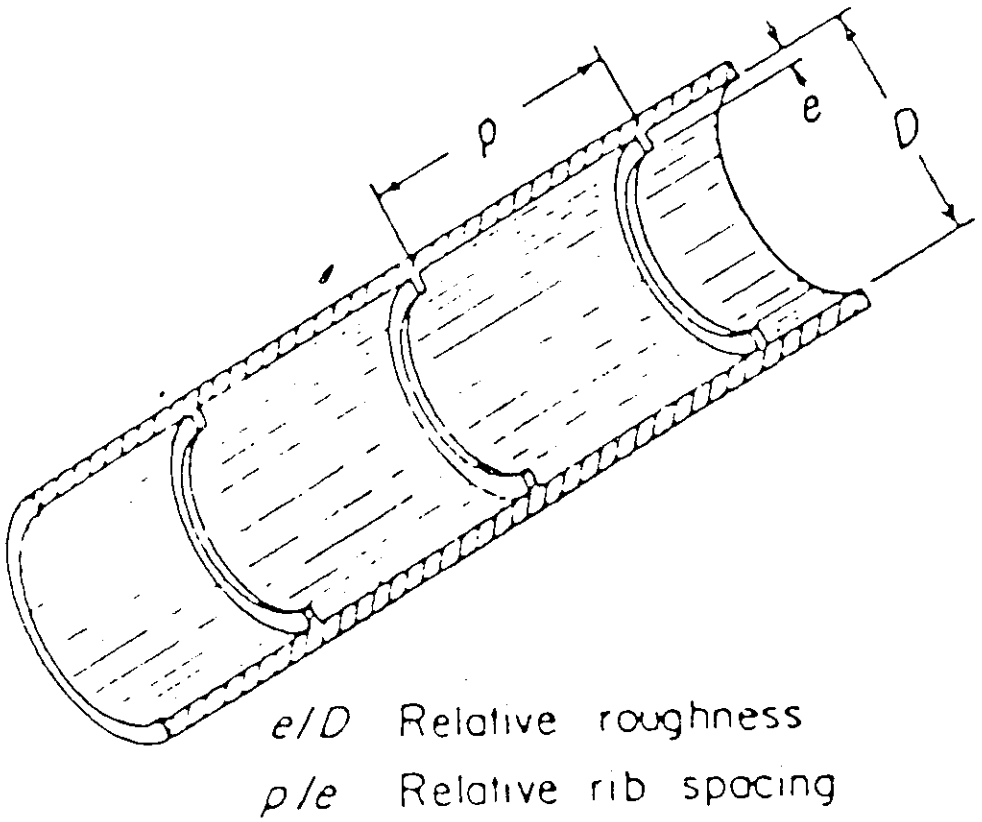

Figure 2.2 Characteristic Dimensions of Repeated-Rib Roughness.

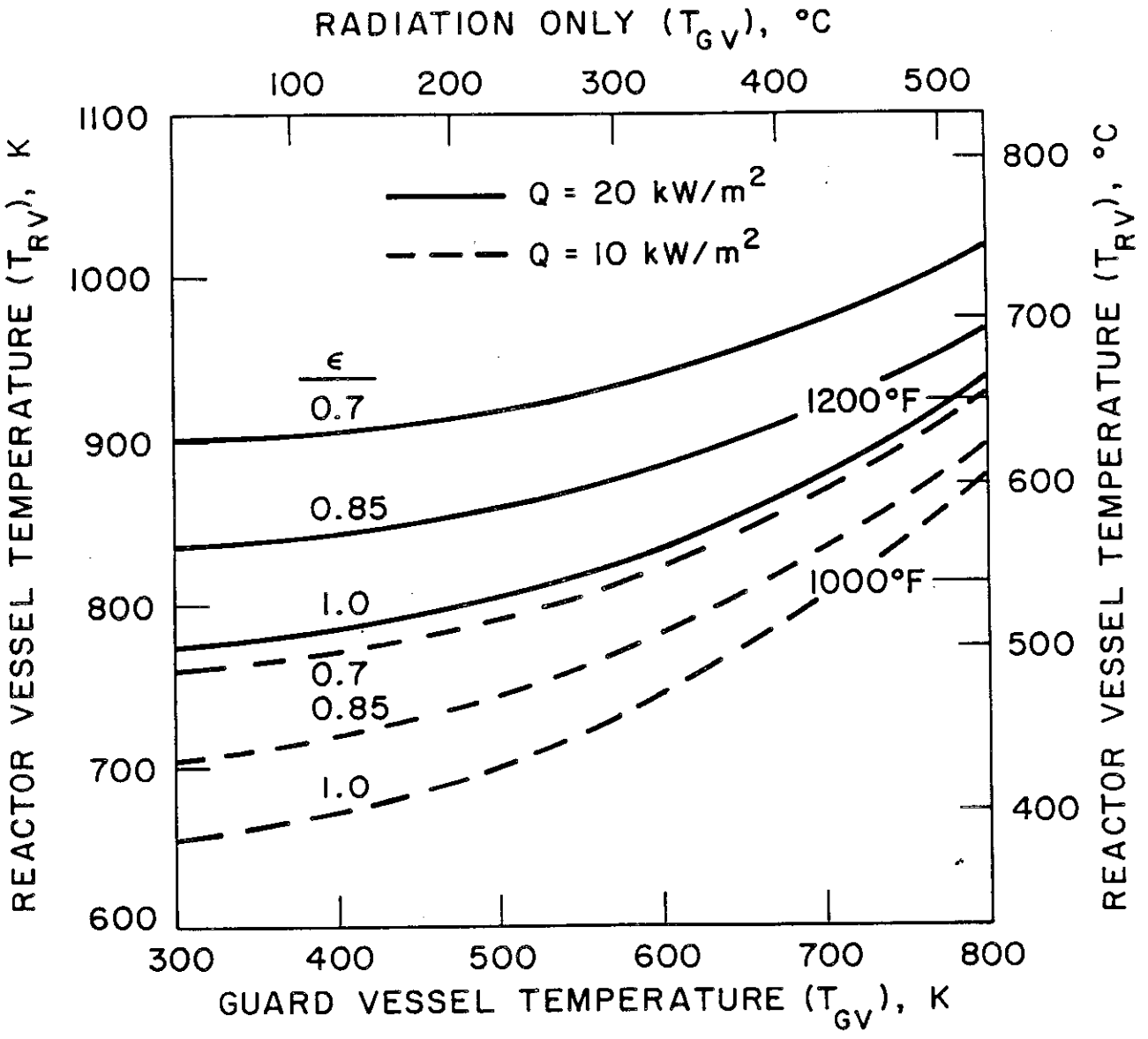

Figure 2-3 Reactor Vessel Temperature as Function of Guard Vessel Temperature for Various Heat Fluxes and Surface Emissivity (radiation only).

3.0 PHYSICAL MODEL

Since R >> H, the guard vessel and the duct wall may be treated as two parallel flat walls. To the first approximation, the air cooling system may be divided into a number of individual flow channels, each of which has the same shape as the one depicted in Fig. 3-1. For design options C, D, and E, the parameter S is simply the fin spacing and the total number of flow channels is determined by the total number of fins. For design options A and B, however, there is only one continuous flow channel and therefore, the parameter S must go to infinity. In all cases, the total length of the channel is L whereas the length of the heated section is L_h. The difference $(L - L_h)$ represents the stack height which is a parameter of the system. Note that at any elevation z, measured from the bottom of the air circulation channel, the temperatures T_1 and T_2 of the two adjacent fins may be different than the guard vessel temperature T_w and the temperature T_s of the duct wall. To analyze the flow and heat transfer in the channel, the following simplifying assumptions are employed.

(1) The air cooling system is operates at steady state and the operating conditions can be described in a quasi-steady manner.

(2) The guard-vessel wall, the duct wall, and each of the two adjacent fins form a separate flow channel. This is equivalent to assuming C = 0. For design A and B, the flow channel is simply the gap between two parallel walls.

(3) The flow is buoyancy-driven, incompressible and turbulent. The mass flow rate is constant along the channel.

(4) The guard vessel wall is heated externally under a constant-heat-flux conditions, i.e., Q_w is independent of space and time.

(5) Radiation heat flux may be calculated based on the average surface temperatures. Gray surfaces are assumed. In addition, the air is not participating in the radiation transfer process.

(6) The friction factors and heat transfer coefficients may be obtained from the data for forced flow in channels with or without repeated ribs.

(7) All physical properties are constant except density variation in the buoyancy force. In particular, the surface emissivity does not vary with time during the operation of the air cooling system.

Under steady-state natural circulation conditions, the pressure drop in the entire flow channel including inlet and outlet losses must be balanced by the buoyancy force. This gives

$$\Delta P = g \int_{o}^{L} (\rho_\infty - \rho)\, dz \tag{3-1}$$

where g is the acceleration due to gravity, ρ the local air density, and ρ_∞ the ambient air density. Assuming a linear relationship between the density and the temperature, we have

$$\rho = \rho_\infty [1 - \beta (T_a - T_\infty)] \tag{3-2}$$

where β is the isobaric coefficient of thermal expansion, T the local air temperature, and T_∞ the ambient air temperature. Ignoring the relatively small heat loss from the duct wall to the environment, the local air temperature T_a must rise in the flow direction according to

$$\frac{dT_a}{dz} = Q_w / \rho C_p u H \quad , \quad T_a(o) = T_o \tag{3-3}$$

where C_p is the specific heat, u the air velicity to be determined in the course of the analysis, and T_o the inlet air temperature which can be different from the ambient air temperature T_∞. In writing Eq. (3-3), the flow has been assumed adiabatic in the upper unheated section where $L \leq z \leq L_h$. Note that the quantity $(\rho u H)$ represents the mass flow rate of air and is a constant under steady-state operating conditions. Integration of Eq. (3-3) gives

$$T_a = \begin{cases} T_o + (Q_w/\rho C_p u H)\, z & \text{for } 0 \leq z \leq L_R \\ T_o + Q_w L_h/\rho C_p u H & \text{for } L_h \leq z \leq L \end{cases} \tag{3-4}$$

Combining Eqs. (3-1), (3-2), and (3-4), we have

$$\Delta P = \rho_\infty g\beta\left[(T_o - T_\infty)\, L + Q_w L_h \left(L - \frac{1}{2} L_h\right)/\rho C_p u H\right] \tag{3-5}$$

In terms of the friction factor f, the pressure drop is also given by

$$\Delta P = 2f\rho u^2 L_h/D_h + \Delta P_{loss} \tag{3-6}$$

where ΔP_{loss} represents the inlet and outlet losses and D_h is the hydraulic diameter defined by

$$D_h = 2SH/(S + H) \tag{3-7}$$

For design options A and B, we have

$$S \to \infty \quad \text{and} \quad D_h = 2H \tag{3-8}$$

Introducing a parameter $\Omega = \Delta P_{loss}/\Delta P$ into Eq. (3-6), we obtain

$$\Delta P = 2f\rho u^2 L_h/(1 - \Omega)\, D_h \tag{3-9}$$

where Ω is a positive quantity always less than unity. The relation between Ω and the overall inlet-exit loss coefficient is given in Appendix 1. For the GE RVACS system, preliminary estimates suggest that Ω is in the range $0.4 < \Omega < 0.8$. The above equations are applicable to all design options under consideration. To determine the air flow rate and the temperatures of the duct wall, the guard vessel, and the reactor vessel, the friction factor and the heat transfer coefficient must be specified for each design option.

3.1 Design Option A -- Smooth Channel

For turbulent channel flows, the Blasius formula gives

$$f = \begin{cases} 0.0791\ Re^{-1/4} & \text{for } 2300 \leq Re \leq 2 \times 10^4 \\ 0.046\ Re^{-1/5} & \text{for } Re \geq 2 \times 10^4 \end{cases} \tag{3-10}$$

where $Re = \rho u D_h/\mu$ is the Reynolds number and D_h is given by Eq. (3-8). The heat transfer coefficient is given by [13]

$$h = \frac{0.023\ k}{D_h} Re^{0.8} \left(\frac{\nu}{\alpha}\right)^{0.4} \tag{3-11}$$

In terms of the width, H, of the channel, the above expression becomes

$$h = \frac{0.020\ k\ u^{0.8}}{H^{0.2}\ (\alpha\nu)^{0.4}} \tag{3-12}$$

Combining Eqs. (3-5), (3-9), and (3-10), we yield an implicit expression for the average air velocity

$$u = H^{5/11} \left\{ \frac{\rho_\infty g\beta(1 - \Omega) \left[(T_o - T_\infty)\, uL + Q_w L_h \left(L - \frac{1}{2} L_h \right) / \rho C_p H \right]}{0.0665\, \rho^{3/4}\, \mu^{1/4}\, L_h} \right\}^{4/11} \tag{3-13}$$

For the special case of $T_o = T_\infty$, the above expression reduces to

$$u = H^{5/11} \left\{ \frac{\rho_\infty g\beta(1 - \Omega)\, Q_w \left(L - \frac{1}{2} L_h \right)}{0.0665\, \rho^{7/4}\, C_p\, \mu^{1/4}\, H} \right\}^{4/11} \tag{3-14}$$

Thus the air flow rate is not sensitive to the change in the channel width since $u \sim H^{0.1}$ but is sensitive to the value of external pressure losses since $u \sim (1-\Omega)^{0.36}$.

To determine the steady-state temperature distribution of the system, the following equations are employed.

$$Q_w = h(T_{GV} - T_a) + \frac{\sigma(\overline{T}_{GV}^4 - \overline{T}_D^4)}{\frac{1}{\varepsilon_{GV}} + \frac{1}{\varepsilon_D} - 1} \tag{3-15}$$

$$h(T_D - T_a) = \frac{\sigma(\overline{T}_{GV}^4 - \overline{T}_D^4)}{\frac{1}{\varepsilon_{GV}} + \frac{1}{\varepsilon_D} - 1} \tag{3-16}$$

$$\bar{T}_R = \left[\bar{T}_{GV}^4 + \frac{Q_w}{\sigma}\left(\frac{1}{\varepsilon_R} + \frac{1}{\varepsilon_{GV}} - 1\right)\right]^{1/4} \tag{3-17}$$

where

$$\bar{T}_D = \frac{1}{L_h}\int_o^{L_h} T_D dz \tag{3-18a}$$

$$\bar{T}_{GV} = \frac{1}{L_h}\int_o^{L_h} T_{GV} dz \tag{3-18b}$$

$$\bar{T}_R = \frac{1}{L_h}\int_o^{L_h} T_R dz \tag{3-18c}$$

where the subscript D refers to the duct wall, GV the guard vessel, and R the reactor vessel. Equations (3-15) to (3-18) may be solved with the aid of Eq. (3-12) to determine $T_D(z)$, $T_{GV}(z)$, and $\bar{T}_R$.

3.2 Design Option B -- Repeated-Rib Roughness

The following analysis is for repeated rib roughness on both the guard vessel and duct wall. The analysis is based upon the results of Webb et al. [2]. The preliminary analysis for roughness on just one wall is presented in Section 4.2. For given values of roughness height, e, and pitch, p, the friction factor may be approximately represented by [2]

$$f = \begin{cases} 2\left[2.5 \ln (H/e) + u_e^+ - 3.75\right]^{-2} & \text{for } e^+ < 25 \\ 2\left[2.5 \ln (H/e) + 0.95 (p/e)^{0.53} - 3.75\right]^{-2} & \text{for } e^+ > 35 \end{cases} \quad (3\text{-}19)$$

where e^+ is referred to as the roughness Reynolds number.

$$e^+ = (e/2H)\, Re\, (f/2)^{1/2} \quad (3\text{-}20)$$

$$u_e^+ = 2.64\, (p/e)^{0.53}\, (1 - 0.18 \ln e^+) \qquad \text{for } e^+ < 25 \quad (3\text{-}21)$$

Interpolation may be used for $25 < e^+ < 35$. In terms of f, the air velocity is given by

$$u = \left\{\frac{\rho_\infty g\beta(1 - \Omega)\, H \left[(T_o - T_\infty)\, uL + Q_w L_h \left(L - \frac{1}{2} L_h\right)/\rho C_p H\right]}{\rho f L_h}\right\}^{1/3} \quad (3\text{-}22)$$

For the special case of $T_o = T_\infty$, the above expression reduces to

$$u = \left\{\frac{\rho_\infty g\beta(1 - \Omega)\, Q_w \left(L - \frac{1}{2} L_h\right)}{\rho^2 C_p f}\right\}^{1/3} \quad (3\text{-}23)$$

Note that e^+, u_e^+, and f are functions of u so that Eqs. (3-19) to (3-23) must be solved iteratively in the numerical calculation. With the average air velocity determined, the heat transfer coefficient may be evaluated according to the following expression [2]:

$$h = \rho C_p uf/2A \quad (3\text{-}24)$$

where

$$A = \begin{cases} 1 + (f/2)^{1/2} \left[4.5 \left(e^{+}\right)^{0.28} Pr^{0.57} - 0.95 \left(p/e\right)^{0.53}\right] & \text{for } e^{+} > 35 \\ 1 + (f/2)^{1/2} \left[11.1\ Pr^{0.57} - u_e^{+}\right] & \text{for } e^{+} < 25 \end{cases} \tag{3-25}$$

The reactor temperature, guard-vessel temperature, and duct-wall temperature can be determined by solving Eqs. (3-15) to (3-18) using the above expression for h.

3.3 Design Option C -- Fins on the Guard Vessel Only

In the GE/RVACS design, the fins will not be placed on the guard vessel. Nonetheless, we shall include this option in the mathematical formulation for reference, although no calculation will be made for this case. To simplify the analysis, heat conduction, Q_c, from the fins to their bases per unit fin spacing is included by using the following steady-state expression

$$Q_c = \left(\frac{b_f}{s}\right) \left[\frac{2\ K_F}{H} \left(T_b - T_F\right)\right] \tag{3-26}$$

where T_F is the average temperature of the fins, T_b the average temperature of their bases, b_f the fin half width, and K_F the fin conductivity. When all the fins are located on the guard-vessel wall, we have $T_b = T_{GV}$. The fin efficiency is defined by

$$\eta = \frac{h_F\left(T_F - T_a\right) + \left(Q_r\right)_F}{h_b\left(T_b - T_a\right) + \left(Q_{rb}\right)F} \tag{3-27}$$

which is an output quantity. Since the local velocity variation is ignored in the analysis, we shall take $h_F = h_{GV} = h$, where h is given by Eq. (3-11). Under steady-state conditions, the following relations must be satisfied by the various temperatures:

$$Q_w = h(T_{GV} - T_a) + (Q_r)_{GV} + 2Q_c \tag{3-28}$$

$$(Q_r)_D + h(T_D - T_a) = 0 \tag{3-29}$$

$$Q_c = \frac{H}{S}\left[h(T_F - T_a) + (Q_r)_F\right] \tag{3-30}$$

where Q_r's are the net radiant heat fluxes and the subscript F refers to the fins. Combining Eqs. (3-28) to (3-30), we have

$$Q_w = h(T_{GV} - T_a) + (Q_r)_{GV} + 2\frac{H}{S}\left[h(T_F - T_a) - (Q_r)_F\right] \tag{3-31}$$

Equations (3-29) and (3-31) may be solved for $T_{GV}(z)$ and T_D along with the following equations governing the radiant heat fluxes:

$$(Q_r)_{GV} = \varepsilon_{GV}\left[\sigma\overline{T}^4_{GV} - F_{GD}J_D - (1 - F_{GD})\,J_F\right] \tag{3-32}$$

$$(Q_r)_D = \varepsilon_D\left[\sigma\overline{T}^4_D - F_{GD}J_{GV} - (1 - F_{GD})\,J_F\right] \tag{3-33}$$

$$(Q_r)_F = \varepsilon_F\left\{\sigma\overline{T}^4_F - \frac{S}{2H}(1 - F_{GD})\,(J_{GV} + J_D) - \left[1 - \frac{S}{H}(1 - F_{GD})\right] J_F\right\} \tag{3-34}$$

where F_{GD} is the shape factor between the guard-vessel wall and the duct wall which is a function of H and S, and the J's are radiosities given by

$$J_{GV} = \varepsilon_{GV}\sigma\bar{T}_{GV}^4 + (1 - \varepsilon_{GV}) [F_{GD}J_D + (1 - F_{GD}) J_F] \tag{3-35}$$

$$J_D = \varepsilon_D\sigma\bar{T}_D^4 + (1 - \varepsilon_D) [F_{GD}J_{GV} + (1 - F_{GD}) J_F] \tag{3-36}$$

$$J_F = \varepsilon_F\sigma\bar{T}_F^4 + (1 - \varepsilon_F) \{\frac{S}{2H} (1 - F_{GD}) (J_{GV} + J_D) + [1 - \frac{S}{H} (1 - F_{GD})] J_F\} \tag{3-37}$$

The averaged wall temperatures are given by

$$\bar{T}_{GV} = \frac{1}{L_h} \int_o^{L_h} T_{GV}\, dz \tag{3-38a}$$

$$\bar{T}_D = \frac{1}{L_h} \int_o^{L_h} T_D\, dz \tag{3-38b}$$

$$\bar{T}_F = \frac{1}{L_h} \int_o^{L_h} T_F\, dz \tag{3-38c}$$

where from Eq. (3-4), we have

$$\bar{T}_a = T_o + Q_w L_h/2\rho C_p uH \tag{3-39}$$

Once T_{GV} is determined, the average temperature $\bar{T}_R$ of the reactor vessel can be obtained from Eq. (3-17). Note from Eqs. (3-31) to (3-37) that Q_w is equal to the sum of convective cooling by air at the bounding surfaces, i.e.,

$$Q_w = h[(T_{GV} - T_a) + (T_D - T_a) + 2\frac{H}{S}(T_F - T_a)] \tag{3-40}$$

3.4 Design Option D -- Fins on the Duct Wall Only

When all the fins are located on the duct wall, we have

$$Q_c = (\frac{b_f}{s})[\frac{2K_F}{H}(T_D - T_F)] \tag{3-41}$$

Under steady-state conditions, the following relations must be satisfied by the various temperatures:

$$Q_w = h(T_{GV} - T_a) + (Q_r)_{GV} \tag{3-42}$$

$$(Q_r)_D + h(T_D - T_a) + 2Q_c = 0 \tag{3-43}$$

$$Q_c = \frac{H}{S}[h(T_F - T_a) + (Q_r)_F] \tag{3-44}$$

where Q_c is now the conductive heat flux from the duct wall to the fins. Combining Eqs. (3-43) and (3-44) gives

$$(Q_r)_D + h(T_D - T_a) + 2\frac{H}{S}[h(T_F - T_a) + (Q_r)_F] = 0 \tag{3-45}$$

Again, Eqs. (3-31) to (3-37) can be solved along with Eqs. (3-42) and (3-45) to get $T_{GV}(z)$ and $T_D(z)$. Once T_{GV} is determined, $\bar{T}_R$ can be obtained from Eq. (17). Note that, in this case, we have

$$Q_w = h\left[\left(T_{GV} - T_a\right) + \left(T_D - T_a\right) + 2\,\frac{H}{S}\left(T_F - T_a\right)\right] \qquad (3\text{-}46)$$

From Eqs. (3-14), (3-40), and (3-46), it is evident that for given values of Q_w, K_F, and H/S, a lower guard-vessel temperature can be achieved by using Design Option C rather than Design Option D.

Figure 3-1. Physical Model

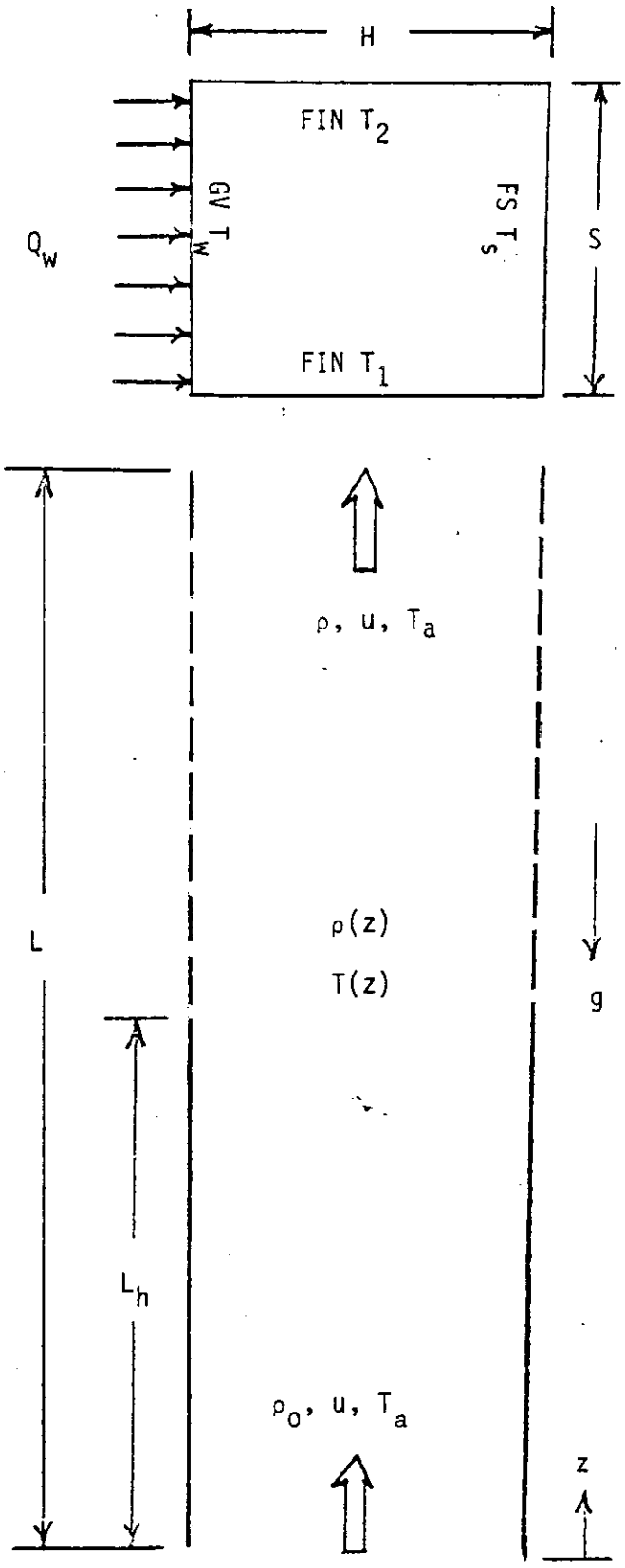

4. NUMERICAL SOLUTIONS

This section presents numerical results for a variety of RVACS design configurations and assumed operating conditions. A fairly exhaustive set of parametrics are presented for each design option to examine performance senstivity to individual parameter variation and also show the comparative performance of the various design options. The calculations were made by computer; the models presented in Section 3 were coded and program listings are presented in Appendix 2.

4.1 Smooth Channel Results

The basis for comparison for any design option should be the results of the smooth channel option (Option A). Option A has the least impact upon reactor design. Table 4.1 shows the results of a parametric evaluation of RVACS performance of the following parameters; channel width, heat flux, emissivity, stack height, heated length, and loss parameter Ω. Comparison between the various cases may be highlighted by examining the values of reactor vessel temperature, exit air temperature, duct wall temperature and convective heat transfer coefficient. The results of this evaluation lead to the following key observations

1. Reactor vessel temperatures are weakly influenced by air-side temperatures/parameters provided that the overall air flow rates are sufficiently high ($>$ 3 m/s) as is the case for $\Omega \leq 0.8$ and $H > 0.0254$ m. On the other hand, heat flux levels and/or surface emissivities have strong effects.

2. Both the outlet air temperature and the guard-vessel temperature, T_{GV}, increase with Q_w according roughly to $(Q_w)^m$ were $m \simeq 0.6$ based

upon a rough fit to the preliminary numerical results. This also can be derived from equations (3-4) and (3-14) along with the fact that $(T_{GV} - T_a)$ is a constant based upon the present model.

3. Assuming steady-state surface-to-surface radiation heat transfer between the reactor vessel and the guard vessel, the reactor-vessel temperature can be shown to vary with Q_w according to

$$T_R \sim Q_w^n, \quad 0.25 < n < 0.6 \tag{4-1}$$

The value of n will depend on the relative resistance to heat transfer. (1) from the reactor vessel to guard vessel and 2) from the guard vessel to air.)

4. The wall temperatures are not sensitive to the stack height as long as the stack height is comparable to the heated length. Increasing the stack height would only slightly decrease the outlet air temperature and moderately increase the air flow rate.

5. Decreasing the inlet air temperature would moderately lower the air flow rate and the wall temperatures.

4.2 Smooth Channel (Option A) vs. Repeated-Rib Roughness on Both Walls (Option B)

Roughening the surface(s) in the heated zone of the air flow channel has the potential to increase RVACS heat removal capability as noted previously. The possible benefit accrues from the tendency of the circumferential ribs to

increase the convective heat transfer coefficient, thereby reducing guard vessel and duct wall temperatures. However, because the friction factor of a roughness geometry is greater than that of a smooth channel (for the same Reynolds number), the pressure drop of the rough channel will be greater than that of a smooth channel. Hence, for a natural convection problem having a constant channel spacing, flow length, and heat input, the flow rate will be smaller in a rough channel geometry than in a smooth channel. This flow rate reduction will reduce the potential benefits of the rough channel in two ways. First, the heat transfer coefficient will be smaller than if it were possible to operate at the same flow rate as the smooth surface channel. Second, the required heat transfer must be accomplished at a reduced flow rate, which increases the average air temperature. Hence, it is necessary to select a roughness size that will provide a reasonably high heat transfer coefficient with the smallest possible pressure drop increase.

To explore the effects of surface roughening quantitatively, a large number of calculations were performed assuming repeated ribs on both the guard vessel and duct wall surfaces and, for comparison, companion calculations for a smooth channel (i.e. no fins or ribs). Results are presented in Tables 4.2 and 4.3 for the case of zero stack height. Additional results for the case of non-zero stack height are presented in Appendix 3. Table 4.6 provides a nomenclature list for tables in this Section.

Tables 4.2 and 4.3 show the calculated performance of roughened guard vessel and duct wall as compared to a smooth channel for two methods of prediction. The first method of calculation was presented in Section 3.2. The second method of calculation was used by Webb and a more detailed description of the method will be reported separately. The stack height was set equal to zero for both cases. In both tables comparisons are highlighted

by presenting the values of reduced guard vessel temperatures, $\Delta\bar{T}_{GV}$, and relative gain in heat transfer coefficients, h_R/h_S, for roughened walls. Method 2 (Table 4.3) shows more improvement than does Method 1 (Table 4.2) by ~ 15 percent. This is attributed to two differences in the calculational techniques, viz.; (1) Method 2 accounts for air property variation with temperature whereas Method 1 does not and, (2) different correlations are used for friction factor f and heat transfer coefficient h. In Method 1, the expressions for f and h given in Section 3 are employed. In Method 2, special equations were formulated to describe the heat transfer and friction characteristics of the traverse-rib roughness geometry; these correlations are given by Webb et al. [2]. The heat transfer and friction coefficients are functions of the "roughness Reynolds number," ($e^+ = eu^*/\nu$). The roughness performance was calculated for $16 < e^+ < 250$ for each roughness type. The roughness geometry is characterized by the rib spacing/height ratio (p/e) and the relative roughness size (e/D), where:

e = the roughness height

p = the roughness spacing

D = the flow channel hydraulic diameter (twice its spacing, H)

For a given roughness type (p/e = constant) variation of e/D changes the value of e^+.

The objective of the roughness is to maintain a low temperature of the guard vessel wall. Examination of the computer output shows that all roughness geometries yield the minimum wall temperature at $e^+ \sim 50$. Table 4.3 summarizes the rough surface data for the $e^+ = 50$ condition. The table compares the performance of the roughness geometries with that of the smooth surface at the same channel spacing (see [14] for the effect of different channel width). The term G_R/G_S is the ratio of flow rates in the rough and

smooth channel designs. Examination of Table 4.3 offers the following conclusions:

1. The p/e = 10 geometry provides the greatest reduction of the guard vessel wall temperature - 58-65°C for the two values of H.

2. The air flow rate for the p/e = 10 geometry is 62-65% of that of the smooth channel case.

3. Quite small roughness height and spacing are required for the p/e = 10 geometry - 2.4 mm height and 24 mm spacing.

One may offer practical objections to the very small roughness height and spacing of the p/e = 10 geometry. It may be costly to install, and it may be susceptible to surface fouling by dust and lint in the air. Use of the p/e = 40 geometry requires approximately the same roughness height, but its spacing is increased by a factor of four (to 101 mm). The wall temperature reduction is 50 C, as compared to 58 C for the p/e = 10 geometry with H = 254 mm.

If the largest roughness size and spacing are desired, one may choose the p/e = 40 geometry operated at $e^+ = 250$. For H = 254 mm, it reduces the wall temperature by 38 C (as compared to 58 C for the p/e = 10 geometry operated at $e^+ = 50$). However, the values of p and e for the p/e = 40 geometry operated at $e^+ = 250$ are 11.7 mm (0.46 in.) and 468 mm (18.4 in.), respectively. This roughness may be the most economical and practical to install of both the guard vessel and the duct wall.

In summary indications to date are that repeated rib roughness with roughness on both walls provides some benefit to reducing reactor vessel

temperatures if the ribs are small (less than 5 mm). For large ribs, reduced air flow effectively cancels the benefit of increase in heat transfer coefficient.

4.3 Repeated-Rib Roughness on the Guard Vessel Only vs. Roughness on Both Walls (Option B)

The above discussed analysis uses roughness on both the guard vessel and the duct wall. Analysis has been performed for the case of roughness that is placed only on the guard vessel wall. The duct wall is smooth. It is expected that the flow rate reduction will not be as great, possibly resulting in a lower guard-vessel temperature than is obtained for a geometry having roughness on both the guard vessel and duct walls. The analytical formulation of this case will be presented later in a separate report.

A considerable effort was required to obtain heat transfer and friction data for flow in a rib-roughened wall having only one rough wall. Actually, a considerable amount of data have been taken on this geometry. But, nearly all of these data have been "transformed" to allow its interpretation for the case of both walls rough. These publications do not include their test results for the asymmetric geometry. Much of these data were taken in the England and Germany in support of their gas-cooled nuclear reactor programs.

After much searching, a publication of Wilkie et al. [15] was located, which includes test data for p/e = 10 transverse-rib roughness in a parallel plate channel. The paper provides data for both walls rough, and for one rough and one smooth. Wilkie's data for e/D = 0.0056 was used. This e/D provides a roughness height of 2.82 mm for a 254 mm channel spacing. The paper provides only friction factor data (no heat transfer data were taken) for air flow at $25{,}000 < Re < 121{,}000$.

A modified analysis method was required to predict the heat transfer characteristics from [15]. It was assumed that the heat transfer coefficient can be predicted, if the friction factor for the p/e = 10 geometry is known, using the heat transfer correlation of Webb et al. [2]. Hence, the first step was to calculate results for the case of both walls rough using the Wilkie data for p/e = 10 and e/D = 0.056, a function of e^+. Then, using the friction factor data for the one wall rough case, the flow rate in the rough guard vessel wall-smooth duct wall channel was predicted. At this known Re, the heat transfer coefficient for the case of both walls rough (same e) was calculated. Sheriff and Gumley [16] show that the heat transfer coefficient in a channel with only one wall rough is approximately 8% less than that of a channel having the same roughness on both walls. Hence, the heat transfer coefficient for one rough wall was obtained by reducing the value for two rough walls 10% (both at the same Re). This heat transfer coefficient was applied only to the rough guard vessel wall. The heat transfer coefficient on the smooth duct wall was taken to be that for a smooth channel at the same Reynolds number. The actual heat transfer coefficient on the smooth duct wall should be a little higher than the value used here.

Table 4.4 shows the results for the case of roughness on only the guard vessel wall. Again, the stack height was set equal to zero. The first line of the table is for a smooth channel (H = 254 mm). The second line is for both walls rough, using Wilkie's measured friction factor for the tabled p/e and e/D. Line 3 shows the results for roughness on the guard vessel wall only. Examination of lines 1, 2 and 3 of Table 4.4 shows that roughness on one wall results in a higher wall temperature (18 C higher) than the value for both walls rough. The benefit of the higher flow rate is more than offset by the reduced heat transfer coefficient on the duct wall. The heat transfer

coefficient on the duct wall is reduced from 24.9 W/m^2-K to 12.5 W/m^2-K for the smooth duct wall. Because the duct wall runs at a quite high temperature, a high heat transfer coefficient is of considerable benefit on this surface too. The analysis method assumed that the heat transfer coefficient on the smooth duct wall is the same as that on the rough guard wall. This provides a prediction that is on the conservative side.

4.4 Fins on the Duct Wall Only (Option D)

The governing system for this case given in Section 3.4 constitutes a set of nonlinear equations. These equations were solved using subroutine HYBRD from MINPACK-1 package of subprograms [17]. This subroutine utilizes combination of Newton and scaled gradient directions method with Jacobian approximated with forward differences at the starting guess. This is very proven software and highly optimized and requires very small computational times.

A large number of calculations were performed to examine the effects of fin spacing, fin height, wall heat flux, stack height, inlet-outlet losses, and surface emissivity. Results are summarized in Table 4.5. The corresponding results for the case of smooth channel are presented in Table 4.1. Comparison between Table 4.5 and the results given in Table 4.1 for the smooth channel indicates that under all conditions studied in the analysis, heat loss occurs mainly on the guard-vessel side since $\overline{T}_{GV}$ is much higher than $\overline{T}_{D}$. Placing the fins on the duct wall would actually have negative effects (relative to the case of smooth channel) on the overall performance of the RVACS air cooling system. This is true as long as Ω is not larger than 0.8. Physically this is attributed to the fact that the air flow rate would decrease substantially due to the increase in wall friction by placing the

fins on the duct wall. The slight increase in the heat removal capacity on the duct-wall side is more than offset by the drop in the heat transfer coefficient for the guard-vessel wall. Additional calculations not reported here indicate that for a high value of the loss parameter Ω there is some benefit to placing the fins on the duct wall. A high Ω results in low velocities and correspondingly low heat transfer coefficients and high duct wall temperatures.

Table 4.1 Parametrics for Smooth RVACS Channel--Design Option A

Case No.	H(m)	Q_w (kW/m^2)	L_s (m)	L_h (m)	Ω	ε	U (m/s)	Ta (K)	$\bar{T}_R$(K)	T_{GVO} (K)	T_{GV} (K)	T_{DO} (K)	T_D (K)	h (W/m^2-K)
1	0.3048	10.0	15.24	12.192	0.5	0.7	10.0	326	818	571	605	398	431	26
2	0.2540	"	"	"	"	"	9.9	334	817	566	607	395	435	27
3	0.4572	"	"	"	"	"	10.4	314	820	582	604	407	429	25
4	0.3048	5.0	"	"	"	"	7.8	314	683	472	494	348	369	21
5	"	15.0	"	"	"	"	11.6	336	911	647	690	450	493	29
6	"	20.0	"	"	"	"	12.9	345	987	711	763	501	553	32
7	"	10.0	7.62	"	"	"	8.5	332	827	594	633	428	467	23
8	"	"	22.86	"	"	"	11.2	323	811	556	586	381	410	28
9	"	"	15.24	"	0.0	"	12.9	319	805	538	563	362	388	32
10	"	"	"	"	0.4	"	10.7	324	814	562	593	387	419	27
11	"	"	"	"	0.8	"	7.2	339	840	620	666	467	513	20
12	"	"	"	"	0.5	0.5	10.0	326	904	593	626	376	409	26
13	"	"	"	"	"	0.6	"	326	857	582	615	387	421	26
14	"	"	"	"	"	0.8	"	326	783	562	595	407	441	26
15	"	"	"	"	"	1.0	"	326	724	544	577	425	458	26
16	"	"	"	3.048	"	0.7	9.2	302	819	587	596	410	419	24
17	"	"	"	6.096	"	0.7	9.5	311	818	581	599	405	423	25
18	"	"	"	9.144	"	0.7	9.8	319	818	576	602	402	427	26

Note: Above values based on air inlet temperature of 293 K.

Table 4.2 Comparative Results Summary for Both Wall Rough vs. Smooth Channel-Method 1 (see Section 3.2)

H			E	P		$\overline{T}_{GV}$	$\Delta\overline{T}_{GV}$	$\overline{T}_D$	$\overline{T}_a$	h	
m	P/E	e^+	mm	mm	G_R/G_S	K	K	K	K	$W/m^2.K$	hR/hs
0.254	Smooth surface			-	1.00	682	0	540	326	18.9	-
0.254	10	53	2.39	23.9	0.61	664	18	516	348	22.2	1.17
0.254	20	53	2.45	49.0	0.66	668	14	521	344	21.5	1.14
0.254	40	52	2.53	101.2	0.73	673	9	528	339	20.6	1.09
0.381	Smooth surface			-	1.00	686	0	542	314	18.0	0
0.381	10	49	2.28	22.8	0.63	664	22	514	327	20.5	1.14
0.381	20	49	2.34	46.8	0.68	669	17	506	325	19.9	1.11
0.381	40	48	2.41	96.4	0.74	676	10	530	322	19.1	1.06

Table 4.3 Comparative Results Summary for Both Walls Rough vs. Smooth Channel-Method 2*

H m	P/E	e^+	E mm	P mm	G_R/G_S	$\bar{T}_{GV}$ K	$\Delta\bar{T}_{GV}$ K	$\bar{T}_D$ K	$\bar{T}_a$ K	h $W/m^2.K$	hR/hs
0.254	Smooth surface			-	1.00	721	0	599	342	16.9	-
0.254	10	50	2.39	23.9	0.62	663	58	519	361	23.4	1.38
0.254	20	"	2.54	49.0	0.67	666	55	522	358	22.7	1.34
0.254	40	"	2.52	101.2	0.74	671	50	527	353	21.9	1.30
0.381	Smooth surface			-	1.00	725	0	602	331	16.2	-
0.381	10	50	2.28	22.8	0.65	659	66	509	341	22.1	1.36
0.381	20	"	2.34	46.8	0.69	664	61	515	340	21.6	1.33
0.381	40	"	2.41	96.4	0.76	668	57	521	337	20.9	1.29

*Method of R. Webb (consultant) to be reported separately.

Table 4.4 Roughness on One Wall vs. Two Walls

H m	P/E	e^+	E mm	P mm	G_R/G_S	$\overline{T}_{GV}$ K	$\Delta\overline{T}_{GV}$ K	$\overline{T}_D$ K	Case
0.254	Smooth surface			-	1.00	721	0	599	Smooth
0.254	10	59	2.82	28.2	0.58	656	65	581	Both rough
0.254	10	75	2.82	28.2	0.70	674	47	535	One rough
0.381	Smooth surface			-	1.00	725	0	602	Smooth
0.381	10	118	4.23	42.3	0.57	661	64	512	Both rough
0.381	10	119	4.23	42.3	0.69	668	57	574	One rough

Table 4.5 Parametrics for Fins on Duct Wall-Design Option D

Remarks	Case No.	H(m)	S(m)	Q_w (kW/m^2)	L_s(m)	L_h(m)	Ω	ε	U (m/s)	Ta (K)	T_R (K)	T_{GVO} (K)	T_{GV} (K)	T_{FO} (K)	T_F (K)	T_{DO} (K)	T_D (K)	h (W/m^2-K)
Base case (H=12")	1	0.3048	0.3048	10	15.24	12.192	0.5	0.7	7.32	339	818	566	611	344	389	349	395	23.3
H=10"	2	0.254	0.254	"	"	"	"	"	7.2	349	818	560	616	342	398	347	402	23.8
H=18"	3	0.4572	0.4572	"	"	"	"	"	7.59	322	819	576	605	347	376	354	383	22.1
S=H/2	4	0.3048	0.1524	"	"	"	"	"	6.09	348	822	571	626	324	378	352	406	21.8
S=2H	5	"	0.6096	"	"	"	"	"	8.34	333	818	568	608	371	411	350	390	24.4
Q_W=5	6	"	0.3048	5	"	"	"	"	5.69	322	685	473	502	320	349	322	352	19.0
Q_W=15	7	"	"	15	"	"	"	"	8.48	352	910	634	693	367	426	376	435	26.2
Q_W=20	8	"	"	20	"	"	"	"	9.42	364	982	690	760	391	462	402	473	28.5
L_S=75'	9	"	"	10	22.86	"	"	"	8.18	334	813	555	595	335	376	340	381	25.4
L_S=25'	10	"	"	"	7.620	"	"	"	6.23	346	825	581	634	358	411	364	418	20.5
L_H=30'	11	"	"	"	15.24	9.144	"	"	7.50	326	815	565	599	341	374	346	379	23.8
L_H=20'	12	"	"	"	"	6.096	"	"	7.68	315	813	565	587	339	360	343	365	24.2
L_H=10'	13	"	"	"	"	3.048	"	"	7.85	304	811	565	575	337	347	340	351	24.6
Ω=0	14	"	"	"	"	12.192	0.0	"	9.42	328	807	540	575	326	362	331	366	28.5
Ω=0.4	15	"	"	"	"	"	0.4	"	7.82	336	815	559	602	338	381	344	386	24.5
Ω=0.8	16	"	"	"	"	"	0.8	"	5.24	357	834	597	660	376	440	384	447	17.8
ε=0.5	17	"	"	"	"	"	0.5	0.5	7.32	339	905	592	637	336	381	339	384	23.3
ε=0.6	18	"	"	"	"	"	"	0.6	7.32	339	858	578	623	340	385	344	390	23.3
ε=0.8	19	"	"	"	"	"	"	0.8	7.32	339	783	555	600	347	392	353	399	23.3
ε=1.0	20	"	"	"	"	"	"	1.0	7.32	339	723	536	581	352	398	361	407	23.3
H=6"	21	0.1524	0.1524	"	"	"	"	0.7	6.87	390	819	544	641	339	437	342	439	25.4
Copper fin	22	0.3048	0.3048	"	"	"	"	0.7	7.32	339	818	566	611	345	391	346	391	23.3

For Cases 1-21 the fin conductivity is equal to that of stainless steel.

Table 4.6

Nomenclature (for Tables 4.1 to 4.5 and A.3.1 and A.3.2)

E = Rib height (mm).

e^+ = Surface roughness parameter--see Ref. 2.

G_R = Air mass flow rate for rough surface ($kg/s.m^2$).

G_s = Air mass flow rate for smooth surface ($kg/s.m^2$).

H = Fin height or channel spacing (m).

h = Convective heat transfer coefficient (W/m^2-K).

L_h = Heated height of RACS (m).

L_s = Stack height (m).

$L_h + L_s = L$ = total height of RACS (m).

P = Rib pitch (mm).

Q_w = RACS heat flux (W/m^2).

S = Azimuthal distance between fins (m).

T_a = Exit air temperature (K).

$\overline{T}_a$ = Axially averaged air temperature (K).

T_{DO} = Duct wall temperature at entrance (K).

T_D = Duct wall temperature at exit (K).

$\overline{T}_D$ = Axially averaged duct wall temperature (K).

T_{FO} = Fin temperature at base (K).

T_F = Fin temperature at the exit (K).

T_{GVO} = Guard vessel temperature at entrance (K).

T_{GV} = Guard vessel temperature at exit (K).

$\overline{T}_{GV}$ Axially averaged guard vessel temperature (K).

$\Delta\overline{T}_{GV}$ = Reduction in average guard vessel temperature relative to smooth surface (K).

$\overline{T}_R$ = Axially averaged reactor vessel temperature (K).

U = Air velocity (m/s).

ε = Surface emissivity.

Ω = Pressure loss parameter.

5. SIMPLIFIED CASES -- BOUNDING CALCULATION

If we consider the flow channel as an enclosure of three gray surfaces (i.e., the guard-vessel wall, the fins, and the duct wall) exchanging radiant energy with one another, there will be three surface resistances and three spatial resistances. Using the electric analog for a three-surface gray enclosure, it can be shown that maximum radiation cooling occurs when the effect of multi-reflection is neglected. Also, we shall assume that the fin temperature can be expressed in terms of its base temperature by $T_F = T_a + \eta (T_b - T_a)$, where η is assumed to be given with a maximum value of unity. Thus bounding calculations may be performed for designs C and D.

5.1 Design Option C -- Fins on the Guard Vessel Only

If the effect of multi-reflection is neglected, Eqs. (3-28) to (3-37) reduces to

$$Q_w = h\left[\left(1 + 2\frac{H}{S}\eta\right)\left(T_{GV} - T_a\right) + \left(T_D - T_a\right)\right] \tag{5-1}$$

$$\frac{\sigma(\overline{T}_{GV}^4 - \overline{T}_D^4)}{\frac{1}{\varepsilon_{GV}} + \frac{1}{\varepsilon_D} + \frac{1}{F_{GD}} - 2} + \frac{2H\sigma(\overline{T}_F^4 - \overline{T}_D^4)}{S\left[\frac{1}{\varepsilon_F} - 1 + \frac{H}{S}\left(\frac{2}{1 - F_{GD}} + \frac{1}{\varepsilon_D} - 1\right)\right]} = h(T_D - T_a) \tag{5-2}$$

where $\overline{T}_{GV}$, $\overline{T}_D$, and $\overline{T}_F$ are given by Eqs. (3-38). Once $T_{GV}(z)$ and $T_D(z)$ are determined from Eqs. (5-1) and (5-2), $\overline{T}_R$ can be obtained from Eq. (3-17). To facilitate the task of numerical solution, it is desirable to expand T_{GV} and T_D in series of z:

$$T_{GV} = a_{GV} + b_{GV} z + c_{GV} z^2 + d_{GV} z^3 + \ldots . \tag{5-3}$$

$$T_D = a_D + b_D z + c_D z^2 + d_D z^3 + \ldots . \tag{5-4}$$

where the various coefficients are functions of Q_w, H, S, η, L_h, L, T_o, T_∞, Ω, and the material properties including ε_{GV}, ε_D, and ε_F. Substituting these expressions into Eqs. (3-38), we have

$$\bar{T}_{GV} = a_{GV} + \frac{1}{2} b_{GV} L_h + \frac{1}{3} c_{GV} L_h^2 + \frac{1}{4} d_{GV} L_h^3 + \ldots . \tag{5-5}$$

$$\bar{T}_D = a_D + \frac{1}{2} b_D L_h + \frac{1}{3} c_D L_h^2 + \frac{1}{4} d_D L_h^3 + \ldots . \tag{5-6}$$

$$\bar{T}_F = \eta a_{GV} + (1 - \eta) \left[T_o + Q_w L_h / 2\rho c_p u H\right] \cdot$$

$$+ \eta\left[\frac{1}{2} b_{GV} L_h + \frac{1}{3} c_{GV} L_h^2 + \frac{1}{4} d_{GV} L_h^3 + \ldots .\right] \tag{5-7}$$

We note from Eq. (3-4) that the air temperature, T_a, is a linear function of z in the heated section. It can be shown from Eqs. (5-1) and (5-2) that the following relations must be satisfied by the various coefficients:

$$a_D - T_o + \left(1 + 2 \frac{H}{S} \eta\right) \left(a_{GV} - T_o\right) = Q_w / h \tag{5-8}$$

$$b_{GV} = b_D = Q_w/\rho c_p uH \tag{5-9}$$

$$h(a_D - T_o)/\sigma = \frac{(a_{GV} + \frac{1}{2} b_{GV} L_h)^4 - (a_D + \frac{1}{2} b_{GV} L_h)^4}{\frac{1}{\varepsilon_{GV}} + \frac{1}{\varepsilon_D} + \frac{1}{F_{GD}} - 2}$$

$$+ 2 \frac{H}{S} \frac{[\frac{1}{2} b_{GV} L_h + \eta a_{GV} + (1 - \eta) T_o]^4 - (a_D + \frac{1}{2} b_{GV} L_h)^4}{\frac{1}{\varepsilon_F} + \frac{H}{S} (\frac{2}{1 - F_{GD}} + \frac{1}{\varepsilon_D} - 1) - 1} \tag{5-10}$$

$$C_{GV} = d_{GV} = \ldots = 0 \quad \text{and} \quad C_D = d_D = \ldots = 0 \tag{5-11}$$

Once F_{GD} is given, a_{GV}, a_D, b_{GV}, and b_D can be determined from which $T_{GV}(z)$ and $T_D(z)$ can be obtained. Note that in the 1-D model, the wall temperatures are linear functions of z as long as Q_w is a constant.

5.2 Design Option D -- Fins on the Duct Wall Only

Following the same analysis as the one described in the preceding section, we have

$$a_{GV} - T_o + (1 + 2 \frac{H}{S} \eta) (a_D - T_o) = Q_w/h \tag{5-12}$$

$$b_{GV} = b_D = Q_w/\rho c_p uH \tag{5-13}$$

$$h\left(1 + 2\frac{H}{S}\eta\right)(a_D - T_o)/\sigma = \frac{(a_{GV} + \frac{1}{2} b_{GV} L_h)^4 - (a_D + \frac{1}{2} b_{GV} L_h)^4}{\frac{1}{\varepsilon_{GV}} + \frac{1}{\varepsilon_D} + \frac{1}{F_{GD}} - 2}$$

$$+ \frac{(a_{GV} + \frac{1}{2} b_{GV} L_h)^4 - [\frac{1}{2} b_{GV} L_h + \eta a_D + (1 - \eta) T_o]^4}{\frac{1}{\varepsilon_{GV}} + \frac{2}{1 - F_{GD}} - 1 + \frac{S}{H}(\frac{1}{\varepsilon_F} - 1)} \tag{5-14}$$

$$C_{GV} = d_{GV} = \ldots = 0 \quad \text{and} \quad C_D = d_D = \ldots = 0 \tag{5-15}$$

Again, a_{GV}, a_D, b_{GV}, and b_D can be determined once F_{GD} is given. The wall temperatures can be obtained from Eqs. (3-17) and (3-38). The results for the three design options are presented in Table (5-1).

Table 5-1 Parametrics for Finned Channels

Design Options	H(m)	Q_w (kW/m^2)	L_s (m)	L_h (m)	S (m)	U (m/s)	Ta (K)	T_{GVO} (K)	T_{GV} (K)	T_{DO} (K)	T_D (K)
C	0.254	10.0	15.24	12.19	0.254	11.7	350	407	446	330	369
D	0.254	10.0	15.24	12.19	0.254	11.7	350	550	589	337	380
C	0.381	10.0	15.24	12.19	0.381	13.4	334	402	425	328	351
D	0.381	10.0	15.24	12.19	0.381	13.4	334	545	457	335	358
C	0.254	21.0	15.24	12.19	0.254	14.4	375	468	532	364	428
D	0.254	21.0	15.24	12.19	0.254	14.4	375	660	724	368	432
C	0.254	10.0	7.62	12.19	0.254	9.9	357	417	462	343	389
D	0.254	10.0	7.62	12.19	0.254	9.9	357	558	604	345	391
C	0.254	10.0	15.24	12.19	0.127	9.7	360	376	424	318	366
D	0.254	10.0	15.24	12.19	0.127	9.7	360	542	590	333	381
C	0.381	10.0	15.24	12.19	0.191	11.2	339	372	399	319	346
D	0.381	10.0	15.24	12.19	0.191	11.2	339	537	564	332	359

6. DISCUSSION OF THE ANALYTICAL RESULTS

6.1 Major Findings

From the results presented in Sections 4 and 5, the following conclusions can be drawn:

(1) Indications to date are that repeated rib roughness provides some benefit to reducing reactor vessel temperatures provided that the ribs are smaller than 5 mm. For large ribs, reduced air flow effectively cancels the benefit of increase in heat transfer coefficient. Placing the ribs on the guard vessel alone would not improve the performance compared to the case with ribs on both the guard vessel and the duct wall. Further studies are needed.

(2) Preliminary results for fins on the duct wall with Ω not larger than 0.8 show marginal or no improvement in performance over a smooth channel. Fin efficiency is low unless high conductivity material is used for the fins. However, additional calculations not presented show that for the case of high Ω (high inlet and exit losses), fins can have significant impact on reactor vessel temperature.

(3) Reactor vessel temperatures are weakly influenced by air-side temperatures. On the other hand, heat flux levels and/or surface emissivities have strong effects.

(4) Outlet air temperature may be lowered by increasing the flow area, i.e., by increasing fin spacing, S, and fin height, H.

(5) The guard-vessel temperature may be lowered by increasing the effective heat transfer area, i.e., by increasing the ratio H/S.

(6) Both the outlet air temperature and the guard-vessel temperature, T_{GV}, increase with Q_w according roughly to $(Q_w)^m$ were $m \simeq 0.6$ based upon a rough fit to the preliminary numerical results. This can

also be derived from equations (3-4) and (3-14) noting the fact that $(T_{GV}-T_a)$ is a constant based upon the present model.

(7) Assuming steady-state surface-to-surface radiation heat transfer between the reactor vessel and the guard vessel, the reactor-vessel temperature can be shown to vary with Q_w according to

$$T_r \sim Q_w^n, \quad 0.25 < n < 0.6$$

(8) The wall temperatures are not sensitive to the stack height as long as the stack height is comparable to the heated length. Increasing the stack height would only slightly decrease the outlet air temperature and moderately increase the air flow rate.

(9) Decreasing the inlet air temperature would moderately lower the air flow rate and the wall temperatures.

(10) The flow is highly turbulent since the Reynolds number is of the order of 1×10^5 in all the cases studied. The entrance effect which has been ignored can be important and will further lessen the guard vessel temperature; however, the effect on the reactor vessel temperatures will not be as large.

(11) Factors such as local buoyancy (see below), increasing stack height, and reducing Ω improve the performance of smooth channel and make it less attractive to consider the use of fins or ribs.

6.2 Discussion of Assumption--Need for Future Work

Two important quantities that need to be accurately predicted in the evaluation of air-side RVACS performance are the air flow rate and the convective heat flux from the channel wall to the air draft. In the foregoing analysis these two quantities are expressed in terms of the friction factor and the heat transfer coefficient, respectively. The flow is assumed to be

symmetrical along the centerline of the channel and the heat transfer coefficient is assumed to be the same for both the guard vessel and the duct wall. By further assuming that the flow is fully developed and that the effect of local buoyancy is negligible, the friction factor and the heat transfer coefficient are obtained directly from the correlations for turbulent forced convection in fully developed channel flow such as those given in [2,13]. For a typical radial heat flux of ~ 10 kW/m^2 that is required to balance the decay power at 24 hours and for a typical channel width of ~ 0.3 m, the present results indicate that the average air velocity is 5 to 10 m/s for low entrance and exit losses ($\Omega \sim 0.5$), the average guard vessel temperature is of the order of ~ 600 K, the average duct wall temperature is of the order of ~ 400 K, and the air temperature ranges from 320 K to ~ 360 K at the outlet. Evidently, the flow is highly turbulent since the Reynolds number is of the order of $Re \sim 1 \times 10^5$.

It is known that a fully developed flow can be expected in a channel only if $L/D_h \gg 10$ where L is the length of the flow channel and D_h is the hydraulic diameter. This condition, however, is not met in the RVACS air cooling system since L has a typical value of 12 m and D_h has a typical value of 0.6 m. On the other hand, the local buoyancy effect can be neglected only if $Gr \ll Re^2$ where Gr is the Grashof number of the flow. From the results presented in previous sections, it can be shown that Gr is of the order of 1×10^{10}, or $Gr \sim Re^2$. This implies that the local buoyancy has important effect on the flow. Since the guard vessel temperature is much higher than the duct wall temperature, the velocity profile is not symmetrical but skewed. A much higher local velocity can be expected near the guard vessel wall. As a result, the heat transfer coefficient for the guard vessel can be much higher than the heat transfer coefficient for the duct wall. Consequently, the

present results may underpredict the shutdown heat removal capacity of the system. A realistic modeling of the air-side RVACS dictates the study of the local buoyancy and the entrance effects. This is supported by the results in HEDL IDS experiments [18] which indicate an increase in heat transfer coefficient over forced flow correlations. A 3-D formulation of the problem is given in the next section.

7.0 FUTURE EXTENSION

7.1 Modeling of Heat Transfer Coefficient, Wall Friction and Fin Efficiency

The analyses to date have allowed for evaluation of the numerous design options and the selection of the most promising options. The analyses have several deficiencies such as noted in Section 6.0 that need to be addressed. The purpose of this section is to address future modeling effort by ANL to allow a detailed evaluation. The analysis is presented for fins on the guard vessel but it is equally applicable to fins on the duct wall or a smooth channel.

The study of heat transfer from finned surfaces is traditionally carried out by one-dimensional approximations provided of course one has a prior knowledge of heat transfer coefficients. For forced convection flows the study of heat transfer coefficients, though highly empirical, is more extensive than for the natural convection flows. Natural convection flows with radiation heat transfer are more geometry dependent than forced convection flows. There appears to be neither experimental nor analytical studies available that could be extended to study heat transfer in combined natural convection and radiation modes from longitudinal fins in RVACS configurations.

The natural convection flows pertaining to RVACS are driven by density differential (between the ambient air and that in RVACS cylinder outside the guard vessel) caused by heat loss from the guard vessel along its height. However, the maximum temperature that air in RVACS passage outside the guard vessel can attain depends significantly on its geometry, such as on the presence or the absence of fins or roughness. Because of the fairly small driving force in these natural convection flows, the frictional characteristics of the passages become very important. Consequently, it is very

important to the design and functioning of RVACS system that thermal and flow characteristics of RVACS passages are adequately known.

To achieve adequate rates of heat transfer to the air some form of designed augmentation of heat transfer such as through the use of fins may be needed in RVACS passages. However, if longitudinal fins are used then in the presence of turbulent flow the local heat transfer between the fluid and the fin surface and the guard vessel or duct wall may be dominated by the secondary flows which are generated by Reynolds stress gradients acting in the corner regions between the fin surfaces and guard or duct wall. These secondary flows will also significantly affect the efficiency of fins as well. These secondary flows can lead to formation of "hot spots" in the corner regions. Consequently, it is of primary importance that we are able to predict local flows and heat transfer behavior. A further complication that arises in RVACS configurations is the presence of the radiation mode of heat transfer which is very comparable in magnitude to the convection mode. Although the air is transparent to the radiation, the surfaces present in the RVACS passage interact very significantly with this mode of energy transfer. Consequently, the effect of radiation must be accounted for in studying conduction through the fins for the purposes of determining fin efficiency and heat transfer to the air.

In determining frictional and heat transfer characteristics of the surfaces in three-dimensional flows including the effect of buoyancy one needs to analyze the behavior near the walls. Since these flows are "recirculating" in nature, they are consequently, elliptic, that is, there is strong coupling between velocity and pressure fields. In dealing with behavior near the wall a finer grid to cover the low-Reynolds-number region is not practical in an elliptic flow, as the coupling between velocity and pressure requires an

iterative solution. This in turn implies considerably greater computer times (about two-orders of magnitude greater than for a parabolic problem such as three-dimensional boundary layers) and considerably greater storage requirements. The traditional approach through the use of wall functions is not suitable for buoyancy driven flows because the determination of wall functions is made through a mixture of analysis and experimental data. Such a recourse is not available for buoyancy driven flows because of complete lack of data and analyses near the wall for systems even remotely similar to RVACS passages. In fact, even for flows that are forced driven, the universal behavior of these wall functions is not guaranteed. Consequently, an alternative approach for analyzing behavior near the wall must be adopted for buoyancy driven flows. Very recently a scheme has been devised by Iacovides and Launder [19] in which the region near the wall is parabolized by neglecting the variation of pressure adjacent to a wall where low Reynolds numbers prevail. Consequently, it is not required to solve for the pressure and the use of finer mesh becomes practicable.

7.2 Governing Equations for Heat Transfer Coefficient and Friction Factor

Since buoyancy driven flows are very geometry dependent, we can utilize experimental data if available for a given configuration of the flow passage, to determine heat transfer coefficients and friction factors. However, their extension to another configuration such as accomplished by varying fin design or varying surface roughness is highly questionable. In design studies, one invariably needs to perform optimization studies. Such studies are not feasible, unless one devises "universally applicable" analytical tools which have sound physical basis and have been experimentally verified for a number of passage configurations. It is with this objective we propose the following analysis.

The presence of fins renders the flow to be three dimensional. However, a considerable simplification can be made by recognizing that the flow is predominant in the vertical direction along which diffusion of momentum and energy can be neglected. In the spirit of these observations, it is plausible to assume that the flow is parabolic in nature along the longitudinal or vertical direction, and elliptic in the two cross stream directions. These simplifications were first introduced by Patankar and Spalding [20]. Since then a number of other works have successfully utilized these assumptions in calculating a wide varity of three-dimensional flows; see for example Refs. [21,22]. This assumption implies that the pressure P can be written as [21]

$$P(r,\theta,z) = \bar{p}(z) + p(r,\theta) \tag{7-1}$$

where $\bar{p}$ is the pressure averaged over the duct cross section and p is the small pressure variation in the two cross-stream directions. Let u, v and w be the time averaged velocity components in the r, θ and z cylindrical coordinate system shown in Fig. 7.1. Let T be the temperature and u', v', and w' be the fluctuating components of velocity in r, θ and z directions. In view of previous discussions the governing equations can be written as

continuity:

$$\frac{1}{r}\frac{\partial}{\partial r}(ru) + \frac{1}{r}\frac{\partial v}{\partial \theta} + \frac{\partial w}{\partial z} = 0 \tag{7-2}$$

r-momentum

$$u\frac{\partial u}{\partial r} + \frac{v}{r}\frac{\partial u}{\partial \theta} + w\frac{\partial u}{\partial z} = -\frac{1}{\rho}\frac{\partial p}{\partial r} + \nu\left(\frac{\partial^2 u}{\partial r^2} + \frac{1}{r}\frac{\partial u}{\partial r} + \frac{1}{r^2}\frac{\partial^2 u}{\partial \theta^2} - \frac{u}{r^2} - \frac{2}{r^2}\frac{\partial v}{\partial \theta}\right) - \frac{1}{r}\frac{\partial}{\partial r}\overline{ru'^2} - \frac{1}{r}\frac{\partial}{\partial \theta}\overline{u'v'} + \frac{\overline{v'^2}}{r} \tag{7-3}$$

θ-momentum

$$u\frac{\partial v}{\partial r} + \frac{v}{r}\frac{\partial v}{\partial \theta} + w\frac{\partial v}{\partial z} + \frac{uv}{r} = -\frac{1}{\rho r}\frac{\partial p}{\partial \theta} + \nu\left(\frac{\partial^2 v}{\partial r^2} + \frac{1}{r}\frac{\partial v}{\partial r} + \frac{1}{r^2}\frac{\partial^2 v}{\partial \theta^2}\right.$$

$$\left. - \frac{v}{r^2} + \frac{2}{r^2}\frac{\partial u}{\partial \theta}\right) - \frac{1}{r}\frac{\partial \overline{v'^2}}{\partial \theta} - \frac{\partial \overline{v'u'}}{\partial r} - 2\frac{\overline{u'v'}}{r} \qquad (7\text{-}4)$$

z-momentum

$$u\frac{\partial w}{\partial r} + \frac{v}{r}\frac{\partial w}{\partial \theta} + w\frac{\partial w}{\partial z} = -\frac{1}{\rho}\frac{\partial \bar{p}}{\partial z} + \nu\left[\frac{\partial^2 w}{\partial r^2} + \frac{1}{r}\frac{\partial w}{\partial r} + \frac{1}{r^2}\frac{\partial^2 w}{\partial \theta^2}\right]$$

$$- \frac{1}{r}\frac{\partial r\overline{u'w'}}{\partial r} - \frac{1}{r}\frac{\partial \overline{v'w'}}{\partial \theta} - g \qquad (7\text{-}5)$$

energy

$$u\frac{\partial T}{\partial r} + \frac{v}{r}\frac{\partial T}{\partial \theta} + w\frac{\partial T}{\partial z} = \alpha\left[\frac{1}{r}\frac{\partial}{\partial r}\left(r\frac{\partial T}{\partial r}\right) + \frac{1}{r^2}\frac{\partial^2 T}{\partial \theta^2}\right] - \frac{1}{r}\frac{\partial\, \overline{ru'T'}}{\partial r} - \frac{1}{r}\frac{\partial\, \overline{v'T'}}{\partial \theta} \qquad (7\text{-}6)$$

The overall mass conversation is given as

$$\rho w dA = \dot{m} = \text{constant} = \rho_o w_o A \qquad (7\text{-}7)$$

In arriving at the above equations we have neglected both laminar and turbulent diffusion in z-direction keeping in with our previous discussions.

Traditionally the closure law for turbulent quantities for ducts has been specified through use the k~ε model which require solution of two additional partial differential equations describing transport of turbulent kinetic energy and dissipation. However, an algebraic model proposed by Gessner and Emergy [23] for square ducts has had a considerable success in

predicting heat transfer in a square duct with constant-property incompressible flow. Since the geometry of square ducts bear similarity with the geometry formed with fins in RVACS passage, we propose to use their algebraic model together with the method proposed by Iacovides and Launder [19] for treatment of the wall region. Thus, various turbulent quantities occurring in Eqs. (7-2)-(7-6) are determined through the following algebraic model [23]:

$$\overline{u'^2} = -\frac{(2\,a_{12} + \gamma_1 - 2)}{\gamma_2}\,\ell_p^2\left(\frac{\partial w}{\partial r}\right)^2 + \frac{a_{12}\,\ell_p^2}{\gamma_2}\left[\left(\frac{\partial w}{\partial r}\right)^2 + \left(\frac{1}{r}\frac{\partial w}{\partial \theta}\right)^2\right] \tag{7-8}$$

$$\overline{v'^2} = -\frac{2\,a_{12} + \gamma_1 - 2}{\gamma_2}\,\ell_p^2\left(\frac{1}{r}\frac{\partial w}{\partial \theta}\right)^2 + \frac{a_{12}\,\ell_p^2}{\gamma_2}\left[\left(\frac{\partial w}{\partial r}\right)^2 + \left(\frac{1}{r}\frac{\partial w}{\partial \theta}\right)^2\right] \tag{7-9}$$

$$\overline{u'w'} = -\ell_p^2\frac{\partial w}{\partial r}\left[\left(\frac{\partial w}{\partial r}\right)^2 + \left(\frac{1}{r}\frac{\partial w}{\partial \theta}\right)^2\right]^{1/2} \tag{7-10}$$

$$\overline{v'w'} = -\ell_p^2\frac{1}{r}\frac{\partial w}{\partial \theta}\left[\left(\frac{\partial w}{\partial r}\right)^2 + \left(\frac{1}{r}\frac{\partial w}{\partial \theta}\right)^2\right]^{1/2} \tag{7-11}$$

$$\overline{u'v'} = -\frac{(2\,a_{12} + \gamma_1 - 2)}{\gamma_2}\,\ell_p^2\left(\frac{\partial w}{\partial r}\right)\left(\frac{1}{r}\frac{\partial w}{\partial \theta}\right) \tag{7-12}$$

The effects of buoyancy production of the various turbulent transport quantities have been ignored. Utilizing the definition of turbulent Prandtl number, scalar transport quantities can be written as

$$\overline{u'T'} = -\frac{\overline{u'w'}}{Pr_t}\frac{(\partial T/\partial r)}{(\partial w/\partial r)} \tag{7-13}$$

$$\overline{v'T'} = -\frac{\overline{v'w'}}{Pr_t}\frac{(\partial T/r\partial\theta)}{(\partial w/r\partial\theta)} \tag{7-14}$$

Here, $\ell_p(r,\theta,z)$ is the mixing length and is prescribed through an expression obtained by Gessner and Emergy [24] which gives its variation both in cross stream and axial directions. The various constants occurring in Eqs. (7-8)-(7-12) are given as [22]

γ_1	γ_2	a_{12}
0.94	0.26	0.535

Since the flow is driven by bouyancy only, we must represent this driving force by using Boussinesq model as

$$\rho_\infty = \rho[1 + \beta\ (T - T_\infty)] \tag{7-15}$$

where ρ_∞ is the density of the ambient fluid.

If p_∞ is the ambient (that is, in stagnant air outside) pressure at location z and p_o is fixed pressure such as at inlet to RVACS duct, we have the following relationship:

$$p_o = p_\infty + \rho_\infty\ g\ z \tag{7-16}$$

Let $\tilde{p}$ be pressure difference between cross section average pressure and ambient pressure p_∞ at some location z, we then have

$$\tilde{p} = \overline{p} - p_\infty \tag{7-17}$$

The use of Eq. (7-16) gives

$$\bar{p} = \tilde{p} + p_o - \rho_\infty g z \tag{7-18}$$

which gives

$$-\frac{1}{\rho}\frac{\partial \bar{p}}{\partial z} - g = -\frac{1}{\rho}\frac{\partial \tilde{p}}{\partial z} + \left(\frac{\rho_\infty - \rho}{\rho}\right)g \tag{7-19}$$

The substitution of Eq. (7-15) in Eq. (7-19) gives

$$-\frac{1}{\rho}\frac{\partial \bar{p}}{\partial z} - g = -\frac{1}{\rho}\frac{\partial \tilde{p}}{\partial z} + \beta g (T - T_\infty) \tag{7-20}$$

The substitution of Eq. (7-20) in Eq. (7-5) yields

$$u\frac{\partial w}{\partial r} + \frac{v}{r}\frac{\partial w}{\partial \theta} + w\frac{\partial w}{\partial z} = -\frac{1}{\rho}\frac{\partial \tilde{p}}{\partial z} + \beta g (T - T_\infty) + \nu\left[\frac{\partial^2 w}{\partial r^2} + \frac{1}{r}\frac{\partial w}{\partial r}\right.$$

$$\left. + \frac{1}{r^2}\frac{\partial^2 w}{\partial \theta^2}\right] - \frac{1}{r}\frac{\partial \overline{ru'w'}}{\partial r} - \frac{1}{r}\frac{\partial \overline{v'w'}}{\partial \theta} \tag{7-21}$$

The boundary conditions that these equations must satisfy are:

At the inlet to the duct (z = 0)

$$w(r,\theta,0) = w_o \tag{7-22}$$

$$u(r,\theta,0) = v(r,\theta,0) = 0 \tag{7-23}$$

$$\tilde{p}(0) = 0 \tag{7-24}$$

$$T(r,\theta,0) = T_o \tag{7-25}$$

At the duct outlet (z=L)

$$\tilde{p}(L) = 0 \tag{7-26}$$

At the fin surface and passage walls

$$u = v = w = 0 \tag{7-27}$$

$$-k \frac{\partial T_i}{\partial n} = q_{ci} = h(T_i - T_b) \tag{7-28}$$

where subscript i denotes a surface of the passage or fin surface (see Fig. 7.1), k is thermal conductivity of fluid, T_i is the fluid temperature at surface i, q_{ci} is the convective component of heat flux from a surface, and h is the heat transfer coefficient. The above equations complete the description of the problem on the fluid side. However, we still need to give the methodology for determining wall fluxes q_{wi} which also include the contribution from radiation interacting with surfaces. We may further mention that boundary conditions (7-22), (7-24) and (7-26) are not independent because of parabolization of equations in z direction. In other words, conditions at exit are not necessary if inlet flow w_o were known a priori. Since this is not the case, we utilize the additional condition at the exit to determine w_o. Assign some value to w_o, then determine the value of z at which $\tilde{p}$ becomes zero. When a series of runs have been made, one can readily deduce the value of w_o for a prescribed height L.

7.3 Heat Flux from Fins, Guard Vessel, and Duct Wall

Heat is transported from the guard vessel and the fins attached to it both by radiation to adjacent surfaces and by natural convection, that is,

$$q_{wi} = q_{ci} + q_{Ri} \tag{7-29}$$

where q_{Ri} is the radiation component of heat flux. In order to calculate these fluxes we make the following assumptions:

1. All surfaces are gray, diffuse and have constant radiation properties (i.e., emissivity ε_i of a surface i is independent of temperature) and the fluid is transparent to radiation.

2. Heat conduction through the fins, fin shrouds and guard vessel, is one-dimensional.

3. The thickness, b_G, of guard vessel is very small compared to the radius, R_G, of the guard vessel i.e. $b_G/R_G << 1$ and half thickness b_f of fins is small compared to height H of the fins, i.e., $b_f/H << 1$. Furthermore, the width (H+C) of the RVACS passage is small compared to $(R_s + R_G)/2$, i.e. $(H+C)/(R_s + R_G)/2 << 1$, where R_s is the radius of the duct wall, and C is the fin clearance. These assumptions permit us to neglect the currature effects on radiation and conduction calculations and we can treat the fins as if they are placed on a flat surface as shown in Fig. 7.2.

In view of the above assumptions, the governing equations are:

Guard Vessel

$$\frac{\partial^2 T_w}{\partial x^2} = 0 \tag{7-30}$$

with boundary conditions as

at $x = - b_G$

$$- k_w \left.\frac{\partial T_w}{\partial x}\right| = q_w \tag{7-31}$$

$$T_w(x=0) = T_1 \tag{7-32}$$

Fins

$$b_f K_2 \frac{\partial^2 T_2}{\partial x^2} = q_{2R}(x,z) + \bar{h} (T_2(x,z) - T_b) \tag{7-33}$$

where

$$q_{2R}(x,z) = B_2(x,z) - H_2(x,z) \tag{7-34}$$

$$B_2(x,z) = \varepsilon_2 \sigma T_2^4(x,z) + (1 - \varepsilon_2) H_2(x,z) \tag{7-35}$$

$$H_2(x,z) = \int_{A_4} B_4(x',z)\ dF_{d2-d4} + \int_{A_1} B_1(y,z)\ dF_{d2-d1}$$

$$+ \int_{A_3} B_3(y',z)\ dF_{d2-d3} \qquad (7\text{-}36)$$

$$B_1(y,z) = \varepsilon_1\ \sigma\ T_1^{\,4} + (1 - \varepsilon_1)\ H_1\ (y,z) \qquad (7\text{-}37)$$

$$H_1(y,z) = \int_{A_2} B_2(x,z)\ dF_{d1-d2} + \int_{A_3} B_3(y',z)\ dF_{d1-d3}$$

$$+ \int_{A_4} B_4(x',z)\ dF_{d1-d4} \qquad (7\text{-}38)$$

$$B_3(y',z) = \varepsilon_3\ \sigma\ T_3^{\,4} + (1 - \varepsilon_3)\ H_3(y',z) \qquad (7\text{-}39)$$

$$H_3(y',z) = \int_{A_2} B_2(x,z)\ dF_{d3-d2} + \int_{A_4} B_4(x',z)\ dF_{d3-d4}$$

$$+ \int_{A_1} B_1(y,z)\ dF_{d3-d1} \qquad (7\text{-}40)$$

$$B_4(x',z) = B_2(x,z) \quad \text{when} \quad x' = x \qquad (7\text{-}41)$$

$$\bar{h} = \int_{\substack{\text{wetted} \\ \text{perimeter}}} h\ d\ s \qquad (7\text{-}42)$$

ds is the elemental perimeter of the passage as shown in Fig. 2.

The boundary conditions that Eq. (7-33) must satisfy are

$$-\frac{S}{2} K_w \left.\frac{\partial T_w}{\partial x}\right|_{x=0} = -b_f K_2 \left.\frac{\partial T_2}{\partial x}\right|_{x=0} + \bar{h} (T_1 - T_b) + q_{1R} \tag{7-43}$$

$$-k \left.\frac{\partial T_2}{\partial x}\right|_{x=H} = \bar{h} (T - T_b) + (B_T - H_T) \tag{7-44}$$

where

$$q_{1R} = B_1 - H_1 \tag{7-45a}$$

$$B_T = \varepsilon_2 \sigma T^4 + (1 - \varepsilon_2) H_T \tag{7-45b}$$

$$H_T = \int_{A_3} B_3(y',z) \, dF_{dA_T - dA_3} \tag{7-46}$$

Here subscript T denotes tip and $B_3(y',z)$ is given by Eq. (7-39).

7.4 Fin Efficiency and Effectiveness

Fin efficiency η is defined as ratio of the actual fin heat dissipation to that from an ideal fin whose temperature is at the same as the base (i.e. if the fin had an infinite thermal conductivity). Thus

$$\eta = \frac{\int_{L_h} Q_f \, dz}{\int_{L_h} Q_{ideal} \, dz} + \frac{-k_2(2 b_f) \int \left.\frac{dT}{dx}\right|_{x=0} dz}{\int Q_{ideal} \, dz} \tag{7-47}$$

where Q_{ideal} is the heat loss from the fin when $T_2 = T_1$ (base temperature)

$$Q_{ideal} = \int [2H \bar{h}(T_2 - T_a) + 2H(B_2^0 - H_2^0)] \, dz \tag{7-48}$$

$$B_2^0 = \varepsilon_2 \sigma T_1^4 + (1 - \varepsilon_2) H_2^0 \tag{7-49}$$

$$H_2^0 = \int_{A_1} B_1 \, dF_{d2-d1} + \int_{A_4} B_4^0 \, dF_{d2-d4} + \int_{A_3} B_3 \, dF_{d2-d3} \tag{7-50}$$

$$B_4^0 = B_2^0 \tag{7-51a}$$

$$dF_{d2-d4} = dF_{d4-d2} \tag{7-51b}$$

$$B_1^0 = \varepsilon_1 \sigma T_1^4 + (1 - \varepsilon_1) H_1^0 \tag{7-52}$$

$$H_1^0 = \int_{A_2} B_2^0 \, dF_{d1-d2} + \int_{A_4} B_4^0 \, dF_{d1-d4} + \int_{A_3} B_3 \, dF_{d1-d3}$$

or

$$H_1^0 = 2 \int_{A_2} B_2^0 \, dF_{d1-d2} + \int_{A_3} B_3 \, dF_{d1-d3} \tag{7-53}$$

$$B_3^0 = \varepsilon_3 \sigma T_3^4 + (1 - \varepsilon_3) H_3^0 \tag{7-54}$$

$$H_3^0 = \int_{A_1} B_1 \, dF_{d3-d1} + 2 \int_{A_2} B_2^0 \, dF_{d3-d2} \tag{7-55}$$

The use of Eq. (7-51a) in Eq. (7-50) gives

$$H_2^0 = \int_{A_1} B_1 \, dF_{d2-d1} + \int_{A_4} B_2^0 \, dF_{d2-d4} + \int_{A_3} B_3 \, F_{d2-d3} \tag{7-56}$$

Equations (7-49)-(7-56) allow us to determine radiosities B_i° and irradiations H_i° for all surfaces. Equation (7-47) can also be recast as

$$\eta = \frac{\bar{h} \int \{ \int_0^H (T_2(x,z) - T_a)\, dx + \int_0^H [B_2(x,z) - H_2(x,z)]\, dx \}\, dz}{\bar{h} \int [(T_1 - T_a) + (B_2^0 - H_2^0)]\, dz} \tag{7-57}$$

Fin system effectiveness ξ is given as

$$\xi = \frac{\int_{L_h} Q_f\, dz}{\int_{L_h} Q_w\, dz} \tag{7-58}$$

where Q_w is total heat dissipation without fins and is given as

$$Q_w = \{S[(B_1 - H_1) + \bar{h}\,(T_1 - T_b)]\}\, dz \tag{7-59}$$

Equation (7-58) can then be written as

$$\xi = \frac{\bar{h} \int \{ \int_0^H [T_2(x,z) - T_a]\, dx + \int_0^H [B_2(x,z) - H_2(x,z)]\, dx \}\, dz}{\int \{S\,[\bar{h}\,(T_1 - T_a) + (B_1 - H_1)]\}\, dz} \tag{7-60}$$

Although in the present formulation we have not included the governing equations for fins on the duct wall, subsequently we will extend the analysis to include this case and the case of double fins, that is, fins placed both on the guard vessel and on the duct wall. Fins on these two walls may be staggered or placed opposite each other. We will also allow for two-dimensional effects of heat transfer in the guard vessel/duct wall due to the presence of fins.

7.5 Fully Developed Flow

In a long channel of constant cross section and surface characteristics, one expects that after some initial length the flow under forced flow conditions will become fully developed. However, the natural convection flow of a RVACS as driven by density gradients caused by heat flux along the length of the vertical channel, cannot become fully developed. In a RVACS system the cross-section of the passage may not remain constant because of interruptions in the length of the fins to accommodate axial thermal expansion and, in addition, some bypassing of the flow from outer channel to inner channel (e.g., in GE design) may also be present. These conditions will further prevent the flow from becoming fully developed. Whether fully developed flow conditions really ever exist in a RVACS channel, it is nevertheless a very powerful assumption that greatly simplifies the study of effectiveness of a finned system in dissipating the shut down heat from the reactor to the atmosphere and permits a valid first detailed analysis.

For fully developed flow, the velocity components $u = v = 0$ and the axial velocity $w(r,\theta,z) = w(r,\theta)$, i.e., w is independent of axial distance. Under these assumptions Eqs. (7-2)-(7-6) simplify to

$$\frac{\partial w}{\partial z} = 0 \tag{7-61}$$

$$\frac{1}{\rho}\frac{\partial \bar{p}}{\partial z} + g = \nu\left(\frac{\partial^2 w}{\partial r^2} + \frac{1}{r}\frac{\partial w}{\partial r} + \frac{1}{r^2}\frac{\partial^2 w}{\partial \theta^2}\right) - \frac{1}{r}\frac{\partial r\overline{u'w'}}{\partial r} - \frac{1}{r}\frac{\partial \overline{v'w'}}{\partial \theta} \tag{7-62}$$

$$w\frac{\partial T}{\partial z} = \alpha\left[\frac{1}{r}\frac{\partial}{\partial r}\left(r\frac{\partial T}{\partial r}\right) + \frac{1}{r^2}\frac{\partial^2 T}{\partial \theta^2}\right] - \frac{1}{r}\frac{\partial r\overline{u'T'}}{\partial r} - \frac{1}{r}\frac{\partial \overline{v'T'}}{\partial \theta} \tag{7-63}$$

Equation (7-61) implies that

$$w = w_o = \text{constant.} \tag{7-64}$$

From the definition of stress components, we have

$$\tau_{rz} = \tau_{zr} = \rho\nu \frac{\partial w}{\partial r} - \rho\overline{u'w'} \tag{7-65a}$$

$$\tau_{\theta z} = ou \frac{\rho\nu}{r} \frac{\partial w}{\partial \theta} - \rho\overline{v'w'} \tag{7-65b}$$

Introducing these definitions in Eq. (7-62), we obtain

$$\frac{\partial \bar{p}}{\partial z} + g\rho = \frac{1}{r} \frac{\partial}{\partial r} (r\, \tau_{rz}) + \frac{1}{r} \frac{\partial\, \tau_{\theta z}}{\partial \theta} \tag{7-66}$$

Integrating above equation over a channel formed by pair of fins and the fin shroud and guard vessel wall.

$$\iint \frac{\partial \bar{p}}{\partial z}\, r d\theta dr + \iint g\rho r d\theta dr = \iint \frac{1}{r} \frac{\partial}{\partial r} (r\, \tau_r z)\, r d\theta dr + \iint \frac{1}{r} \frac{\partial\, \tau_{\theta z}}{\partial \theta}\, r d\theta dr$$

which gives

$$\begin{aligned} A \frac{\partial \bar{p}}{\partial z} + gA\, \bar{\rho}(z) &= \int r_2\, \tau_{rz}(r_2,\theta) d\theta - \int r_1\, \tau_{rz}\, (r_1,\theta) d\theta \\ &+ \int \tau_{\theta z}\, (r,\, \theta_2)\, dr - \int \tau_{\theta z}\, (r_1 \theta_1) dr \\ &= \int_{S_2} \tau_{rz}\, (r_2,\theta)\, ds_2 - \int_{S_1} \tau_{rz}(r_1,\theta)\, ds_1 \\ &+ \int \tau_{\theta z}\, (r,\theta_2) dr - \int \tau_{\theta z}(r,\theta_1) dr \end{aligned} \tag{7-67}$$

where $\bar{\rho}(z)$ is the cross sectional averaged density, and S_1 and S_2 are the wetted perimeters along guard vessel and duct wall, respectively. Consistent with fully developed flow assumptions and the Boussinesq approximation (that variation of density is considered important only in the buoyancy term) and Eqs. (7-61), (7-65) the right-hand of Eq. (7-67) is independent of z. We can rewrite Eq. (7-67) as

$$\frac{\partial \bar{p}}{\partial z} + g\bar{\rho}(z) = \frac{1}{A}\{S_2\,\bar{\tau}_{rz}(r_2) - S_1\,\bar{\tau}_{rz}(r_1) + [\bar{\tau}_{\theta z}(\theta_2) - \bar{\tau}_{\theta z}(\theta_1)]H\} \tag{7-68}$$

where $r_1 = R_G + b_G$, and $r_2 = R_s$.

In regard to the sign convention for shear stresses, we note that the shear stress $\bar{\tau}_{rz}(r_1)$ is in the plane at $r = r_1$ whose normal is directed in a direction opposite to r, $\bar{\tau}_{rz}(r_2)$ is in the plane at $r = r_2$ whose normal is directed along r, and similarily $\bar{\tau}_{\theta z}(\theta_1)$ is in the plane at $\theta = \theta_1$ whose normal direction is opposite to the positive direction of θ and normal to the plane of $\bar{\tau}_{\theta z}(\theta_2)$ is along the direction of θ. However, all of these shear stresses oppose motion. Introducing the perimeter averaged stress τ_w as

$$\begin{aligned} -S_w\tau_w &= S_2\,\bar{\tau}_{rz}(r_2) - S_1\,\bar{\tau}_{rz}(r_1) + [\bar{\tau}_{\theta z}(\theta_2) - \bar{\tau}_{\theta z}(\theta_1)]\,H \\ &= -S_w\frac{\rho_\infty w^2}{2} f \end{aligned} \tag{7-69}$$

where $S_w = S_1 + S_2 + 2H$, the wetted perimeter of the channel, f is the average friction factor, and w is the cross-section averaged velocity. The use of Eq. (7-69) in Eq. (7-68) yields

$$\frac{\partial \bar{p}}{\partial z} + g\,\bar{\rho}(z) + \left(\frac{4}{D_h}\right)\frac{\rho_\infty w^2}{2} f = 0 \tag{7-70}$$

where $D_h = 4A/S_w$.

The use of Eq. (7-16) into Eq. (7-70) gives

$$\frac{\partial(\bar{p} - p_\infty)}{\partial z} + g(\bar{\rho}(z) - \rho_\infty) + \frac{4}{D_h}\frac{\rho_\infty w^2}{2} f = 0 \tag{7-71}$$

Returning now to the energy equation, fully developed conditions for the temperature profile occurs under constant heat flux conditions.

Integrating Eq. (7-63) over the cross-sectional area, we obtain

$$\int w \frac{\partial T}{\partial z}\, dA = \frac{1}{\rho C_p} \int [q_r(r_2) - q_r(r_1)]ds + \frac{1}{\rho C_p}\int [q_\theta(\theta_2) - q_\theta(\theta_1)]dr$$

$$= [S_2\, \bar{q}_r(r_2) - S_1\, \bar{q}_r(r_1)] + [\bar{q}_\theta(\theta_2) - \bar{q}_\theta(\theta_1)]H$$

$$= S\, q_w/\rho C_p \tag{7-72}$$

where S is the pitch and q_w is the heat flux into the guard vessel. Clearly, if q_w is constant, then Eq. (7-72) becomes

$$w \frac{\partial T}{\partial z} = \frac{S}{A} q_w \tag{7-73}$$

The substitution of the relation, $\bar{\rho}(z) = \rho_\infty[1 - \beta\,(T - T_\infty)]$ in Eq. (7-71) gives

$$\frac{\partial(\bar{p} - p_\infty)}{\partial z} - g\beta\rho_\infty\,(T - T_\infty) + \frac{2}{D_h}\rho_\infty w^2 f = 0 \tag{7-74}$$

Equations (7-73) and (7-74) form the basis of the simplified analysis presented in Section 3.

Method of Solution

The equations governing heat transfer in the fins and surfaces will be solved by the boundary element method using a constant element as the approximating function for the boundary temperature distribution. This method will allow fins and surfaces to be treated as a series of constant temperature elements (or strips of zero thickness) and consequently allow the use of finite shape factors for each of these constant temperature strips. The use of the boundary element method with a constant element is a natural application to the solution of this problem, as the boundary temperature and fluxes are only the desired quantities required for the present analysis. The temperatures inside the material are not required and therefore computations performed using finite-difference methods would be more wasteful.

The governing system of equations that describe the turbulent, three-dimensional flow of the air in the channel can be solved by a computational scheme that utilizes the explicit differencing method of DuFort-Frankel for the axial momentum and thermal energy equations, and an implicit method for the radial and circumferential momentum equations that accommodates a modified pressure-correction formulation of the Patankar-Spalding technique [20]. This modification is necessary to utilize the simplification of the momentum equations in the near-wall region outlined in Iacovides and Launder [19], which allows a fine-grid analysis of the wall region. In accordance, the radial velocity component in the very thin parabolic sublayer is obtained from application of the contunity equation to each cell, and the radial momentum equation and pressure-correction equation needs to be considered only outside of this near-wall region.

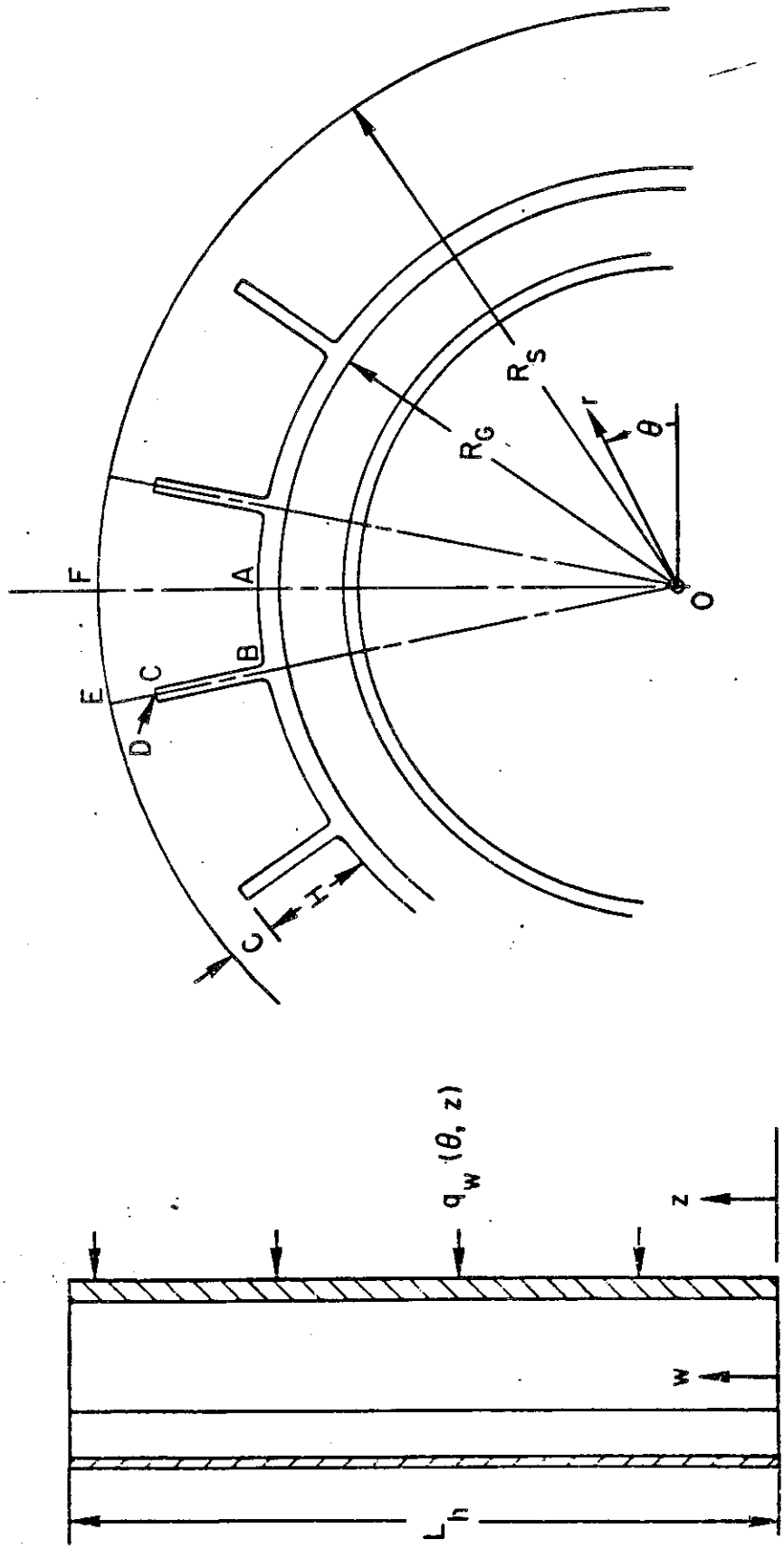

Figure 7-1. Coordinate System with Fins on Guard Vessel.

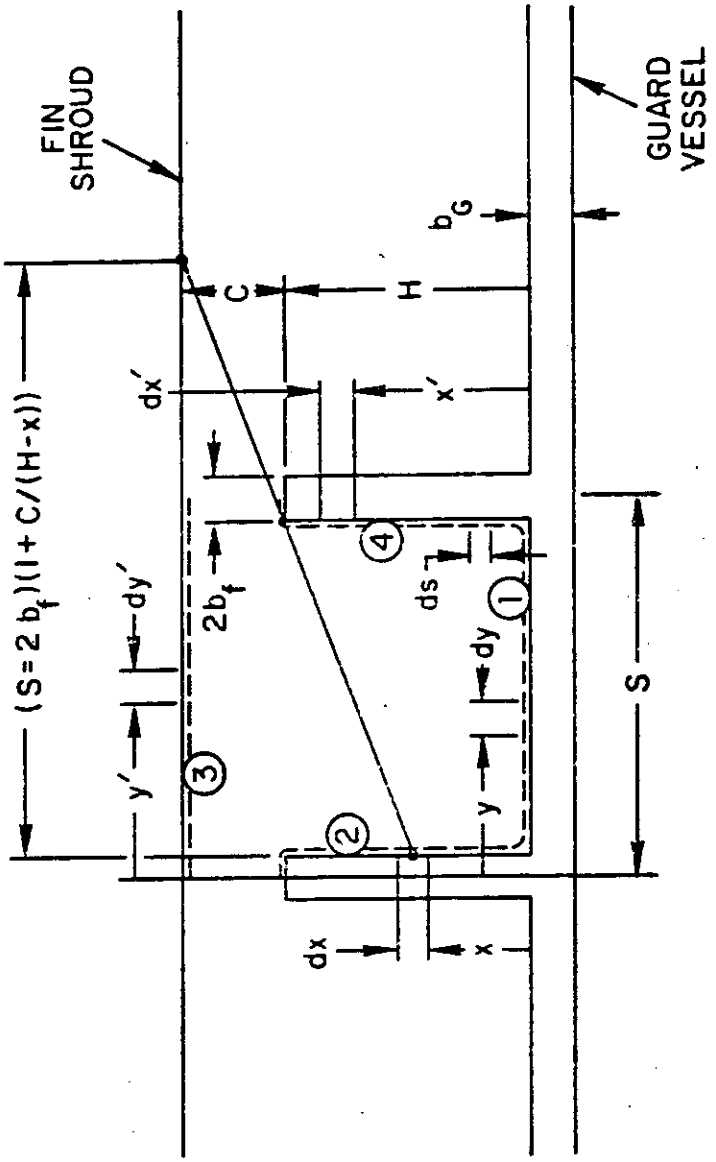

Figure 7-2. Coordinate System for Fins on Guard Vessel.

8. STATUS REPORT ON FULL SCALE SEGMENT TEST

8.1 Introduction

This section describes the status of the Argonne National Laboratory (ANL) out-of-pile test assembly that simulates experimentally the General Electric (GE) Radiant Vessel Auxiliary Cooling System (RVACS). The information presented is preliminary in nature and general in scope. The topics discussed are the design requirements, a description of the structural configuration, the heater control system, and the instrumentation and data acquisition system.

Basically, the test assembly will prototypically simulate a full-size vertical segment of the GE/RVACS the flow channel between the guard vessel and the duct wall. The test assembly includes sufficient instrumentation to determine local wall and air temperatures, velocity profiles, and heat flux rates at various elevations; from such recorded information the heat transport performance characteristics for chosen configurations can be evaluated.

The primary objective of the ANL RVACS program is:

to test theoretically optimized configurations to determine the local heat flux transport rates and associated convective heat transfer coefficients at various elevations, and evaluate their integral performance characteristics for the bounding range of shutdown decay heat removal conditions.

The structural and thermal analysis which formed the basis for the design requirements and structural configuration were described in detail in earlier sections, which show that the requirements [25] will theoretically satisfy the bounding conditions.

8.2 Summary

ANL's Shutdown Heat Removal Test Assembly, referred afterward as the Test Assembly, is an out-of-pile test assembly. It simulates experimentally the GE Radiant Vessel Auxiliary Cooling System (RVACS) which removes decay heat from a reactor vessel through radiation and natural convection to air. The ANL Test Assembly design will support the requirements of the reference General Electric (RVACS) design as well as future modifications. The Phase I design refers to the initial design that was based on a scientific modeling analysis and evaluation to ascertain theoretically the optimum GE/RVACS fundamental configuration. The Phase II design refers to a revised design that will be based on an experimentally improved model and/or general modifications to the initial design.

The Test Assembly is comprised of a structural model, electric heaters, insulation, and instrumentation. Additionally, a computerized control and data acquisition system is employed. The Test Assembly is capable of simulating prototypic reactor vessel temperatures, air flow patterns, and heat removal conditions that would exist for a RVACS system during normal reactor operation and/or a shutdown situation. The Test Assembly will be sufficiently instrumented to determine three-dimensional temperature and velocity profiles. The system is designed to operate in two modes: 1) constant wall temperature or 2) constant heat flux, up to 2.0 kW/ft^2.

The structural model is the result of detailed parametric heat transport analyses for various configurations. It provides a full-scale mock-up of a vertical segment of the air-side RVACS configuration such that tests may be performed to:

a. Determine local and integral performance characteristics for the range of shutdown heat removal conditions expected.

b. Evaluate and characterize key similarity parameters, Reynolds and Grashof numbers, entrance-laminar, developed, and turbulent flow regimes.

c. Develop a data base to permit validation of analytical heat transfer modeling methods.

d. Investigate various design configurations for evaluation and selection of the configuration of optimum performance.

The basic structure of the Test Assembly is illustrated in Figure 8.1; it is 50-ft. vertically, 5-ft. wide, and has a changeable depth of 6-in. to 18-in. The illustrated cross-sectional description of the Test Assembly shown in Fig. 8.2 indicates that the guard vessel wall and the duct wall simulators are flat instead of slightly curved because the curvature of a 5-ft. segment would produce a relatively minor effect on the performance, and for test purposes the rectangular flat-wall geometry is much easier to work with. The structural model is constructed entirely with carbon steel, which may not be entirely prototypic; however, the Phase II tests will be performed with entirely prototypic reactor material. Only the guard vessel and the duct wall are simulated in the Phase I tests. The Test Assembly is being designed to allow for the addition of a reactor vessel simulator in the Phase II testing if the results of the analytical evaluation warrant such test modeling. All Phase I interior surfaces will have an oxide coating to enhance the emissivity, and the emissivity of those surfaces will be examined periodically throughout the testing sequence. The guard vessel wall and duct wall simulators are insulated from each other, but each are attached to the end channels by

bolting as indicated in the Fig. 8.2 illustration. The greater thermal expansion of the hotter guard vessel simulator will be accommodated by specially designed expansion joints. Consistent with prototypic requirements, the guard vessel wall simulator will be insulated from heat conduction to the outer channels, as indicated in Fig. 8.2, with the only points of contact being at the eight bolt contacts on each side of a 10-ft. vertical section. Heat transport from the guard vessel simulator will thus be restricted to radiation and convection.

Heating of the guard-vessel simulator wall (or the reactor-vessel simulator wall in possible Phase II tests) will be achieved with an array of electric plate heaters to simulate up to one and one-half (1.5) times the peak RVACS decay heat transport rate, or a heat flux of approximately 2 kW/ft^2. The heating elements are capable of operating at 1200°F. Thus, the capability exists to provide a constant heat flux of $\sim$ 2 kW/ft^2. A total of 200 heaters will be used over a 20-ft. vertical section. Each heater plate is 12-in. x 6-in. x 1/2-in. The total array of 200 heaters are divided into 2-ft. x 5-ft. modular heating units each containing 20 heaters. Each heater unit will be computer controlled to supply a constant heat flux so that the wall temperature variations will not exceed 20°F. Heat losses through exterior surfaces will be minimized by appropriate materials and thicknesses, and is limited in the design requirements to $\lesssim$ 2%, i.e. $\lesssim$ 500 $Btu/hr.ft^2$.

To control and monitor test conditions, and determine heat transport performance for a given structural configuration, the Test Assembly will be fitted with sensors for measuring wall and air temperatures, air velocities, volume and/or mass flow rates, differential pressure, and air humidity/density conditions. The emissivity of the interior walls will be measured at appropriate times by the removal of coupons attached to the heated walls. The

wall and fin surface temperatures, as well as local air velocities and temperatures will be measured every 4 feet up the 20-ft. vertical height of the test model starting from the 3-ft. elevation point. Inlet and outlet air temperature velocities and volume/mass flow rates will be monitored also. Local air temperatures will be measured with thermocouples that have radiant shields to reduce radiation effects to the extent that the true air temperature is measured. Also, the capability for flow visualization studies will be incorporated into the design of the Test Assembly. The power to the heaters will be controlled with a computer based SCR controllers. The measurement of the power to the electric heaters will be computed from the measured "on-time" voltage (E) and the temperature corrected resistance (R) of the heaters, i.e. $P = E^2/R$. The temperatures of the heaters in each 2-ft. by 5-ft. modular heating unit, are measured by two groups of thermocouples: one group of four for the heaters that cover the outer-end areas, and another group of four for the heaters that cover the adjacent-inner areas. Additionally, local heat flux sensors will be utilized in support of thermocouple measurements.

Control of the air flow through the Test Assembly is provided for by a baffle plate and a variable speed fan arrangement at the outlet. The outlet flow area can be reduced up to 100% of normal and the fan is capable of a variable flow rate up to a maximum of 17,000 CFM. In the final stage of Phase II testing a means for generating and injecting a sodium aerosol can be provided to evaluate surface fouling effects on free convection.

8.3 Test Assembly Design Requirements

Fundamentally, it is required to model theoretically optimized configurations of a full-size vertical segment of the air flow channel between the

guard vessel wall and the RVACS duct wall. At issue is the resolution of uncertainties with respect to local heat fluxes and convective transfer coefficients, and the overall performance characteristics of structurally optimized configurations. For parametric testing it is fundamentally required to obtain precise and accurate knowledge about the air temperature, density, velocity, volumetric and/or mass flow rates at the inlet and throughout the flow region. No less important is the necessity to know the heat generation, heat loss, and heat flux transferred. The parametric test results should provide a credible data base for evaluation and development of the optimum configuration.

8.3.1 Structural Configuration

The Test Assembly is illustrated in Figs. 8.1 and 8.2. Note that the walls of the Test Assembly are flat instead of curved because the curvature of a 5-ft. segment will produce a relatively minor effect on performance, and the rectangular flat-wall geometry is much easier to fabricate and analyze parametrically. As shown in Fig. 8.2, the Test Assembly will consist of a rectangular duct approximately 50-ft. vertically, 5-ft. wide and 1-ft. deep. The initial Phase I testing will be performed without fins on either the duct wall or the guard vessel wall. The lower 20-ft. of the test structure will be heated on the side simulating the guard vessel wall. The wall thicknesses are to be 1-in. for both the G.V. wall and the duct wall, however, the G.V. wall thickness need not be the same as the real case G.V. wall since only the wall heating rate, wall temperature, and wall surface conditions are parameters to be modeled.

The advantage of a full-scale segment test structure is that direct application of the test results can be made to the predicted performance of the actual RVACS design. Also, direct evaluation comparisons are allowed for

geometry effects, key similarity parameters, Reynolds and Grashof numbers, entrance effects as well as fully developed and turbulent velocity profiles, and variations in the heat transfer coefficient.

The central region of the air flow duct is expected to develop prototypic flow and temperature characteristics. The regions near the two side fins of the test structure are not expected to have prototypic temperature or flow distributions due to unprototypic partitioning between the guard vessel and duct simulator walls; however, the unprototypic effects are expected to be small.

8.3.2 Materials and Surface Conditions

Prototypic heat transfer characteristics will be assured because the ANL RVACS mock-up will ultimately duplicate the same materials and surface conditions that have been proposed for the real RVACS. The Phase I required materials and surface conditions are listed in Table 8.1.

The carbon steel shall be ordered with mill-scale to enhance the emissivity. Grinding of the surface will not be permitted except for weld preparation. Emissivity measurements of coupons that are contained within the Test Assembly will be performed on the as received material and periodically at appropriate times during the testing series.

8.3.3 Heating System

The guard vessel simulator wall will be heated with an array of ceramic-plate electric heaters to simulate up to 1.5 times the peak RVACS decay heat transport rate, or approximately 2 kW/ft^2. The heating elements are capable of operating at 1200°F, which will be sufficient to provide a constant temperature of up to ~ 900°F at the air side of the guard vessel wall simulator. Thus, the capability exists to supply a constant heat flux of approximately 2 kW/ft^2. A total of 200 heaters will be used over the lower 20-ft. of

Table 8.1. RVACS Materials and Surface Conditions

Item Description	Material Description	Surface Conditions
Guard vessel simulation	Carbon steel (AISI No. C1017-C1020)	Oxidized (Mill-scale)
Duct wall simulation	Carbon steel (AISI No. C1017-C1020)	Oxidized (Mill-scale)
End fins	Carbon steel (AISI No. C1017-C1020)	Oxidized (Mill-scale)
Interior Fins	Carbon steel (AISI No. C1017-C1020)	Oxidized (Mill-scale)

the vertical structure. The dimensions of a single heater plate are 12-in. x 6-in. x 1/2-in. The total array of 200 heaters are grouped into ten (10) modular units each measuring 2-ft. x 5-ft., containing 20 heaters. Figure 3.1 illustrates the modular 2-ft. x 5-ft. heater arrangement in relation to the overall structural configuration and the location of instrumentation. The power to the electric ceramic-plate heaters will be computed from the measured "on-time" voltage (E) and the temperature corrected resistance (R) of the heaters, i.e., Power = E^2/R. The temperature of the heaters in each 2-ft. by 5-ft. modular unit are measured by eight thermocouples: one group of four for the heaters that cover the outer-end areas, the other group of four for the heaters that cover the adjacent inner areas. The temperature of each heater unit will be computer controlled to supply a constant heat flux. A diagrammatical layout of the heater control and data acquisition system is shown in Fig. 8.4. The system will also have the capability of producing predetermined non-uniform guard vessel wall temperature gradients in the vertical direction. Heat losses through exterior surfaces will be minimized to < 2% (i.e. $\lesssim$ 500 Btu/hr.ft^2) by appropriate thicknesses of insulation materials.

8.3.4 Instrumentation Requirements

Instrumentation of the Test Assembly is required to measure surface temperatures, air temperatures, air velocities and flow rates, and electrical power input to the heaters. These data will be used to evaluate the heat removal performance for the particular configurations to be tested.

Wall Surface Temperature Measurements

Surface temperature measurements of the guard vessel and duct wall simulators are tentatively to be made at the locations indicated in Figure 8.3. Temperature measurements are to be obtained at five locations within the 20-ft. vertically heated region, at 3-ft., 7-ft., 11-ft., 15-ft., and 19-ft. from the bottom of the heated zone. For the open channel (no fins) arrangements shown in Figure 8.3, twelve thermocouples will be required at three of the five locations (i.e. locations A, C, and E indicated in Figure 8.3), and eight thermocouples will be required at each elevation marked B and D in Figure 8.3. Thus, the total number of these measurements will be 52.

Local Channel Air Temperature and Velocity Measurements

Local air temperature measurements will be made at elevations of approximately 3-ft., 7-ft., 11-ft., 15-ft., and 19-ft.; that is, within the heated 20-ft. vertical test channel, air temperature measurements are to be made at elevations similar to the wall temperature measurements and as near to the air velocity measurement locations as possible. These measurements are to be made with removable hot-wire anemometer and/or pitot-tube/temperature transverse probes to eliminate flow interference from instrumentation that would otherwise be fixed in position. Within the heated test region of the structural model the air velocity measurements shall be monitored at 15 symmetrical locations respective to its central axis. Such arrangement for velocity and temperature measurement is indicated in Figure 8.3. The thermocouples for air

temperature measurement shall be shielded from thermal radiation to assure measurement of the actual air, they may also be combined in a combination pitot-static/thermocouple probe for measuring the total and static pressures and the temperature of the flowing air, from which information the air velocity at the various measurement positions can be calculated.

Outlet Air Velocity, Volumetric Flow Rate, and Temperature Measurement

Air temperature measurements will also be made at the outlet location, and perhaps at the inlet, as indicated in Figure 8.3. The outlet measurement location will be fixed at elevation "F" ~ 41-ft., but the inlet measurements would be made with removable sensors to eliminate flow interference at the inlet. However, the final decision is yet to be made on the need for continuously monitoring the inlet velocity, volumetric flow rate, and temperature measurements. The method for measuring the total volumetric flow rate of the air, as well as its velocity and temperature at the outlet, and perhaps occasionally at the inlet, is indicated in Figure 8.3. That method incorporates three multiple total and static pressure sensor traverse probes with ~ 12 TCs riding piggy-back for temperature measurement. The traverse probes have ~ 15 total and static pressure sensors located in one ~ 52-in. probe; thus, three probes will supply ~ 45 such sensors whose measurements are averaged together to give a result which should be within ± 2% uncertainty for the averaged velocity and volumetric rate of air flow.

Electric Power and Heat Flux Measurement

The power to the electric heaters will be controlled with the computer based SCR controller system shown in Figure 8.2. The measurement of the power to the electric heaters will be computed from the measured "on-time" voltage (E) and the temperature corrected resistance (R) of the heaters, i.e. $P = E^2/R$. The temperatures of the heaters in each 2-ft. by 5-ft. modular unit

are measured by two groups of thermocouples; one group of four for the heaters that cover the outer-end areas, and the other group of four TC's for the heaters that cover the adjacent-inner areas. Additionally, local heat flux sensors will be utilized in support of thermocouple measurements. A cross-sectional view of the TC and heat flux sensor arrangement is indicated in Figure 8.3. In a feasibility test, two of the flat, ceramic-plate, nichrome-wound, electric heaters, which are each rated at 2-kW, were flush mounted to a 48-in. by 10-in. by 1/2-in. thick stainless steel plate; at a total power of 3.96-kW (220 volts and 18 amps) the opposite side of the steel plate was heated to ~ 900°F in ~ 4-hrs.

Pressure Measure Measurements

The total and static pitot tube pressure measurements for differential measurements of pressure will be made with high accuracy, temperature compensated, electronic manometers, which are of the variable capacitance differential pressure transmitter type.

Humidity/Density Measurements

The humidity and density of the inlet air will be measured by an appropriate device and/or calculated from other parametric measurements to determine these fundamental properties of the air.

Emissivity Measurements

Emissivity measurements will be made periodically at appropriate times during the testing series of metal coupons whose surfaces are prototypic of the interior surface of the structural model.

Sensor Requirements

Table 8.2 lists the minimum required range, accuracy, and response for the instrument sensors. The range specified is ~ 10% greater than the range of values expected during the test. Specified accuracies are based on the

need to detect a ≤ 20°F variation in temperature, air velocities of approximately 0.10 FPS variation, and air volume flow rates of ± 2% uncertainty. The accuracy of the electric power input metering is desired to be known also within ± 2% of the total value. Accuracies of other parametric measurements are to be appropriately consistent within the ± 2% of full scale. The sensor response is based on the expected rate of change of the measured parameters, and the data acquisition rate. Wall temperatures as well as air inlet and outlet temperatures and velocities are expected to change slowly. However, local channel air temperatures and velocities are expected to fluctuate more rapidly due to local flow mixing and/or turbulence, thus, a fast response time for those sensors is desirable. Table 8.2 also indicates the type of sensor required for the parameters to be measured.

Flow Visualization Studies

Thermally adequate windows shall be locatable at any desired elevation by removal of a selection of insulation between the guard vessel and the end plates and insertion of the window. Fundamentally, the provision will exist for flow visualization at any desired elevation.

8.3.5 Data Acquisition System

The data acquisition system is shown interfaced with the heater control system in Figure 8.4. Data loggers capable of 198 measurement channels will be interfaced with a PDP-11 computer with on-line graphics display and hardcopy capability.

8.3.6 Other Requirements

Guard Vessel, Duct Wall and Fins

The structural model will provide the capability of evaluating various configurations. Its design will allow for changing the gap between the guard vessel wall simulator and the end of the fin, when tests with fins are

performed. The design shall be capable of making gap adjustments without requiring complete disassembly of the test assembly. Phase I tests will be performed without fins.

Inlet Air Temperature Control

No provisions have been incorporated into the design to increase or decrease the inlet air temperature. Tests performed during summer may be with air temperatures up to ~ 100°F, and winter tests may be performed with inlet temperatures of ~ 0°F.

Inlet Air Flow Control

Provision shall be available to control the air flow rate. The air velocity shall be variable from natural free convective flow to forced flow conditions of 30 FPS.

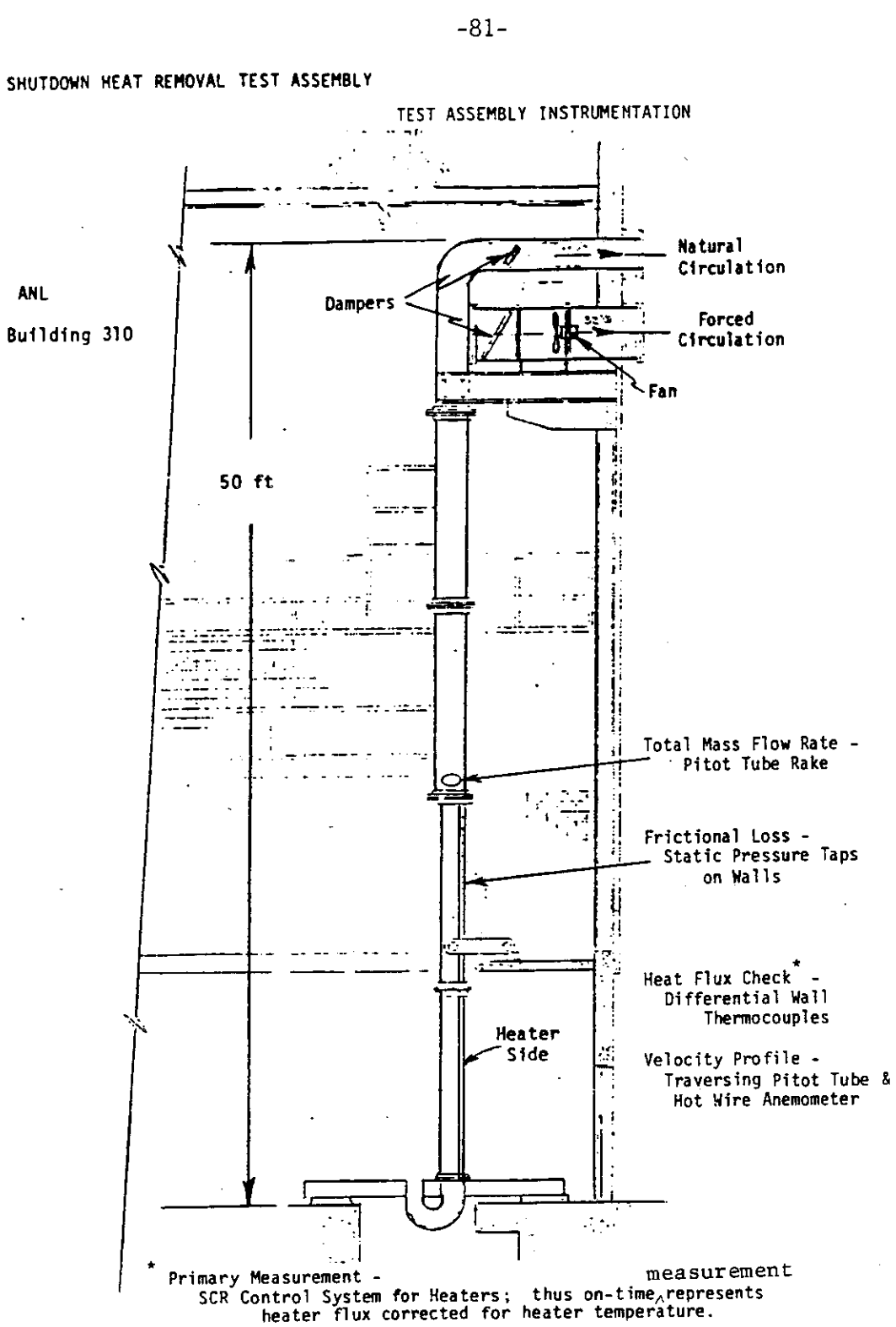

Figure 8-1. Illustration of the Basic Structure of the ANL Shutdown Heat-Removal Test Assembly.

SHUTDOWN HEAT REMOVAL TEST ASSEMBLY

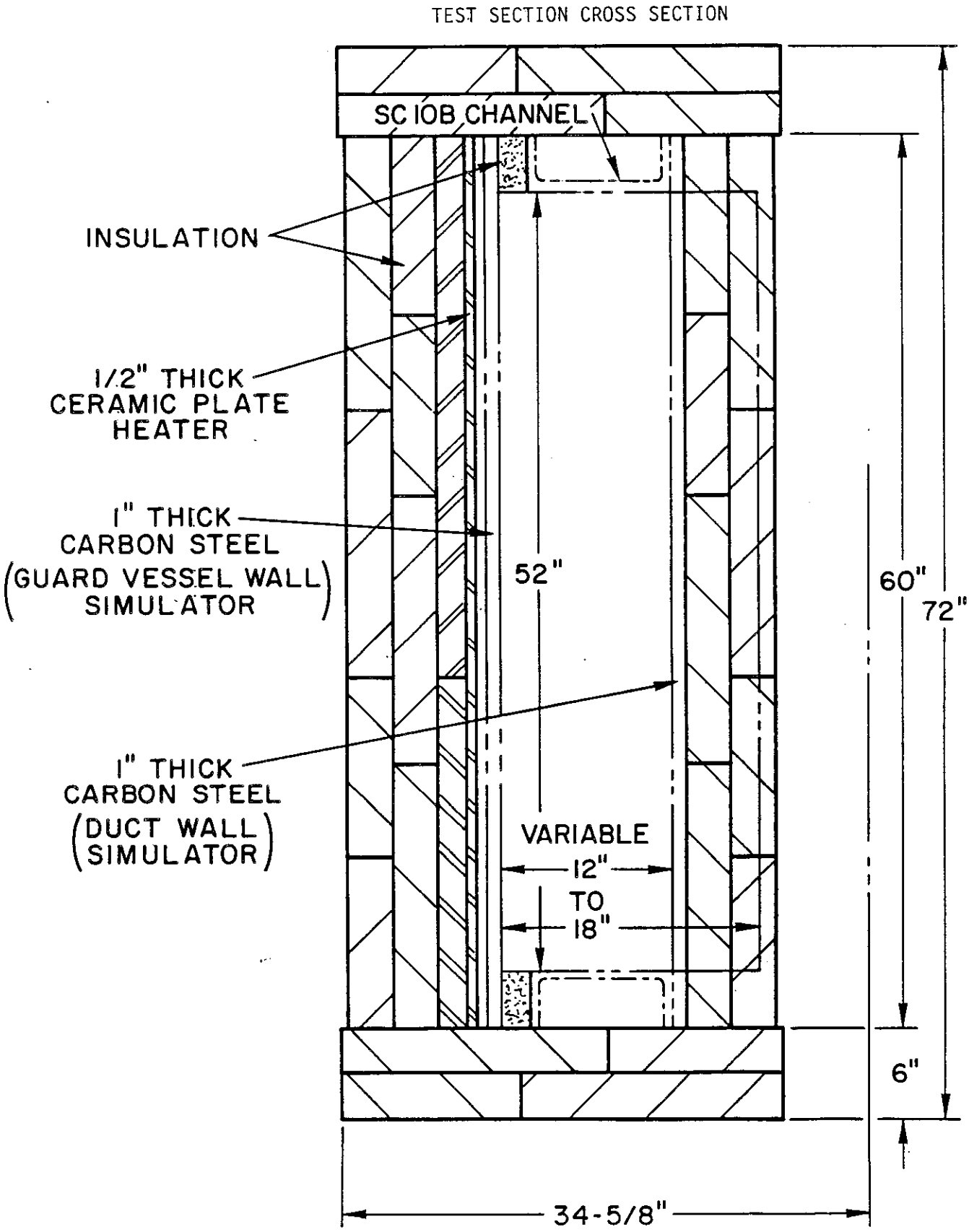

Figure 8-2 Illustrated Cross-Sectional Description of the Basic Structure of the ANL Shutdown Heat-Removal Test Assembly.

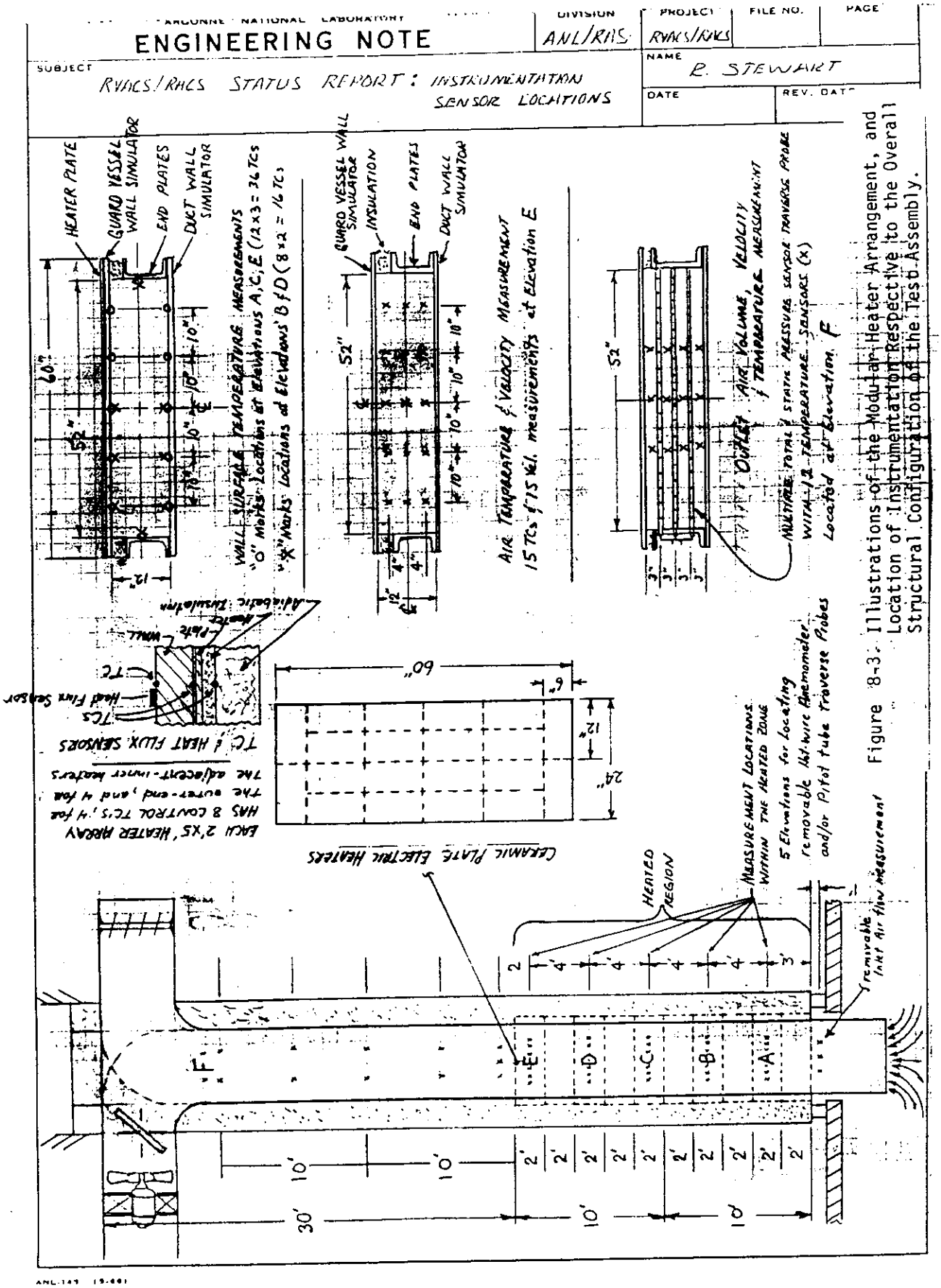

Figure 8-3. Illustrations of the Modular Heater Arrangement, and Location of Instrumentation Respective to the Overall Structural Configuration of the Test Assembly.

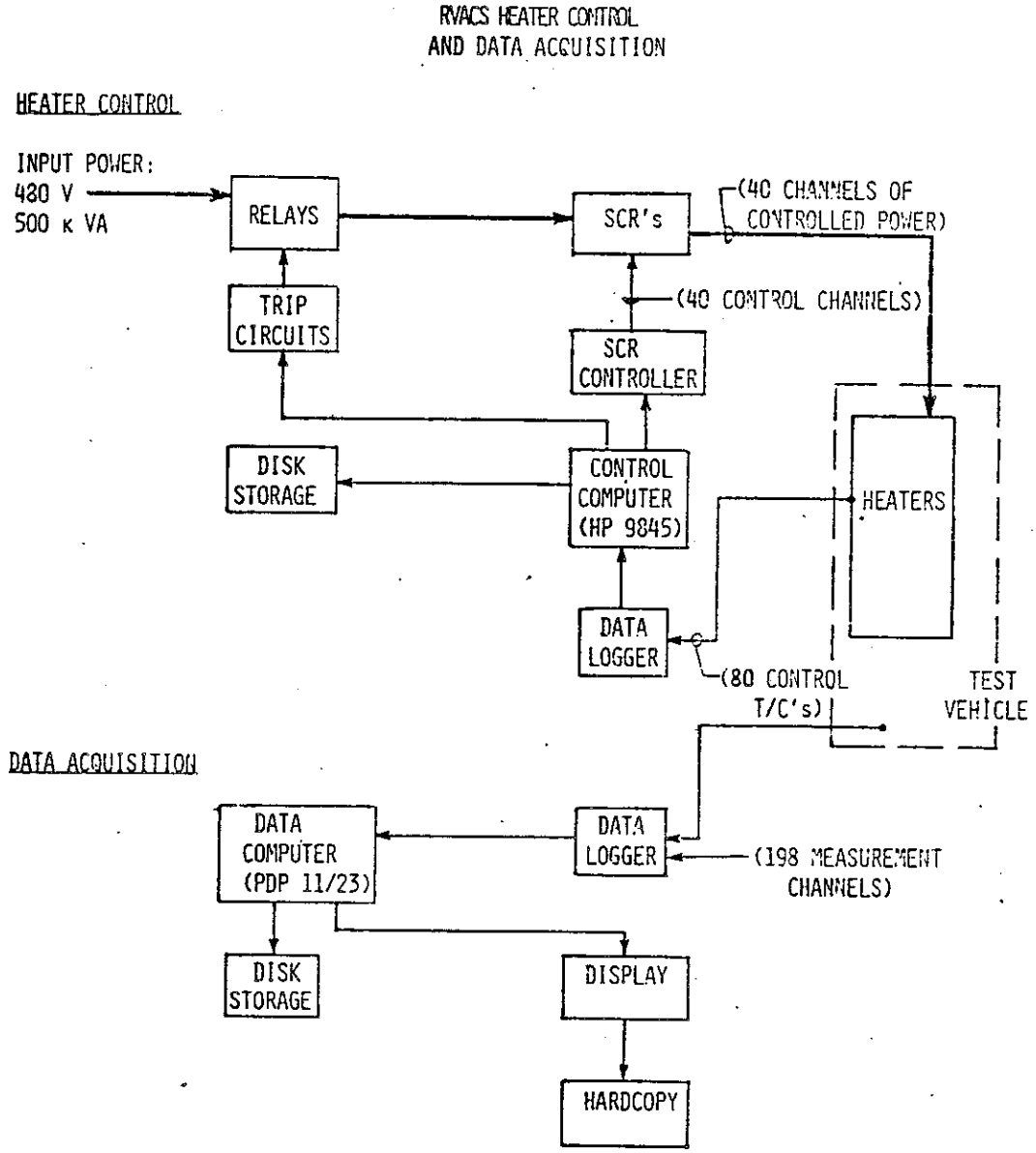

Figure 8-4. A Diagramatical Layout of the RVACS/RACS Heater Control and Data Acquisition System.

TABLE 8-2. INSTRUMENTATION REQUIREMENTS[1]

ITEM DESCRIPTION	Sensor Type	Quantity[2] 10' sect.	Quantity[2] Total	Minimum Required Values Range	Minimum Required Values Accuracy[3]	Minimum Required Values Response[4]
Guard Vessel Thermocouples	C/A type-K 24 AWG High temp. glass	TBD	52	0 to 1000°F	± 2% of FR	30 sec.
Duct Wall Thermocouples	C/A type-K 28 AWG glass braid	TBD	52	0 to 500°F	± 2% of FR	30 sec.
Fin Thermocouples[5]	C/A type-K 28 AWG glass braid	TBD	54	0 to 800°F	± 2% of FR	30 sec.
Air Thermocouples						
Inlet	C/A type-K 28 AWG, glass		12	0 to 150°F	± 2% of FR	30 sec.
Outlet	C/A type-K 28 AWG, glass		12	0 to 300°F	± 2% of FR	30 sec.
Local	C/A type-K 28 AWG, glass	TBD	15	0 to 500°F	± 2% of FR	3 sec.
Inlet Air Velocity and Flow Rate Sensor	Air Vol/Vel Traverse Probe		1	0 to 30 FPS	± 2% of FR	30 sec.
Outlet Air Velocity and Flow Rate Sensor	Air Vol/Vel Traverse Probe		1	0 to 30 FPS	± 2% of FR	30 sec.
Local Air Velocity Sensors[6]	Hot-Wire Anemometers	TBD	3	0 to 30 FPS	± 2% of FR	3 sec.
	Pitot Tube Traverse Probe	TBD	4	0 to 30 FPS	± 2% of FR	3 sec.
Electric Power Input Meter (for calibration)		TBD	TBD	TBD	± 0.5% of FR	--
Static Pressure Taps	MKS Baratron Capacitance manometer	1	5	1 mm Hg (FR)	± .08% FR	30 sec.
Humidity/Density Measurement	TBD	TBD	3	Std. for air	± 2% FR	30 sec.

1. Surface emissivity measurement to be performed separately.
2. Data acquisition limited to 198 channels.
3. Including linearity and repeatability.
4. Time required to equal 63% of instantaneous change.
5. Locations and installation method addressed elsewhere.
6. Movable sensor.

9.0 References

1. N. Sheriff and P. Gumley, "Heat Transfer and Friction Properties of Surfaces with Discrete Roughness," Int. J. Heat Mass Transfer, Vol. 9, pp. 1297-1320, 1966.

2. R. L. Webb, E. R. G. Eckert, and R. J. Goldstein," Heat Transfer and Friction in Tubes with Repeated-Rib Roughness," Int. J. Heat Mass Transfer, Vol. 14, pp. 601-617, 1971.

3. A. P. Watkinson, D. L. Miletti, and P. Tarassoff," Turbulent Heat Transfer and Pressure Drop in Internally Finned Tubes," AIChE Symp. Ser., Vol. 69, No. 131, pp. 94-103, 1973.

4. A. P. Watkinson, D. L. Miletti, and G. R. Kubanek, "Heat Transfer and Pressure Drop of Forge-Fin Tubes in Turbulent Air Flow," ASHRAE Paper No. 2347, 1975.

5. T. C. Carnavos, "Cooling Air in Turbulent Flow with Internally Finned Tubes," AIChE Paper No. 4, 17th Natl. Heat Transfer Conf., 1977.

6. S. V. Patankar, M. Ivanovic, and E. M. Sparrow, "Analysis of Turbulent Flow and Heat Transfer in Internally Finned Tubes and Annuli," J. Heat Transfer 101, pp. 29-37, 1979.

7. T. C. Carnarvos, "Heat Transfer Performance of Internally Finned Tubes in Turbulent Flow," Adv. Enhanced Heat Transfer, ASME, New York, pp. 61-67, 1979.

8. S. Faggiani and F. Gori, "Heat Transfer Coefficient for Liquid Metals in Turbulent Flow Between Parallel Plates," J. Heat Transfer, Vol. 102, pp. 292-296, 1980.

9. E. R. G. Eckert, A. J. Diaguila, and A. N. Curren, "Experiments on Mixed Free and Forced Convective Heat Transfer Connected with Turbulent Flow through a Short Tube," NACA TN2974, 1953.

10. A. Steiner, "On the Reverse Transition of a Turbulent Flow under the Action of Buoyance Force," J. Fluid Mech., Vol. 47, pp. 503-508, 1971.

11. J. P. Easby, "The Effect of Buoyancy on Flow and Heat Transfer for a Gas Passing Down a Vertical Pipe at Low Turbulent Reynolds Numbers," Int. J. Heat Mass Transfer, Vol. 21, pp. 791-801, 1978.

12. M. Nakajima, K. Fukui, H. Ueda, and T. Mizushina, "Buoyancy Effects on Turbulent Transport in Combined Free and Forced Convection between Vertical Parallel Plates," Int. J. Heat Mass Transfer, Vol. 23, pp. 1325-1336, 1980.

13. F. P. Incropera and D. P. DeWitt, Fundamentals of Heat and Mass Transfer, 2nd ed., Wiley, New York, 1985.

14. R. L. Webb, "A Critical Evaluation of Analytical Solutions and Reynolds Analogy Equations for Turbulent Heat and Mass Transfer in Smooth Tubes," Warme and Stoffubertragung, Vol. 4, pp. 197-204 (1971)

15. D. Wilkie, M. Cowan, P. Burnett and T. Burgoyne, "Friction Factor Measurements in a Rectangular Channel with Walls of Identical and Non-identical Roughness," Int. J. Heat and Mass Transfer, 10:611-621 (1967).

16. N. Sheriff and P. Gumley, "Heat Transfer and Friction Properties of Surfaces with Discrete Roughnesses," Int. J. Heat and Mass Transfer, 9:1296-1320 (1966).

17. J. J. More', B. S. Garbow, and K. E. Hillstrom, "User Guide for MINPACK-1, Argonne National Laboratory Report, ANL 80-74 (Aug., 1980).

18. J. C. Guzek and D. L. Polzin, "Evaluation of Natural Convective Air Cooling Test in FFTF Interim Decay Storage Vessel," Westinghouse Hanford Company Report #HEDL-TC-2683, June 1985.

19. H. Iacovides and B. E. Launder, "PSL-An Economical Approach to the Numerical Analysis of Near-Wall, Elliptic Flow," 106, Journal of Fluids Engineering, pp. 241-242, (1984).

20. S. V. Patankar and D. B. Spalding, "A Calculation Procedure for Heat, Mass and Momentum Transfer in Three-Dimensional Parabolic Flows," Int. J. Heat Mass Transfer, 15, pp. 1787-1806 (1972).

21. C. Prakash and Ye-Di Liu, "Buoyancy Induced Flow in a Vertical Internally Finned Circular Duct," Journal of Heat Transfer, 107, pp. 118-123 (1985).

22. A. F. Emery, P. K. Neighbors, and F. B. Gessner, "The Numerical Prediction of Developing Turbulent Flow and Heat Transfer in a Square Duct," Journal of Heat Transfer 102, pp. 51-57 (1980).

23. F. B. Gessner and A. F. Emery, "A Reynolds Stress Model for Turbulent Corner Flows-Part I: Development of the Model," Journal of Fluids Engineering, 98 pp. 261-268 (1976).

24. F. B. Gessner and A. F. Emery, "A Length-Scale Model for Developing Turbulent Flow in a Rectangular Duct," Journal of Fluids Engineering, 99, pp. 347-356 (1977).

25. R. R. Stewart, F. B. Cheung, D. R. Pedersen, J. H. Tessier, "Design Requirements for the Shutdown Heat Removal Test Assembly," ANL/RAS Doc. No. R0408-1000-SA, June 29, 1985.

Appendix 1

Relationship Between Loss Parameter, Ω, and the Overall inlet and Exit Loss Coefficient

In Section 3.0 of the text the loss parameter Ω was defined to be the ratio of the entrance and exit losses to the total pressure loss. In this appendix the relationship between Ω and the overall inlet and exit loss coefficient, K, will be developed.

The parameter Ω is defined as

$$\Omega = \frac{\Delta P_{loss}}{\Delta P_{total}} \tag{A-1}$$

where

$$\Delta P_{loss} = K \rho \frac{u_e^2}{2} \tag{A-2}$$

$$\Delta P_{tot} = \Delta P_{loss} + \Delta P_H \tag{A-3}$$

$$\Delta P_H = \frac{2 f \rho u^2 L_H}{D_H} \tag{A-4}$$

K = overall inlet and exit loss coefficient

u_e = velocity in entrance region

u = velocity in heated zone

In equation (A-2) it is assumed that the entrance/exit flow area, A_e, is not equal to the flow area in the heated zone, A_H, thus the velocity u_e is related to the velocity in the heated zone by the following relation

$$u_e = \frac{A_H}{A_e} u \qquad \text{(A-5)}$$

where A_H = flow area in heated zone

A_e = flow area in entrance exit zone

Thus inserting (A-2) to (A-5) in equation (A-1) and solving for K yields

$$K = \frac{\Omega\ 4\ f\ L_H\ A_E^2}{(1 - \Omega)\ D_H\ A_H^2}$$

or solving for Ω

$$\Omega = \frac{K}{K + \dfrac{4\ f\ L_H\ A_E^2}{D_H\ A_H^2}}$$

Appendix 2. Computer Program Listing

This appendix presents listings of FORTRAN computer programs used to obtain the results given in Section 4 of this report. The following listings are provided:

Program 1 - Smooth Channels

Program 2 - Repeated Ribs: $e^+ > 35$

Program 3 - Repeated Ribs: $e^+ < 25$

Program 4 - Fins on Guard Vessel

Program 5 - Penn State University - Program for Smooth Channel and Repeated Ribs

Program 1

FILE: SMOOTH FORTRAN A1 ANL VM/SP 335 CMS

```
C                                                                       SMO00010
C     $$$$$$$$$$$$$$$$$$$$$$$$   THIS IS A SMOOTH CHANNEL MODEL-NO FINS SMO00020
C                                                                       SMO00030
C     OR RIBS  $$$$$$$$$$$$$$$$$$$$$$$$$$$$$$$$$$$$$$$$$$$$$$$$$$$$$$SMO00040
C                                                                       SMO00050
C                                                                       SMO00060
C     THIS PROGRAM IS FOR RACS WITHOUT FINS OR RIBS I.E. FOR SMOOTH     SMO00070
C     CHANNELS.  IT IS BASED ON EQ'S. DERIVED BY F. B. CHEUNG.          SMO00080
C     $$$$$$$$$$$$$$$$$$$$$$$$$$$$$$$$$$$$$$$$$$$$$$$$$$$$$$$$$$$$$$SMO00090
C                                                                       SMO00100
C     UNITS OF OUTPUTS ARE METERS,KELVIN,METERS/SEC. & KW/M**2          SMO00110
C                                                                       SMO00120
C     $$$$$$$$$$$$$$$$$$$$$$$$$$$$$$$$$$$$$$$$$$$$$$$$$$$$$$$$$$$$$$SMO00130
      REAL L,LH,NU,NU,K,LSTACK                                          SMO00140
      DATA RHO,G,BETA,T0,CP,MU,ALPHA,NU,K,SIGMA                         SMO00150
     1 /1200.,9.8,0.00367,293.,1.0,0.019,                               SMO00160
     2  2.23E-5,1.59E-5,0.027,5.67E-8/                                  SMO00170
      DATA CCONV/0.1/                                                   SMO00180
1     WRITE(6,3)                                                        SMO00190
3     FORMAT(1X,'INPUT H IN INCHES')                                    SMO00200
      READ(5,*) H                                                       SMO00210
      WRITE(6,4)                                                        SMO00220
4     FORMAT(1X,'ENTER STACK HEIGHT AND HEATED LENGTH IN FEET')         SMO00230
      READ(5,*) LSTACK,LH                                               SMO00240
      LH=0.3048*LH                                                      SMO00250
      LSTACK=0.3048*LSTACK                                              SMO00260
      L=LSTACK+LH                                                       SMO00270
      WRITE(6,5)                                                        SMO00280
5     FORMAT(1X,'ENTER VALUE OF OMEGA=DELP(LOSS)/DELP(TOTAL) AND EMMISIVSMO00290
     1ITY')                                                             SMO00300
      READ(5,*) OMEGA,EPS                                               SMO00310
      H=H/39.37                                                         SMO00320
      WRITE(6,6) H,LH,LSTACK,OMEGA,EPS                                  SMO00330
      WRITE(50,6) H,LH,LSTACK,OMEGA,EPS                                 SMO00340
6     FORMAT(1X,'H=',F10.4,2X,'LH=',F10.4,2X,'LSTACK=',F10.4,2X,        SMO00350
     1'OMEGA=',F10.4,2X,'EPS=',F10.4,///)                               SMO00360
7     WRITE(6,8)                                                        SMO00370
8     FORMAT(1X,'ENTER VALUE OF HEAT FLUX IN KW/M**2')                  SMO00380
      READ(5,*) QW                                                      SMO00390
      QW=1.E3*QW                                                        SMO00400
      EPSW=EPS                                                          SMO00410
      EPSS=EPS                                                          SMO00420
C     THE FOLLOWING ASSIGNMENT OF AW=400 IS AN INITIAL GUESS            SMO00430
      AW=400.                                                           SMO00440
      TERM1=RHO*G*BETA*(1.0-OMEGA)                                      SMO00450
      TERM2=QW*LH*(L-0.5*LH)/(RHO*CP*H)                                 SMO00460
      TERM3=0.0665*(RHO**(3./4.))*(MU**0.25)*LH                         SMO00470
      U=H**(5./11.)*(TERM1*TERM2/TERM3)**(4./11.)                       SMO00480
      HW=(0.02*K*(U** 0.8))/((H**0.2)*(ALPHA*NU)**0.4)                  SMO00490
      HS=HW                                                             SMO00500
      BW=QW/(RHO*CP*U*H)                                                SMO00510
      BS=BW                                                             SMO00520
10    AS=T0+(QW-HW*(AW-T0))/HS                                          SMO00530
      TERM4=(AW+BW*LH/2.)**4                                            SMO00540
      TERM5=(AS+BS*LH/2.)**4                                            SMO00550
```

Program 1 (cont'd)

FILE: SMOOTH FORTRAN A1 ANL VM/SP 305 CMS

```
      TERM5=HS*(1.0/EPSH+1.0/EPSS-1.0)                                  SMO00560
      ASMIN=T0+SIGMA*(TERM4-TERM5)/TERM5                                SMO00570
      DELAS=ASMIN-AS                                                    SMO00580
      IF(ABS(DELAS).LT.0.1) GO TO 30                                    SMO00590
      AW=AW-DELAS*CCONV                                                 SMO00600
      GO TO 10                                                          SMO00610
30    WRITE(6,40) DELAS                                                 SMO00620
40    FORMAT(1X,'ERROR IN CALCULATED VALUE OF AS=',F10.4)               SMO00630
      TA=T0+QW*LH/(RHO*CP*U*H)                                          SMO00640
      TGV=AW+BW*LH                                                      SMO00650
      TFS=AS+BS*LH                                                      SMO00660
      QW=QW*1.E-3                                                       SMO00670
      WRITE(6,44) QW                                                    SMO00680
      WRITE(50,44) QW                                                   SMO00690
44    FORMAT(1X,'HEAT FLUX-(KW/M**2)=',F10.4)                           SMO00700
      WRITE(6,45)                                                       SMO00710
      WRITE(50,45)                                                      SMO00720
45    FORMAT(5X,'H',10X,'U',10X,'TA',10X,'TGV0',6X,'TGV',8X,'TFS0',     SMO00730
     Y6X,'TFS',6X,'HW')                                                 SMO00740
      WRITE(50,50) H,U,TA,AW,TGV,AS,TFS,HW                              SMO00750
      WRITE(6,50) H,U,TA,AW,TGV,AS,TFS,HW                               SMO00760
50    FORMAT(1X,8F10.4)                                                 SMO00770
      WRITE(6,60)                                                       SMO00780
60    FORMAT(1X,'ENTER POSITIVE NUMBER TO RERUN; NEGATIVE TO TERMINATE') SMO00790
      READ(5,*) IRUN                                                    SMO00800
      IF(IRUN) 100,100,1                                                SMO00810
100   STOP                                                              SMO00820
      END                                                               SMO00830
```

Program 2

FILE: BIGRIBS FORTRAN A1 ANL VM/SP 305 CMS

```
C                                                                       BIG00010
C     $$$$$$$$$$$$$$  THIS IS A MODEL FOR BIG RIBS-E+ > 35 $$$$$$$$$$$$ BIG00020
C                                                                       BIG00030
C     THIS PROGRAM IS FOR RACS/RVACS WITH RIBBED SURFACES.  IT IS       BIG00040
C     ONE OF TWO SUCH PROGRAMS: THIS ONE FOR LARGE RIBS(E+ > 35)        BIG00050
C     THE OTHER,SMALLRIB FORTRAN FOR SMALL RIBS(E+ < 25).               BIG00060
C                                                                       BIG00070
C     THIS PROGRAM IS BASED ON EQ'S. DEVELOPED BY F. B. CHEUNG          BIG00080
C     BASED ON WORK PERFORMED BY R. WEBB(PENN. STATE).  THE CORRELATIONSBIG00090
C     ARE VALID FOR E+ > 35. FOR SMALLER VALUES OF E+ (E+ < 25.) THE    BIG00100
C     PROGRAM SMALLRIB FORTRAN SHOULD BE USED.                          BIG00110
C                                                                       BIG00120
C     $$$$$$$$$$$$$$$$$$$$$$$$$$$$$$$$$$$$$$$$$$$$$$$$$$$$$$$$$$$$$$$BIG00130
C     UNITS OF OUTPUTS ARE IN METERS,KELVIN,METERS/SEC & KW/M**2        BIG00140
C     $$$$$$$$$$$$$$$$$$$$$$$$$$$$$$$$$$$$$$$$$$$$$$$$$$$$$$$$$$$$$$$BIG00150
      REAL L,LH,MU,NU,K,NUM,LSTACK                                      BIG00160
      DATA RHO,G,BETA,T0,CP,MU,ALPHA,NU,K,SIGMA                         BIG00170
     1 /1200.,9.8,0.00367,293.,1.0,0.019,                               BIG00180
     2  2.25E-5,1.58E-5,0.027,5.67E-8/                                  BIG00190
1     WRITE(6,3)                                                        BIG00200
3     FORMAT(1X,'INPUT H IN INCHES')                                    BIG00210
      READ(5,*) H                                                       BIG00220
      WRITE(6,4)                                                        BIG00230
4     FORMAT(1X,'ENTER STACK HEIGTH AND HEATED LENGTH IN FEET')         BIG00240
      READ(5,*) LSTACK,LH                                               BIG00250
      LH=0.3048*LH                                                      BIG00260
      LSTACK=0.3048*LSTACK                                              BIG00270
      L=LSTACK+LH                                                       BIG00280
      WRITE(6,5)                                                        BIG00290
5     FORMAT(1X,'ENTER VALUE OF OMEGA=DELP(LOSS)/DELP(TOTAL)AND EMMISIVIBIG00300
     1TY')                                                              BIG00310
      READ(5,*) OMEGA,EPS                                               BIG00320
      WRITE(6,6)                                                        BIG00330
6     FORMAT(1X,'INPUT E IN INCHES')                                    BIG00340
      READ(6,*) E                                                       BIG00350
      H=H/39.37                                                         BIG00360
      E=E/39.37                                                         BIG00370
      WRITE(6,7)                                                        BIG00380
7     FORMAT(1X,'INPUT VALUE P/E I.E. MULTIPLIER OF E TO GET P')        BIG00390
      READ(6,*) PE                                                      BIG00400
      WRITE(6,12) H,LH,LSTACK,OMEGA,EPS,E,PE                            BIG00410
      WRITE(50,12) H,LH,LSTACK,OMEGA,EPS,E,PE                           BIG00420
12    FORMAT(1X,'H=',F8.4,1X,'LH=',F8.4,1X,'LSTACK=',F8.4,1X,           BIG00430
     1'OMEGA=',F4.2,1X,'EPS=',F4.2,1X,'E=',F8.6,1X,'PE=',F8.4,///)      BIG00440
       P=PE*E                                                           BIG00450
      EPSW=EPS                                                          BIG00460
      EPSS=EPS                                                          BIG00470
      WRITE(6,13)                                                       BIG00480
13    FORMAT(1X,'ENTER VALUE OF HEAT FLUX IN KW/M**2')                  BIG00490
      READ(5,*) QW                                                      BIG00500
      QW=QW*1.E3                                                        BIG00510
8     FORMAT(1X,'INPUT INITIAL GUESS OF AW IN KELVIN')                  BIG00520
      WRITE(6,8)                                                        BIG00530
      READ(5,*) AW                                                      BIG00540
      F=2.0/(2.5*ALOG(H/E)+0.95*(P/E)**0.53-3.75)**2                    BIG00550
```

Program 2 (cont'd)

FILE: BIGRIBS FORTRAN A1 ANL VM/SP 305 CMS

```
      TERM1=G*BETA*(1.0-OMEGA)                                          BIG00550
      TERM2=QW*LH*(L-0.5*LH)/CP                                         BIG00570
      TERM3=RHO*F*LH                                                    BIG00580
      U=(TERM1*TERM2/TERM3)**(1./3.)                                    BIG00590
      RE=2.*RHO*U*H/NU                                                  BIG00600
      ESTAR= (E/(2.0*H))*RE*SQRT(F/2.0)                                 BIG00610
      NUM=RHO*CP*U*F/2.0                                                BIG00620
      DEN1=SQRT(F/2.0)                                                  BIG00630
      DEN2=4.5*((ESTAR)**0.28)*(NU/ALPHA)**0.57                         BIG00640
      DEN3=0.95*(P/E)**0.53                                             BIG00650
      DEN=DEN1*(DEN2-DEN3)                                              BIG00660
      HW=NUM/(1.0+DEN)                                                  BIG00670
      HS=HW                                                             BIG00680
      BW=QW/(RHO*CP*U*H)                                                BIG00690
      BS=BW                                                             BIG00700
10    AS=T0+(QW-HW*(AW-T0))/HS                                          BIG00710
      TERM4=(AW+BW*LH/2.)**4                                            BIG00720
      TERM5=(AS+BS*LH/2.)**4                                            BIG00730
      TERM6=HS*(1.0/EPSW+1.0/EPSS-1.0)                                  BIG00740
      ASNEW=T0+SIGMA*(TERM4-TERM5)/TERM6                                BIG00750
      DELAS=ASNEW-AS                                                    BIG00760
      IF(ABS(DELAS).LT.0.1) GO TO 30                                    BIG00770
      AW=AW-DELAS/2.0                                                   BIG00780
      GO TO 10                                                          BIG00790
30    AS=ASNEW                                                          BIG00800
      WRITE(6,40) DELAS                                                 BIG00810
40    FORMAT(1X,'ERROR IN CALCULATED VALUE OF TGV0=',F10.4)             BIG00820
      TGV0=AW                                                           BIG00830
      TFS0=AS                                                           BIG00840
      TA=T0+QW*LH/(RHO*CP*U*H)                                          BIG00850
      TGV=AW+BW*LH                                                      BIG00860
      TFS=AS+BS*LH                                                      BIG00870
      QW=QW*1.E-3                                                       BIG00880
      WRITE(6,45)                                                       BIG00890
      WRITE(50,45)                                                      BIG00900
45    FORMAT(5X,'H',10X,'E',10X,'P',10X,'U',6X,'TA',10X,'TGV0',         BIG00910
     Y6X,'TGV',6X,'TFS0',7X,'TFS',8X,'HW')                              BIG00920
      WRITE(6,50) H,E,P,U,TA,TGV0,TGV,TFS0,TFS,HW                       BIG00930
      WRITE(50,50) H,E,P,U,TA,TGV0,TGV,TFS0,TFS,HW                      BIG00940
50    FORMAT(1X,10F10.4)                                                BIG00950
      WRITE(6,51) F,RE,ESTAR,QW                                         BIG00960
      WRITE(50,51) F,RE,ESTAR,QW                                        BIG00970
51    FORMAT(1X,'F=',F10.4,2X,'RE=',F12.2,2X,'ESTAR=',F10.4,2X,'QW=',F10BIG00980
     Y.4)                                                               BIG00990
      WRITE(6,60)                                                       BIG01000
60    FORMAT(1X,'ENTER POSITIVE NUMBER TO RERUN; NEGATIVE TO TERMINATE')BIG01010
      READ(5,*) IRUN                                                    BIG01020
      IF(IRUN) 100,100,1                                                BIG01030
100   STOP                                                              BIG01040
      END                                                               BIG01050
```

Program 3

FILE: SMALRIBS FORTRAN A1 ANL VM/SP 305 CMS

```
C                                                                       SMA00010
C     $$$$$$$$$$$$$$$$$$$$$$  THIS IS A MODEL FOR SMALL RIBS-E+ < 25 $$$SMA00020
C                                                                       SMA00030
C     THIS PROGRAM HAS DEVELOPED USING EQ'S. DEVELOPED BY F. B. CHEUNG. SMA00040
C     CORRELATIONS DERIVED FROM WORK BY R. WEBB-PENN. STATE ARE USED.   SMA00050
C                                                                       SMA00060
C     $$$$$$$$$$$$$$$$$$$$$$$$$$$$$$$$$$$$$$$$$$$$$$$$$$$$$$$$$$$$$$SMA00070
C     UNITS OF OUTPUTS ARE METERS,KELVIN,METERS/SEC. & KW/M**2          SMA00080
C     $$$$$$$$$$$$$$$$$$$$$$$$$$$$$$$$$$$$$$$$$$$$$$$$$$$$$$$$$$$$$$SMA00090
      REAL L,LH,MU,NU,K,NUM,LSTACK                                      SMA00100
      DATA RHO,G,BETA,TO,CP,MU,ALPHA,NU,K,SIGMA                         SMA00110
     1 /1200.,9.8,0.00367,293.,1.0,0.019,                               SMA00120
     2  2.25E-5,1.58E-5,0.027,5.67E-8/                                  SMA00130
1      WRITE(6,3)                                                       SMA00140
3     FORMAT(1X,'INPUT H IN INCHES')                                    SMA00150
      READ(5,*) H                                                       SMA00160
      WRITE(6,4)                                                        SMA00170
4     FORMAT(1X,'ENTER STACK HEIGHT AND HEATED LENGTH IN FEET')         SMA00180
      READ(5,*) LSTACK,LH                                               SMA00190
      WRITE(6,5)                                                        SMA00200
      LH=LH*0.3048                                                      SMA00210
      LSTACK=LSTACK*0.3048                                              SMA00220
      L=LSTACK+LH                                                       SMA00230
5     FORMAT(1X,'ENTER VALUE OF OMEGA=DELP(LOSS)/DELP(TOTAL) AND EMMISIVSMA00240
     1ITY')                                                             SMA00250
      READ(5,*) OMEGA,EPS                                               SMA00260
      WRITE(6,6)                                                        SMA00270
6     FORMAT(1X,'INPUT E IN INCHES')                                    SMA00280
      READ(6,*) E                                                       SMA00290
      H=H/39.37                                                         SMA00300
      E=E/39.37                                                         SMA00310
      WRITE(6,7)                                                        SMA00320
7     FORMAT(1X,'INPUT VALUE P/E I.E. MULTIPLIER OF E TO GET P')        SMA00330
      READ(6,*) PE                                                      SMA00340
      WRITE(6,12) H,LH,LSTACK,OMEGA,EPS,E,PE                            SMA00350
      WRITE(50,12) H,LH,LSTACK,OMEGA,EPS,E,PE                           SMA00360
12    FORMAT(1X,'H=',F8.4,2X,'LH=',F8.4,1X,'LSTACK=',F8.4,1X,           SMA00370
     1'OMEGA=',F4.2,1X,'EPS=',F4.2,1X,'E=',F8.6,1X,'PE=',F8.4,///)      SMA00380
      P=PE*E                                                            SMA00390
      WRITE(6,13)                                                       SMA00400
13    FORMAT(1X,'ENTER VALUE OF HEAT FLUX IN KW/M**2')                  SMA00410
      READ(5,*) QW                                                      SMA00420
      QW=QW*1.E3                                                        SMA00430
      EPSW=EPS                                                          SMA00440
      EPSS=EPS                                                          SMA00450
      WRITE(6,8)                                                        SMA00460
8     FORMAT(1X,'INPUT INITIAL GUESS OF AW IN KELVIN')                  SMA00470
      READ(5,*) AW                                                      SMA00480
      F=2.0/(2.5*ALOG(H/E)+0.95*(P/E)**0.53-3.75)**2                    SMA00490
      TERM1=G*BETA*(1.0-OMEGA)                                          SMA00500
      TERM2=QW*LH*(L-0.5*LH)/CP                                         SMA00510
9     TERM3=RHO*F*LH                                                    SMA00520
      U=(TERM1*TERM2/TERM3)**(1./3.)                                    SMA00530
      RE=2.*RHO*U*H/MU                                                  SMA00540
10    ESTAR= (E/(2.0*H))*RE*SQRT(F/2.0)                                 SMA00550
```

Program 3 (cont'd)

FILE: SMALRIBS FORTRAN A1 ANL VM/SP 305 CMS

```
      IF(ESTAR.LE.25.0) GO TO 11                                        SMA00560
      E=E/2.0                                                           SMA00570
      P=PE*E                                                            SMA00580
      GO TO 10                                                          SMA00590
11    GBAR=11.1                                                         SMA00600
      UESTAR=(2.64*(P/E)**0.53)*(1.0-0.18*ALOG(ESTAR))                  SMA00610
      FNEW=2.0/(2.5*ALOG(H/E)+UESTAR-3.75)**2                           SMA00620
      DELF=FNEW-F                                                       SMA00630
      IF(ABS(DELF).LT.0.0001) GO TO 15                                  SMA00640
      F=FNEW-DELF/2.0                                                   SMA00650
      GO TO  9                                                          SMA00660
15    F=FNEW                                                            SMA00670
      NUM=RHO*U*CP*F/2.0                                                SMA00680
      DEN1=GBAR*((NU/ALPHA)**0.57)-UESTAR                               SMA00690
      DEN2=DEN1*SQRT(F/2.0)+1.0                                         SMA00700
      HW=NUM/DEN2                                                       SMA00710
      HS=HW                                                             SMA00720
      BW=QW/(RHO*CP*U*H)                                                SMA00730
      BS=BW                                                             SMA00740
20    AS=T0+(QW-HW*(AW-T0))/HS                                          SMA00750
      TERM4=(AW+BW*LH/2.)**4                                            SMA00760
      TERM5=(AS+BS*LH/2.)**4                                            SMA00770
      TERM6=HS*(1.0/EPSW+1.0/EPSS-1.0)                                  SMA00780
      ASNEW=T0+SIGMA*(TERM4-TERM5)/TERM6                                SMA00790
      DELAS=ASNEW-AS                                                    SMA00800
      IF(ABS(DELAS).LT.0.1) GO TO 30                                    SMA00810
      AW=AW-DELAS/2.0                                                   SMA00820
      GO TO 20                                                          SMA00830
30    AS=ASNEW                                                          SMA00840
      WRITE(6,40) DELAS                                                 SMA00850
40    FORMAT(1X,'ERROR IN CALCULATED VALUE OF TFS0=',F10.4)             SMA00860
      TA=T0+QW*LH/(RHO*CP*U*H)                                          SMA00870
      TGV=AW+BW*LH                                                      SMA00880
      TFS=AS+BS*LH                                                      SMA00890
      TGV0=AW                                                           SMA00900
      TFS0=AS                                                           SMA00910
      H=H*39.37                                                         SMA00920
      E=E*39.37                                                         SMA00930
      P=PE*E                                                            SMA00940
      QW=QW*1.E-3                                                       SMA00950
      WRITE(6,45)                                                       SMA00960
      WRITE(50,45)                                                      SMA00970
45    FORMAT(5X,'H',10X,'E',10X,'P',10X,'U',6X,'TA',10X,'TGV0',         SMA00980
     Y6X,'TGV',6X,'TFS0',7X,'TFS',8X,'HW')                              SMA00990
      WRITE(6,50) H,E,P,U,TA,TGV0,TGV,TFS0,TFS,HW                       SMA01000
      WRITE(50,50) H,E,P,U,TA,TGV0,TGV,TFS0,TFS,HW                      SMA01010
50    FORMAT(1X,F10.4,1X,F12.8,1X,8F10.4)                               SMA01020
      WRITE(6,51) F,RE,ESTAR,QW                                         SMA01030
      WRITE(50,51) F,RE,ESTAR,QW                                        SMA01040
51    FORMAT(1X,'F=',F10.6,2X,'RE=',F12.2,2X,'ESTAR=',F10.4,2X,'QW=',   SMA01050
     1F10.4)                                                            SMA01060
      WRITE(6,60)                                                       SMA01070
60    FORMAT(1X,'ENTER POSITIVE NUMBER TO RERUN; NEGATIVE TO TERMINATE')SMA01080
      READ(5,*) IRUN                                                    SMA01090
      IF(IRUN) 100,100,1                                                SMA01100
```

Program 3 (cont'd)

```
FILE: SMALRIBS FORTRAN  A1  ANL VM/SP 305 CMS

100   STOP                                                    SMA01110
      END                                                     SMA01120
```

Program 4

```
C  TITLE FINS ON GAURD VESSEL CHEUNG'S FORMULATION: 6-22-85
C
C  $$$$$$$$$$$$$$$$$$$$$$$$$$$$$$$$$$$$$$$$$$$$$$$$$$$$$$$$$$$$$$$$$$$$$$$$
C  THIS VERSION IS FOR RACS WITH FINS
      IMPLICIT REAL*8(A-H,O-Z)
      DIMENSION X(9),FVEC(9),WA(200)
      EXTERNAL FCN
      COMMON/PROP/G,BETA,QW,RHOHO,CP,VISK,S,H,TO,FKF,ALPHA,FLH,
     1FL,FK,PR,EGV,ED,EF,SIG,U,FMU,HTC,BFIN,FGD,IFIN
C  $$$$$$$$$$$$$$$$$$$$$$$$$$$$$$$$$$$$$$$$$$$$$$$$$$$$$$$$$$$$$$$$$$$$$$$$
      IFIN=0
C   IFIN=1,FOR FINS ON DUCT WALL: IFIN=0,FOR FINS ON GUARD VESSEL
      QW=1.0D4
      H=0.3048D0
      S=H
      TO=293.D0
      FLH=12.192D0
      FL=27.432D0
      BFIN=0.0127D0
      OMEGA=0.50D0
       G=9.8D0
      ALPHA=2.25D-5
      SIG=5.67D-8
      BETA=0.00367DD0
      RHOHO=1.2D0
      CP=1.D3
      VISK=1.58D-5
      FKF=19.D0
C     FKF=374.D0
      FK=0.027D0
      EGV=0.7D0
      EF=EGV
      ER=EGV
      ED=EGV
CONSTANT G=9.8,BETA=0.00367,RHOHO=1.2,CP=1.,VISK=1.58E-5,FKF=19.,...
C     ALPHA=2.25E-5,FK=0.027,PR=0.7,EGV=0.7,ED=0.7,EF=0.7,ER=0.7,...
C     SIG=5.62E-8,N=9
      N=9
      F1=RHOHO*G*BETA*(1.-OMEGA)*QW*(FL-0.5*FLH)
      FMU=VISK*RHOHO
      F2=0.0665*(RHOHO**1.75)*CP*(FMU**.25)*H
      DH=2.D0*S*H/(S+H)
      DHH=DH/2.D0
      U=(DHH**(5./11.))*(F1/F2)**(4./11.)
      HTC=0.02*FK*(U**.8)/((DHH**.2)*(ALPHA*VISK)**.4)
      FMM=DSQRT(HTC/(FKF*BFIN))
      PHM=FMM*H
      ETAC=DTANH(PHM)/PHM
      LHA=(N*(3*N+13))/2
      XX=H/S
      Y=FLH/S
      DXX=1.+XX*XX
      DY=1.+Y*Y
      DXXS=DSQRT(DXX)
      DYS=DSQRT(DY)
      P1=DLOG(DSQRT(DXX*DY/(DXX+Y*Y)))
      P2=Y*DXXS*DATAN(Y/DXXS)
      P3=XX*DYS*DATAN(XX/DYS)
      P4=-Y*DATAN(Y)-XX*DATAN(XX)
```

Program 4 (cont'd)

```
      FGD=2.*(P1+P2+P3+P4)/(3.14159265*XX*Y)
C  FOR IFIN=0,X(2)=TGV-TF,FOR IFIN=1,X(2)=TD-TF
C  X(1)=TGV-TA,X(3)=TD-TA,X(4)=QRGV,X(5)=QRD,X(6)=QC,
C  X(7)=FJGV,X(8)=FJD,X(9)=FJF
      TOL=1.D-20
      X(1)=100.D0
      X(2)=50.D0
      X(3)=30.D0
      FM=1.-FGD
      AGV=X(1)+TO
      BGV=QW/(RHOHO*CP*U*H)
      BD=BGV
      BF=BGV
      AD=X(3)+TO
      AF=AGV-X(2)
      IF(IFIN.EQ.1)AF=-X(2)+AD
      TGVA=AGV+BGV*FLH/2.
      TDA=AD+BD*FLH/2.
      TFA=AF+BF*FLH/2.
      FJGV=EGV*SIG*TGVA**4
      FJD=ED*SIG*TDA**4
      FJF=EF*SIG*TFA**4
      X(7)=FJGV
      X(8)=FJD
      X(9)=FJF
      QRGV=EGV*(SIG*TGVA**4-FGD*FJD-FM*FJF)
      QRD=ED*(SIG*TDA**4-FGD*FJGV-FM*FJF)
      DTF=AGV-AF
      IF(IFIN.EQ.1)DTF=AD-AF
      QC=2.*FKF*DTF/H
      X(4)=QRGV
      X(5)=QRD
      X(6)=QC
      CALL HYBRD1(FCN,N,X,FVEC,TOL,INFO,WA,LWA)
      FM=1.-FGD
      AGV=X(1)+TO
      BGV=QW/(RHOHO*CP*U*H)
      BD=BGV
      BF=BGV
      AD=X(3)+TO
      AF=AGV-X(2)
      IF(IFIN.EQ.1)AF=-X(2)+AD
      TGVA=AGV+BGV*FLH/2.
      TDA=AD+BD*FLH/2.
      TFA=AF+BF*FLH/2.
      RE=U*DH/VISK
      FRF=0.0791*RE**(-0.25)
      DPLH=2.*FRF*RHOHO*U*U*FLH/DH
      DPL=DPLH*FL/FLH
      DP=DPLH/(1.-OMEGA)
      QRGV=X(4)
      QRD=X(5)
      QC=X(6)
      FJGV=X(7)
      FJD=X(8)
      FJF=X(9)
      TFB=TGVA
      AFB=AGV
      IF(IFIN.EQ.1)TFB=TDA
      IF(IFIN.EQ.1)AFB=AD
```

Program 4 (cont'd)

```
      QRF=EF*(SIG*TFA**4-S*FM*(FJGV+FJD)/(2.*H)-(1.-S*FM/H)*FJF)
      NUMR=EF*SIG*TFB**4+(1.-EF)*(S*FM*(FJGV+FJD)/(2.*H))
      DENM=1.-(1.-EF)*(1.-S*FM/H)
      FJFGV=NUMR/DENM
      QRFGV=EF*(SIG*TFB**4-S*FM*(FJGV+FJD)/(2.*H)-(1.-S*FM/H)*FJFGV)
      ETA=(HTC*(AF-TO)+QRF)/(HTC*(AGV-TO)+QRFGV)
      ETACH=(AF-TO)/(AFB-TO)
      DEVEF=(ETACH-ETAC)*100.D0/ETAC
      TRA=(TGVA**4+QW*(1./ER+1./EGV-1.)/SIG)**.25
      NZ=50
      DZ=FL/DFLOAT(NZ)
      NZP1=NZ+1
      DO 10 I=1,NZP1
      Z=(I-1)*DZ
      TA=TO+QW*Z/(RHOHO*CP*U*H)
      TAF=TO+QW*FLH/(RHOHO*CP*U*H)
      IF(Z.GE.FLH)TA=TAF
      TF=AF-TO+TA
      TGV=AGV-TO+TA
      TD=AD-TO+TA
      DPZ=DPLH*Z/FLH
      QGVC=HTC*(TGV-TA)
      WRITE(6,100)Z,TA,TF,TGV,TD,DPZ
  100 FORMAT(3X,' Z=',E10.3,' TA=',E10.3,' TF=',E10.3,' TGA=',E10.3,
     1'  TD=',E10.3,' DPZ=',E10.3)
   10 CONTINUE
      WRITE(6,110)ETA,TRA,TGVA,TFA,TDA,FGD,U,INFO,HTC,ETAC,ETACH,DEVEF
  110 FORMAT(//, '  ETA=',F7.4,'  TRA=',E10.3,' TGVA=',E10.3,'  TFA
     1=',E10.3,/,' TDA=',E10.3,' FGD=',E10.3,' U=',E10.3,' INFO=',I3,
     2'  HTC=',E10.3,'  ETAC=',E10.3,' ETACH=',E10.3,' DEVEF=',E10.3,//)
      WRITE(6,120)(FVEC(I),I=1,N)
  120 FORMAT(//,' F1=',E10.3,' F2=',E10.3,' F3=',E10.3,' F4=',E10.3,
     1'  F5=',E10.3,' F6=',E10.3,' F7=',E10.3,' F8=',E10.3,' F9=',
     2E10.3,//)
      WRITE(6,130)QGVC,QRGV,QRF,QRD
  130 FORMAT(//,' QGVC=',E10.3,'  QRGV=',E10.3,'  QRF=',E10.3,
     1' QRD=',E10.3,//)
      STOP
      END
      SUBROUTINE FCN(N,X,FVEC,IFLAG)
      IMPLICIT REAL*8(A-H,O-Z)
      DIMENSION X(N),FVEC(N)
      COMMON/PROP/G,BETA,QW,RHOHO,CP,VISK,S,H,TO,FKF,ALPHA,FLH,
     1FL,FK,PR,EGV,ED,EF,SIG,U,FMU,HTC,BFIN,FGD,IFIN
C  FOR IFIN=0,X(2)=TGV-TF,FOR IFIN=1,X(2)=TD-TF
C  X(1)=TGV-TA,X(3)=TD-TA,X(4)=QRGV,X(5)=QRD,X(6)=QC,
C  X(7)=FJGV,X(8)=FJD,X(9)=FJF
      FVEC(1)=HTC*X(1)+X(4)+2.D0*BFIN*(1-IFIN)*X(6)/S-QW
      FVEC(2)=X(5)+HTC*X(3)+IFIN*2.D0*BFIN*X(6)/S
      AGV=X(1)+TO
      BGV=QW/(RHOHO*CP*U*H)
      FM=1.-FGD
      BD=BGV
      BF=BGV
      AD=X(3)+TO
      AF=AGV-X(2)
      IF(IFIN.EQ.1)AF=-X(2)+AD
      TGVA=AGV+BGV*FLH/2.
      TDA=AD+BD*FLH/2.
      TFA=AF+BF*FLH/2.
```

Program 4 (cont'd)

```
      FVEC(3)=X(6)-2.*FKF*X(2)/H
      FVEC(4)=EGV*(SIG*TGVA**4-FGD*X(8)-FM*X(9))-X(4)
      FVEC(5)=ED*(SIG*TDA**4-FGD*X(7)-FM*X(9))-X(5)
      RH6=EF*(SIG*TFA**4-S*FM*(X(7)+X(8))/(2.*H)-(1.-S*FM/H)*X(9))
      FVEC(6)=RH6-2.D0*FKF*BFIN*X(2)/(H*H)+HTC*(AF-TO)
      FVEC(7)=EGV*SIG*TGVA**4+(1.-EGV)*(FGD*X(8)+FM*X(9))-X(7)
      FVEC(8)=ED*SIG*TDA**4+(1.-ED)*(FGD*X(7)+FM*X(9))-X(8)
      RH9=EF*SIG*TFA**4+(1.-EF)*(S*FM*(X(7)+X(8))/(2.*H)+(1.-S*FM/H)
     1*X(9))
      FVEC(9)=RH9-X(9)
      RETURN
      END
```

Program 5

```
      REAL*8   WK(68),X(2),PAR(2),FNORM,LH,MU,K,EPS,XL,XR,XAPP
     >        ,B2,RE,EP
      DIMENSION A1(10),EP1(10),GE1(10),B10(10,3),B1(3),H(2)
      INTEGER SURF
      EXTERNAL F
      EXTERNAL     FCN
      COMMON /DATA1/ SIGMA,EW,ES,HI,A
      COMMON /ROUGH/ B2,EP,RE
C
C **** SURF=1 ( PLAIN ) , SURF=2 ( ROUGH ) *********
C
      READ,(EP1(KK),GE1(KK),(B10(KK,J2),J2=1,3),KK=1,9)
      DO 111 J=1,2
      DO 112 K1=1,2
      SURF=J
      M1=10
      DATA H/0.254,0.381/
C
      IF(SURF.EQ.1)THEN
      WRITE(6,11)
      WRITE(6,14)
      ELSE
      WRITE(6,12)
      END IF
   11 FORMAT(//,10X,'**** PLAIN SURFACE ****')
   12 FORMAT(//,10X,'**** ROUGH SURFACE ****')
   13 FORMAT(/,4X,'EP',3X,'G(E)',2X,'B(PE)',2X,'P(MM)',1X,'E(MM)',3X,
     >  'H',7X,'G',10X,'FR',7X,'FR/FS',5X,'HI',6X,'E/D',
     >  9X,'RE',8X,'TFAV',5X,'TWAV',5X,'TSAV')
   14 FORMAT(/,4X,'H',7X,'G',10X,'FS',
     >   9X,'HI',8X,'RE',5X,'TFAV',5X,'TWAV',5X,'TSAV')
   15 FORMAT(/,20X,'--- P/E=',F5.3,' ---',T30,I2)
C     QW(W/M**2),   H(M),   S(M),   TO(K)
C     LH(M),   RO(KG/M**3),   GR(M/S**2)
C     CP(J/(KG*K)),   MU(N*S/M**2),   BETA(1./K)
C     R(J/(KG*K)),   K(W/(M*K)),
C     SIGMA(W/(M**2*K**4)),   G(KG/(M**2*S))
      QW=10.76E3
      G=10.
      S=100.
      TO=38.+273.
      LH=12.19
      RO=1.1248
      CP=1007.44
      GR=9.8
      R=287.
      SIGMA=5.669E-8
      OMEGA=0.5
      EW=0.7
      ES=0.7
   10 TFAV=TO+QW*LH/(2.*G*H(K1)*CP)
      BETA=1./TFAV
      MU=(3.6945705+0.7217775*TFAV-0.43997518E-3*TFAV**2+
     >     0.13530831E-6*TFAV**3)*10.**(-7)
      K=(-3.0992317+0.12297106*TFAV-0.86889035E-4*TFAV**2+
     >    0.3353232E-7*TFAV**3)*10.**(-3)
      PR=0.84168774-0.69540367E-3*TFAV+0.95679111E-6*TFAV**2-
     >     0.37750492E-9*TFAV**3

      GAM=QW/(G*H(K1)*CP)
```

Program 5 (cont'd)

```
      DELP=(RO*GR*BETA*GAM*LH**2)/2.
      ROAV=(101325.-DELP)/(R*(TO+(GAM*LH/2.)))
      RE=2.*H(K1)*G/MU
C
C ********** PLAIN SURFACES ********************************** C
C
      IF(SURF.EQ.1) THEN
      FS=(1.58*DLOG(RE)-3.28)**(-2)
      GI=((1.-OMEGA)*GR*BETA*ROAV*RO*QW*(LH**3)/(FS*CP))**(1./3)
      IF(ABS(G-GI).GT.0.001)THEN
      G=(G+GI)/2.
      GO TO 10
      END IF
      ST=(FS/2.)/(1.07+12.7*(FS/2.)**0.5*(PR**(2./3)-1.))
      HI=ST*G*CP
      Q=QW*S*LH
      A=S*LH
C  ++++++++++++   IMSL ++++++++++++++++
      PAR(1) =-2.*TFAV - Q/(HI*A)
      PAR(2) = -Q - HI*A*TFAV
      N=2
      NSIG=5
      ITMAX=100
      X(1)=500.
      X(2)=300.
      CALL ZSCNT(FCN,NSIG,N,ITMAX,PAR,X,FNORM,WK,IER)
      TWAV=X(1)
      TSAV=X(2)
      WRITE(6,18) H(K1),G,FS,HI,RE,TFAV,TWAV,TSAV
   18 FORMAT(2X,F5.3,2X,F6.2,2X,F11.7,
     >   2X,F7.2,2X,F10.1,2X,F5.1,2X,F7.1,2X,F7.1)
      END IF
********** ROUGH SURFACE ********************************** C
C          EP/RE=(E/D)/(B(J)-2.5*LOG(2*E/D)-3.75)            C
C                =(E/D)*(F/2)**0.5                           C
C                                                            C
C          LET   X=E/D                                       C
********************************************************** C
      IF (SURF.EQ.2) THEN
      DO 140 JJ=1,3
      WRITE(6,15)M1
      WRITE(6,13)
      DO 100 II=1,6
      DATA A1/16.,25.,50.,100.,150.,250./
      DO 200 MM=1,9
      IF(A1(II).LE.EP1(MM)) GOTO 150
  200 CONTINUE
  150 RATE=(A1(II)-EP1(MM-1))/(EP1(MM)-EP1(MM-1))
      EP=A1(II)
      GE=GE1(MM-1)+RATE*(GE1(MM)-GE1(MM-1))
      B1(JJ)=B10(MM-1,JJ)+RATE*(B10(MM,JJ)-B10(MM-1,JJ))
      B2=B1(JJ)
   20 TFAV=TO+QW*LH/(2.*G*H(K1)*CP)
      BETA=1./TFAV
      MU=(3.6945705+0.7217775*TFAV-0.43997518E-3*TFAV**2+
     >     0.13530831E-6*TFAV**3)*10.**(-7)
      K=(-3.0992317+0.12297106*TFAV-0.86889035E-4*TFAV**2+
     >    0.3353232E-7*TFAV**3)*10.**(-3)
      PR=0.84168774-0.69540367E-3*TFAV+0.95679111E-6*TFAV**2-
     >     0.37750492E-9*TFAV**3
      GAM=QW/(G*H(K1)*CP)
      DELP=(RO*GR*BETA*GAM*LH**2)/2.
      ROAV=(101325.-DELP)/(R*(TO+(GAM*LH/2.)))
      RE=2.*H(K1)*G/MU
```

Program 5 (cont'd)

```
      EPS=1.0E-14
      NSIG=3
      XL=0.00000001
      XR=1000.
      ITMAX=1000
      CALL ZFALSE(F,EPS,NSIG,XL,XR,XAPP,ITMAX,IER)
      XX=XAPP
      FR=2.*(EP/(XX*RE))**2
      GI=((1.-OMEGA)*GR*FETA*ROAV*RO*OW*(LH    )/(FR*CP))**(1./3)
      IF(ABS(G-GI).GT.0.1)THEN
      G=(G+GI)/2.
      GO TO 20
      END IF
      ST=(FR/2.)/(1.+(FR/2.)**0.5*(GE*(PR**0.57)-B2))
      HI=ST*G*CP
      Q=QW*S*LH
      A=S*LH
      E=2000.*H(K1)*XX
      P=E*M1
C  ++++++++++++   IMSL ++++++++++++++++
      PAR(1) =-2.*TFAV - Q/(HI*A)
      PAR(2) = -Q - HI*A*TFAV
      N=2
      NSIG=5
      ITMAX=100
      X(1)=500.
      X(2)=300.
      CALL ZSCNT(FCN,NSIG,N,ITMAX,PAR,X,FNORM,WK,IER)
      TWAV=X(1)
      TSAV=X(2)
 ++++++++++++++++++++++++++++++++++
    WRITE(6,17) EP,GE,B1(JJ),P,E,H(K1),G,FR,FR/FS,HI,
   >    XX,RE,TFAV,TWAV,TSAV
 17 FORMAT(2X,F5.1,1X,F5.1,2X,F4.1,2X,F5.1,1X,F5.2,2X,F5.3,
   >    2X,F6.2,2X,F11.7,4X,F5.2,2X,F7.2,2X,F7.6,2X,F10.1,2X,
   >    F7.1,2X,F7.1,2X,F7.1)
100  CONTINUE
     M1=2.*M1
140  CONTINUE
     ENDIF
112  CONTINUE
111  CONTINUE
     STOP
     END


     SUBROUTINE FCN(X,F,N,PAR)
     REAL*8   X(2),F(2),PAR(2)
     COMMON /DATA1/ SIGMA,EW,ES,HI,A
     F(1)=X(1)+X(2)+PAR(1)
     F(2)=SIGMA/(1./EW+1./ES-1.)*(X(1)**4-X(2)**4)
    >      +HI*A*X(1)+PAR(2)
     RETURN
     END
C


     FUNCTION F(X)
     IMPLICIT REAL*8 (A-H,O-Z)
     COMMON /ROUGH/ B2,EP,RE
     F=X-(B2-2.5*DLOG(2.*X)-3.75)*EP/RE
     RETURN
     END
```

Appendix 3

Detailed Parametrics for Roughened RVACS Channels

As stated in Section 4.2 of this report's main body, this Appendix presents more details on the calculated effects of design parameter variations than shown in Tables 4.2 and 4.3. Extensive parametrics were made for both smooth channels and for channels employing repeated-rib rougheness.

Tables A3.1 and A3.2 show rather extensive results for channels with ribs; Table A3.1 results for very small rib heights such that $e^+ < 25$ and Table A3.2 for larger rib heights such that $e^+ > 35$. (Comparison between various cases may be highlighted by examining the values of reactor vessel average temperatures and values of the convective heat transfer coefficients.)

These results are presented here in addition to those of Section 4.1 for completeness. They permit indications not only of the effects of changes in parameters given a smooth or ribbed design option but also allow comparisons between these options. Preliminary conclusions regarding smooth vs. roughened designs are presented in Section 4.

Table A3.1 Parametrics for RVACS Channels with Repeated Ribs-Design Option B: $e^+ < 25$

Case No.	H(m)	Q_w (kW/m^2)	L_s (m)	L_h (m)	Q	ε	E (m)	P/E	e^+	U (m/s)	Ta (K)	$\bar{T}_R$(K)	T_{GVO} (K)	T_{GV} (K)	T_{DO} (K)	T_D (K)	h (W/m^2-K)
1	0.3048	10.0	15.24	12.192	0.5	0.7	5.08×10^{-4}	10	14.7	7.7	336	821	574	617	403	447	26
2	0.2540	"	"	"	"	"	"	"	14.8	7.5	346	820	567	620	399	452	26
3	0.4572	"	"	"	"	"	"	"	14.4	8.0	321	823	589	616	416	444	24
4	0.3048	5.0	"	"	"	"	"	"	11.5	6.2	320	687	479	506	355	382	20
5	"	15.0	"	"	"	"	"	"	16.9	8.7	350	914	645	702	451	509	29
6	"	20.0	"	"	"	"	"	"	18.6	9.5	363	988	704	774	498	568	32
7	"	10.0	7.62	"	"	"	"	"	12.6	6.7	343	832	600	650	440	490	22
8	"	"	22.86	"	"	"	"	"	16.3	8.4	333	813	555	595	383	422	28
9	"	"	15.24	"	0.0	"	"	"	18.6	9.5	328	804	533	568	360	395	32
10	"	"	"	"	0.4	"	"	"	15.6	8.1	334	816	562	604	391	432	27
11	"	"	"	"	0.8	"	"	"	10.7	5.8	351	849	633	691	489	547	19
12	"	"	"	"	0.5	0.5	"	"	14.7	7.7	337	906	596	640	381*	425	26
13	"	"	"	"	"	0.6	"	"	"	7.7	337	860	584	628	393	436	26
14	"	"	"	"	"	0.8	"	"	"	7.7	337	786	564	607	414	457	26
15	"	"	"	"	"	1.0	"	"	"	7.7	337	728	546	590	431	474	26
16	"	"	"	3.048	"	0.7	"	"	13.5	7.1	305	821	593	605	418	429	24
17	"	"	"	6.096	"	"	"	"	13.9	7.3	316	817	586	609	413	435	24
18	"	"	"	9.144	"	"	"	"	14.2	7.5	326	821	579	613	408	441	25
19	"	"	"	12.192	"	"	2.54×10^{-4}	"	6.9	8.5	332	829	598	637	434	473	22
20	"	"	"	"	"	"	7.62×10^{-4}	"	22.8	7.1	340	815	558	605	398	434	28
21	"	"	"	"	"	"	5.08×10^{-4}	5	15.1	7.2	339	819	568	614	398	444	26
22	"	"	"	"	"	"	"	20	14.1	8.3	333	822	580	621	412	452	25

*Note: Above values based on air inlet value of 293 K.

Table A3.2 Parametrics for RVACS Channels with Repeated Ribs-Design Option B: $e^+ > 35$

Case No.	H(m)	Q_w (kW/m^2)	L_s (m)	L_h (m)	Q	ε	E (m)	P/E	e^+	U (m/s)	Ta (K)	$\overline{T}_R$(K)	T_{GVO} (K)	T_{GV} (K)	T_{DO} (K)	T_D (K)	h (W/m^2-K)
1	0.3048	10.0	15.24	12.192	0.5	0.7	0.0254	10	1051	3.7	383	821	553	642	392	482	28
2	0.2540	10.0	"	"	"	"	"	"	1081	3.5	407	822	544	657	389	502	29
3	0.4572	10.0	"	"	"	"	"	"	995	4.2	347	821	571	624	403	457	26
4	0.3048	5.0	"	"	"	"	"	"	834	3.0	349	684	458	514	341	398	23
5	"	15.0	"	"	"	"	"	"	410	4.3	410	919	627	744	447	564	31
6	"	20.0	"	"	"	"	"	"	1324	4.7	435	997	689	831	502	644	33
7	"	10.0	7.62	"	"	"	"	"	907	3.2	397	831	570	674	417	521	25
8	"	"	22.86	"	"	"	"	"	1164	4.1	374	815	541	622	378	459	30
9	"	"	15.24	"	0.0	"	"	"	1324	4.7	364	809	526	598	362	433	33
10	"	"	"	"	0.4	"	"	"	1117	4.0	377	818	546	630	384	468	29
11	"	"	"	"	0.8	"	"	"	775	2.7	415	844	590	711	448	569	22
12	"	"	"	"	0.5	0.5	"	"	1051	3.7	383	907	574	663	372	461	28
13	"	"	"	"	"	0.6	"	"	"	3.7	383	860	562	652	382	472	28
14	"	"	"	"	"	0.8	"	"	"	3.7	383	787	544	633	402	491	28
15	"	"	"	"	"	1.0	"	"	"	3.7	383	730	528	617	418	507	28
16	"	"	"	3.048	"	0.7	"	"	970	3.4	317	816	572	596	396	420	26
17	"	"	"	6.096	"	"	"	"	999	3.5	340	818	565	612	395	441	27
18	"	"	"	9.144	"	"	"	"	1025	3.6	362	819	558	627	394	462	27
19	"	"	"	12.192	"	"	0.00635	"	224	5.1	358	814	545	611	379	444	30
20	"	"	"	"	"	"	0.0127	"	480	4.4	368	817	548	623	384	459	29
21	"	"	"	"	"	"	0.0381	"	1683	3.2	395	825	555	657	399	501	27
22	"	"	"	"	"	"	0.0508	"	2373	2.9	407	827	556	670	403	517	27
23	"	"	"	"	"	"	0.1270	"	7924	1.6	496	842	544	748	412	615	27
24	"	"	"	"	"	"	0.0254	5	1120	3.3	395	820	543	645	385	487	29
25	"	"	"	"	"	"	"	20	975	4.3	370	823	564	641	402	479	26

Note: Above values based on air inlet temperature of 293 K.

Appendix 4 COMMIX-1A Study of the Potential for Flow Channeling in a RVACS with Fins on the Duct Wall

The COMMIX-1A computer code has been used to model a symmetric section of RVACS with fins installed on the duct wall liner of the concrete blast shield. This model was then used to study the question whether severe air flow maldistributions (channeling) might occur in such a channel.

The model cross section is shown schematically in Fig. A4.1. The fins are assumed to be one inch thick, ten inches high and evenly spaced with a pitch of ten inches. The channel width is assumed to be twelve inches which leaves a two inch clearance between the fin tip and reactor guard vessel. The x, y plane is assumed horizontal with nodalization as depicted in Fig. A4.1.; positive z points vertically upward i.e., opposite the gravity vector. The air flow is parallel to + z and the channel is taken to be forty feet in height. The model divides the channel height into twenty equal-length cells.

Air is assumed to enter the RVACS channel at z = 0 with a uniform velocity in the z-direction of 7 m/s which is a typical value found from ancillary calculations. Four steady state COMMIX-1A calculations were then made, varying inlet temperature and the turbulent viscosity of the air. The values of air inlet temperature chosen were 100°F (~ 38°C) and 200°F (~ 93°C) since no heat generation was included. The turbulent viscosity values were taken as the extremes of the range considered appropriate for this application, viz:

$$70 \leq \frac{\mu_t}{\mu} \leq 100$$

where μ_t and μ are the turbulent and molecular dynamic viscosity respectively. At an air temperature of 350 K, $\mu = 2.075 \times 10^{-5}$ kg/m.s and thus the two values of dynamic turbulent viscosity input to the code were $\mu_t = 1.45 \times 10^{-3}$ and 2.02×10^{-3} kg/m.s.

Results are shown in Fig. A4.2 which presents the computed output velocities at z = 39 feet, i.e., one foot below the exit plane. The I, J nodal values are as indicated in Fig. A4.1

The results show the flow distributions to be quite insensitive to both temperature and viscosity change over the ranges studied. More importantly, the results indicate a conclusion that severe flow maldistributions would not occur in this RVACS geometry.

Figure A4.1 COMMIX-1A Model of RVACS

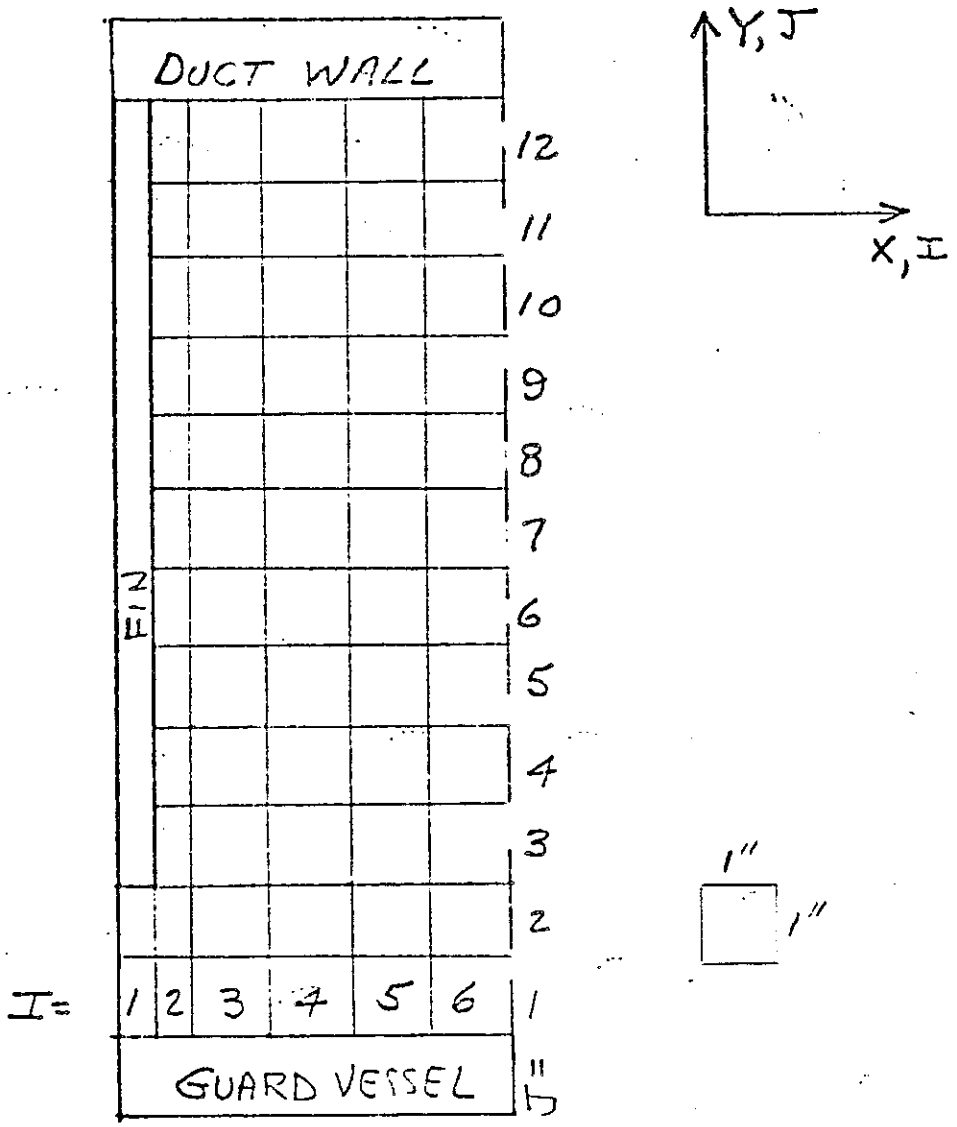

DX(1-2) = 0.5" = 0.0127m
DX(3-6) = 1.0" = 0.0254m
} IMAX = 6

DY(1-12) = 1.0" = 0.0254m : JMAX = 12

DZ(1-20) = 2.0' = 0.0696m : KMAX = 20

Figure A4.2 COMMIX-1A Calculated Velocities Near RVACS Exit for Fins on Duct Wall.

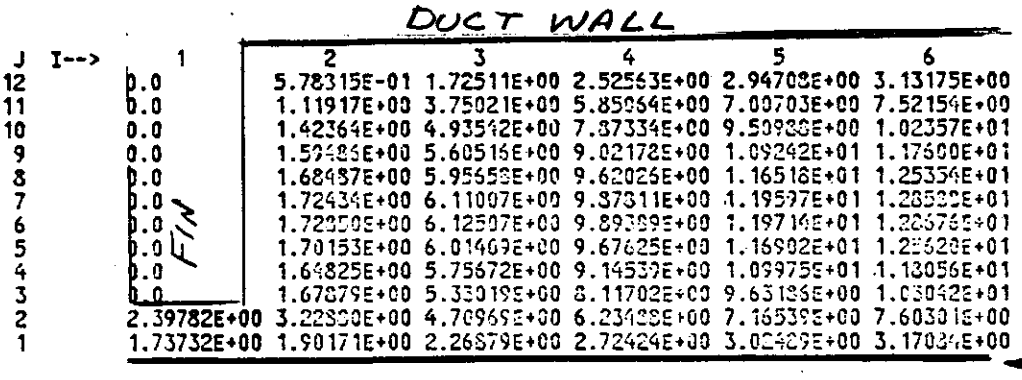

J	I--> 1	2	3	4	5	6
12	0.0	5.78315E-01	1.72511E+00	2.52563E+00	2.94708E+00	3.13175E+00
11	0.0	1.11917E+00	3.75021E+00	5.85064E+00	7.00703E+00	7.52154E+00
10	0.0	1.42364E+00	4.93542E+00	7.87334E+00	9.50988E+00	1.02357E+01
9	0.0	1.59485E+00	5.60516E+00	9.02172E+00	1.09242E+01	1.17600E+01
8	0.0	1.68487E+00	5.95658E+00	9.62026E+00	1.16518E+01	1.25356E+01
7	0.0	1.72434E+00	6.11007E+00	9.87311E+00	1.19597E+01	1.28592E+01
6	0.0	1.72850E+00	6.12507E+00	9.89389E+00	1.19714E+01	1.28676E+01
5	0.0	1.70153E+00	6.01409E+00	9.67625E+00	1.16902E+01	1.25628E+01
4	0.0	1.64825E+00	5.75672E+00	9.14539E+00	1.09975E+01	1.18056E+01
3	0.0	1.67879E+00	5.33019E+00	8.11702E+00	9.63186E+00	1.03042E+01
2	2.39782E+00	3.22800E+00	4.70969E+00	6.23488E+00	7.16539E+00	7.60301E+00
1	1.73732E+00	1.90171E+00	2.26879E+00	2.72424E+00	3.02489E+00	3.17084E+00

$T_{in} = 100°F$

$\frac{Ut}{\mu} = 70$

J	I--> 1	2	3	4	5	6
12	0.0	5.49213E-01	1.64705E+00	2.43410E+00	2.86271E+00	3.05493E+00
11	0.0	1.07044E+00	3.60187E+00	5.67865E+00	6.86703E+00	7.40951E+00
10	0.0	1.37361E+00	4.78559E+00	7.73475E+00	9.45989E+00	1.02510E+01
9	0.0	1.55211E+00	5.48393E+00	8.96992E+00	1.10243E+01	1.19696E+01
8	0.0	1.65022E+00	5.87114E+00	9.65205E+00	1.18042E+01	1.28048E+01
7	0.0	1.69569E+00	6.04673E+00	9.95807E+00	1.22659E+01	1.33180E+01
6	0.0	1.69980E+00	6.06184E+00	9.97550E+00	1.22796E+01	1.33293E+01
5	0.0	1.66727E+00	5.92835E+00	9.71267E+00	1.19294E+01	1.29383E+01
4	0.0	1.60370E+00	5.63192E+00	9.10196E+00	1.11116E+01	1.20274E+01
3	0.0	1.61611E+00	5.16235E+00	7.98592E+00	9.60005E+00	1.03403E+01
2	2.27730E+00	3.07451E+00	4.51550E+00	6.05762E+00	7.03596E+00	7.50495E+00
1	1.64476E+00	1.80444E+00	2.16519E+00	2.62763E+00	2.94277E+00	3.09816E+00

$T_{in} = 100°F$

$\frac{Ut}{\mu} = 100$

J	I--> 1	2	3	4	5	6
12	0.0	5.62111E-01	1.68068E+00	2.47298E+00	2.89789E+00	3.08645E+00
11	0.0	1.09184E+00	3.66733E+00	5.75530E+00	6.92380E+00	7.45992E+00
10	0.0	1.39558E+00	4.85088E+00	7.79764E+00	9.48334E+00	1.02459E+01
9	0.0	1.57039E+00	5.55723E+00	8.99327E+00	1.09796E+01	1.18722E+01
8	0.0	1.66531E+00	5.90773E+00	9.63604E+00	1.17759E+01	1.27324E+01
7	0.0	1.70761E+00	6.07283E+00	9.91893E+00	1.21216E+01	1.31018E+01
6	0.0	1.71175E+00	6.08781E+00	9.93534E+00	1.21343E+01	1.31114E+01
5	0.0	1.68174E+00	5.96462E+00	9.69375E+00	1.18170E+01	1.27620E+01
4	0.0	1.62287E+00	5.68610E+00	9.12035E+00	1.10585E+01	1.19246E+01
3	0.0	1.64323E+00	5.23605E+00	8.04435E+00	9.61437E+00	1.03239E+01
2	2.32862E+00	3.14105E+00	4.59994E+00	6.13553E+00	7.09298E+00	7.54796E+00
1	1.68397E+00	1.84565E+00	2.20895E+00	2.66799E+00	2.97636E+00	3.12733E+00

$T_{in} = 200°F$

$\frac{Ut}{\mu} = 70$

J	I--> 1	2	3	4	5	6
12	0.0	5.37307E-01	1.61648E+00	2.39680E+00	2.82672E+00	3.02111E+00
11	0.0	1.05170E+00	3.54471E+00	5.60395E+00	6.80595E+00	7.35745E+00
10	0.0	1.35429E+00	4.72401E+00	7.67555E+00	9.42364E+00	1.02449E+01
9	0.0	1.53568E+00	5.43744E+00	8.94467E+00	1.10539E+01	1.20367E+01
8	0.0	1.63799E+00	5.83957E+00	9.66220E+00	1.19710E+01	1.30463E+01
7	0.0	1.68520E+00	6.02474E+00	9.98969E+00	1.23861E+01	1.35007E+01
6	0.0	1.68946E+00	6.04031E+00	1.00083E+01	1.24016E+01	1.35134E+01
5	0.0	1.65457E+00	5.89750E+00	9.72529E+00	1.20212E+01	1.30853E+01
4	0.0	1.58680E+00	5.58529E+00	9.08193E+00	1.11490E+01	1.21070E+01
3	0.0	1.59235E+00	5.09936E+00	7.93093E+00	9.57928E+00	1.03442E+01
2	2.23122E+00	3.01606E+00	4.44172E+00	5.98671E+00	6.98039E+00	7.46015E+00
1	1.60904E+00	1.76687E+00	2.12483E+00	2.58857E+00	2.90806E+00	3.06652E+00

$T_{in} = 200°F$

$\frac{Ut}{\mu} = 100$